1991

Effect of process parameters on segregation in a fluidized bed of coal and magnetite

E. Tunc Ulge
Lehigh University

EFFECT OF PROCESS PARAMETERS ON SEGREGATION IN A FLUIDIZED BED OF COAL AND MAGNETITE

by

E. Tunc ULGE

A Thesis Presented to
the Graduate Committee
of Lehigh University
in Candidacy for the Degree of
Master of Science
in
Mechanical Engineering

Lehigh University
Bethlehem, PA
1991

CERTIFICATE OF APPROVAL

This thesis is accepted and approved in partial fulfilment of the requirements of the degree of Master of Science.

Date: August 14, 1991

Professor in Charge: Edward K Levy

(Edward K. Levy)

Chairman of Department: Robert P Wei

(Robert P. Wei)

ACKNOWLEDGEMENTS

My greatest appreciation goes to Prof. E. K. Levy for all of his support and guidance throughout this study.Secondly, I would like thank all of my friends in Bethlehem for giving me support and sharing my times of studying.My special thanks goes to Dr. Bulent Kozanoglu for his support in the first part of this work.I also have a special appreciation for Dr. Fikret Bayat.Last but not least, I would like to thank the Energy Research Center Personnel for their help and friendliness.

TABLE OF CONTENTS

LIST OF TABLES

LIST OF FIGURES

NOMENCLATURE

A_b	Bed cross-sectional area	m^2
C	Coefficient	-
c_p	Tracer concentration in bubble wake	-
c_{po}	Tracer concentration in bubble wake	-
C_E	Volume concentration of component in the emulsion phase	-
C_{w_1}	Volume concentration of component in the first region of the wake phase	-
d_b	Bubble diameter	m
$d_{b,eq}$	Equivalent bubble diameter	m
$d_{b,m}$	Maximum attainable bubble diameter	m
$d_{b,o}$	Bubble diameter just above the distributor	m
d_h	Host diameter	m
d_p	Particle diameter (sieve aperture size)	m
d_r	Size ratio $(d_t-d_h)/d_h$	-
d_{sv}	Particle surface/volume diameter	m
d_t	Tracer diameter	m
D_{bed}	Bed diameter	m
E_p	Probable error	
f_{s_1}	Volume fraction of the first region of the wake	-
f_w	Wake volume fraction	-
F	Mass fraction of particles less than 45 μm	-
F_p	Volumetric flow rate through the bubble wake	m^3/s
g	Gravitational accelaration	m/s^2
g_c	Correction factor	-
GE_p	Generalized performance parameter	-
h	Height from the distributor	m
h_o	Height from the distributor where c_p starts to decrease	m

k	Segregation rate constant based on the cross-sectional area of the emulsion phase	m/s
K_w	Exchange coefficient based on wake volume	1/s
K_1	Exchange coefficient between the emulsion phase and the first region of wake	1/s
L	Bed depth	m
L_{mf}	Level of the bed at minimum fluidization	m
m	Mass of powder	kg
mm	Number of layers occupied by magnetite if the bed is divided into 15 layers of equal thickness	-
N	Number of countable particles	-
N_h	Number of countable host particles	-
N_t	Number of countable tracer particles	-
P	Pressure	Pa
Q	Volumetric flow rate	m^3/s
Q_b	Visible flow rate	m^3/s
Re_b	Reynolds number based on the bubble	-
SG	Specific gravity	-
SGS	Specific gravity of separation	-
t_f	Net fluidization time	s
u_A	Absolute velocity of bubbles in bubbling beds	m/s
u_f	Minimum fluidization velocity of floatsam	m/s
u_j	Minimum fluidization velocity of jetsam	m/s
u_m	Minimum fluidization velocity of the mixture	m/s
u_{mb}	Minimum bubblingvelocity	m/s
u_{mf}	Minimum fluidization velocity	m/s
u_o	Superficial gas velocity	m/s
V	Volume	m^3
x	Weight fraction	-
x_j	Weight fraction of jetsam particles in the bed	-
Y_j	Average segregation distance	m

Y_S	Settling coefficient	-
z	Distance measured from the free surface of the bed	m

Greek

δ	Volume fraction of bubbles and wakes in the bed	
Δx	Displacement of the particles	m
ε	Void fraction	-
ε_{mf}	Void fraction at minimum fluidization	-
γ	Correction factor for visible gas flow	-
μ_f	Absolute viscosity of the fluid	N.s/m^2
ρ_b	Bulk density	kg/m^3
ρ_f	Density of the fluid	kg/m^3
ρ_{fl}	Density of the floatsam	kg/m^3
ρ_h	Host density	kg/m^3
ρ_j	Density of the jetsam	kg/m^3
ρ_p	Particle density	kg/m^3
ρ_r	Density ratio (ρ_t - ρ_h)/ρ_h	kg/m^3
ρ_t	Tracer density	kg/m^3
ϕ	Sphericity	-
ω	Solids circulation rate	m/s

ABSTRACT

The segregation characteristics of a multicomponent fluidized bed of particles composed of coal and magnetite were investigated experimentally and theoretically.The main objective of this study was to determine the impact of operational parameters on the performance of the coal cleaning process, and to determine the most favorable conditions for high efficiency cleaning of coal.

The coal cleaning experiments were conducted with Rushton coal using angular magnetite as the host material.A theoretical model developed previously was used to estimate the degree of segregation and the final coal component distributions under various operational conditions.The outcome of earlier experiments performed to determine the relative displacement of angular particles was used with the theoretical model to predict the stratification of particles in the multi-component coal and magnetite system.Cleaning performance was determined from sulfur and ash distributions, sulfur and ash removal efficiencies, heating value recovery, and generalized distribution curves.The theoretical model agreed with the results from the coal cleaning experiments, showing that the cleaning efficiency is a strong function of operating conditions and bed configuration.The results show that for high cleaning efficiencies, lower bed depths must be selected.Fluidizing gas velocities must also be selected carefully in a certain range.The concentration of the host material was found to affect the coal cleaning performance.The smaller concentrations of magnetite resulted in improved the coal cleaning efficiencies in the case of deep beds.However, cleaning efficiencies was not affected significantly by the magnetite concentration in the case of shallow beds.The cleaning performance generally improved with time, and efficient cleaning obtained with processing periods as short as 30 seconds in the cases of lower bed depths.

I. INTRODUCTION

Cleaning of coal is needed in a more industrialized world for several purposes.Among those are to make it burn environmentally safer, that is to keep poisonous emissions in a more acceptable limit; to keep carbon concentration higher, that is to increase gross calorific value and decrease the weight which must be handled and moved, to decrease ash disposal expenses, and to obtain a more uniform quality product.Since coal is a major source of energy and a primary fuel, unfavorable issues in burning of coal are getting to be more important.Emission of harmful sulfur containing gases and ashes into the atmosphere is a major concern for many societies living on earth.More strict government regulations on emissions are of major concern to industries which utilize coal at high rates.

The mineral impurities present in coal can be classified into two categories consisting of those that form the ash and those that contribute to sulfur.From the standpoint of coal cleaning, each can be considered as impurities which are structurally a part of the coal (organic impurities) and impurities which are not structural (inorganic impurities). Sulfur is accepted as the most important single element which determines the utilization of coal as a clean fuel.Sulfur contents of coals may vary from 0.1 to 10 percent of weight.Pyritic sulfur (FeS_2) is the mineral pyrite present in the coal in the form of discrete and sometimes microscopic particles.It is heavier than pure coal. The specific gravity of mineral pyrite is approximately 5.0 whereas the coal itself has a specific gravity of approximately 1.8.Organic sulfur, which is an integral part of the coal matrix and chemically bonded to coal forms about 30 to 70 percent of the total sulfur.It is agreed that the organic sulfur to total sulfur ratio is highest for low sulfur coals and decreases as the total sulfur content increases.The organic sulfur cannot be removed from the coal unless a chemical treatment is applied.The concentration of organic sulfur determines the upper limit on the cleaning

performance by physical methods.The available methods for controlling sulfur oxide emissions from combustion can be considered as follows: the use of naturally found low sulfur coal, chemical and/or physical cleaning to remove the sulfur, removal of sulfur compounds during the combustion process, removal of sulfur oxides from the combustion flue gas, conversion of coal to another form of cleaner combustible by methods of gasification and/or liquefaction.Among these methods, removal of pyritic sulfur by physical methods is the lowest in cost.

Pyritic sulfur can be separated from the coal after crushing by mechanical cleaning.Cleaning performance is primarily a function of particle size and nature of the distribution of the ash and pyritic sulfur throughout the coal. A commonly used technique is a wet technique. It is a process in which the coal is slurried with water and then by means of one of the well-known methods, the higher density ash and pyrite are removed from the coal.The basic principle of operation is that the specific gravity of coals differs from their impurities, so that there is a relationship between the velocity that the particles fall in water and their relative densities.Coal which has been cleaned by a wet method must be dewatered prior to combustion or transportation.Among other disadvantages of wet cleaning techniques are its contribution to pollution, freezing of coal during shipment and storage and difficulty of flow when the coal is wet.

Mechanical cleaning of coal from its impurities using air instead of water is also possible.Practical application of gas fluidized beds has been increasing for multicomponent solid treatments such as coal and solid waste conversion processes where either good mixing or segregation must be maintained.In a fluidized bed, particles of different size and/or density are moving relative to each other, and a dynamic equilibrium is set up between the competitive mechanisms of mixing and segregation leading to a variation of solid composition over the height of the fluidized bed.A *fluidized bed* is a vertical column of particles where air through a distributor is used to fluidize the column of particles.Previous studies have shown that the particle

motion is caused solely by the bubbles forming in the bed.At low flow rates, the particles are packed and the air flows through the voids naturally present between the particles.In this flow regime, the particles are stationary.At higher flow rates, the particles are suspended in air.Further increasing the flow rate results in a violent mixing as in the boiling of water.At flow rates that the bed is transformed from a packed to a suspended state, the fluidization is referred to as *minimum fluidization*.At above flow rates above minimum fluidization, some of the gas flows through the bed in the form of bubbles or gas voids.As the bubbles move upward through the bed, they cause agitation of the solids leading to a motion of the bed particles.The state of fluidization in which bubbles first form and that is above the minimum fluidization is referred to as *mimimum bubbling*.

It is known that in gas fluidization of multicomponent solid mixtures, particle segregation takes place in the vertical direction of the bed when there is a certain difference in size or density of particles.Denser and bigger particles tend to fall down through the voids relative to the other when an overall motion of paricles are considered to take place under certain operating conditions.Then, the bed is referred to as segregated.The extent of segregation can be easily detected by examining the vertical concentrations of one component of the mixture relative to the others.A component which tends to settle in the downward direction is called as jetsam whereas a component which tends to float is called floatsam.In case of the segregation process, both segregation and mixing occur simultaneously and the segregation performance is determined as a result of these processes competing with each other.It is a major concern of this study to determine the most favorable conditions for a strongly segregating bed of particles of coal and magnetite.It is known that the final distribution of a bed of particles after fluidization can be a function of excess fluidization, that is the rate of fluidization above the minimum fluidization, density and size of the particles, the particle shape, the relative concentration of components and the bed height.

The extent of segregation determines the performance of cleaning in the case of a bed composed of multicomponent coal and magnetite.The results on performance are presented in terms of sulfur and ash distribution, sulfur and ash removal, energy recovery and the generalized distribution curve.

The objective of this study is to to determine the effect of operational parameters such as the depth of the fluidized bed, the concentration of coal, the fluidization velocities above the minimum bubbling velocities, and the size of the host material which is used with coal.Experiments were conducted primarily with Rushton coal with the mesh size -50 +80, and with -100 +120 mesh magnetite.Coal is considered to consist of several components with the same size but with different physical properties such as sulfur, ash and energy content.Each component has also different concentrations.Those components with high sulfur and ash content are heavier and are known to segregate when the bed of particles is fluidized under carefully selected operating conditions.Theoretical results were obtained by a computer program which was previously available for various operating conditions, including the conditions used for the experiments.The computer program is used to calculate the concentration of each coal component and magnetite in equally divided layers of the fluidized bed.Experimental and theoretical results of segregation behavior are presented for a wide range of operational parameters.

II. TERMINOLOGY OF FLUIDIZED BEDS

II.1. States of Fluidization

II.1.A. Minimum Fluidization

The pressure drop will increase linearly upto a certain point with increasing velocity of the gas flowing.Then, it will remain constant independent of the flow velocity.The critical point of flow velocity after which the pressure drop no longer increases is called the *minimum fluidization velocity*.At the minimum fluidization condition, the particles are observed to have transformed from a packed state to a state at which they are suspended individually by the gas and are in the loosest possible condition for moving freely (Fig.2.1).

During the process of fluidization, the bed is observed to expand and the particles relocate themselves to present as little resistance to the flow as possible.After the point of minimum fluidization is passed, the bed continues to expand to allow for additional space between the particles for the passage of the gas.

The state of fluidization is reached when the drag force on the particles by the upward moving gas is equal to the weight of the particles.The drag force is equal to the pressure across the bed times the area of the bed.The weight of the particles can be calculated by knowing the volume of the bed, the specific weight of the particles and the fraction of solids (or voids) in the bed.Then the pressure drop across the bed becomes,

$$\frac{\Delta P}{L_{mf}} = (1-\varepsilon_{mf})(\rho_s - \rho_f)\frac{g}{g^*} \qquad (2.1)$$

Wen and Yu [1] suggests the use of the following correlations,

$$\frac{d_p u_{mf} \rho_f}{\mu_f} = \left[(33.7)^2 + 0.0408 \frac{d_p^3 \rho_f (\rho_s - \rho_f) g}{\mu_f^2} \right]^{0.5} - 33.7 \qquad (2.2)$$

for small particles this becomes,

$$u_{mf} = \frac{d_p^2 (\rho_s - \rho_f) g}{1650 \mu_f} \qquad Re_p < 20 \qquad (2.3)$$

and for large particles,

$$u_{mf} = \left[\frac{d_p^2 (\rho_s - \rho_f) g}{24.5 \rho_f} \right]^{0.5} \qquad Re_p > 1000 \qquad (2.4)$$

When working with air at ambient pressure and temperature, the absolute viscosity term can be included in the numerical constant.Since the fluid density is much smaller than the particle density, eqn. (2.3) becomes,

$$u_{mf} = C \rho_p d_p^2 \qquad (2.5)$$

where C is experimentally determined.For powders in a size range of 50-500 μm, eqn. (2.5) can be written as,

$$u_{mf} = 420 \rho_p d_p^2 \qquad (2.6)$$

where particle density is in kg/m^3, particle size in m, and minimum fluidization velocity in m/s.Measurements of minimum fluidization velocities for different sizes of Rushton coal and angular magnetite are given in Appendix B.

II.1.B. Minimum Bubbling

Fluidized beds of very fine powders expand beyond the state of minimum fluidization without any formation of bubbles. The highest superficial velocity for this state corresponds to the formation of the first bubble and the highest bed height.This state of the fluidization is called the *minimum bubbling velocity*.

A correlation by Abrahamsen and Geldart [2] in terms of the particle and fluid properties is,

$$u_{mb} = 2.07\exp(0.716F)\frac{d_p \cdot \rho_f^{0.06}}{\mu_f^{0.347}} \qquad (2.7)$$

The parameter F is the mass fraction of particles with sizes less than 45 microns.In a fluidized bed, bubbles are the particle-lean regions and are dispersed in a continuous phase of fluidized particles.The continuous phase is termed the dense, particulate or emulsion phase.The rising voids are referred to as *bubbles* if their dimensions are less than that of bed, or *slugs* if their dimensions are close to that of the bed.Measurements of minimum bubbling velocities for different sizes of Rushton coal and angular magnetite are given in Appendix B.

II.1.C. Flow Through Fixed Beds

A *fixed (packed)* bed occurs the solids which form the bed always remain touching each other.In this case, fluid flows through the spaces between the particles, but it is at

low rates that will not cause any disturbance to the particles.The pressure drop in a fixed bed is given by the following equation as a function of the average flow velocity, the fluid viscosity and density, voidage, particle sphericity and size.

$$\frac{\Delta P}{L} g^* = 150 \frac{(1-\varepsilon)^2}{\varepsilon^3} \frac{\mu_f . u_o}{(\phi d_p)^2} + 1.75 \frac{1-\varepsilon}{\varepsilon^3} \frac{\rho_f . u_o^2}{\phi d_p} \qquad (2.8)$$

The first term on the right represents the viscous losses and the second term on the right represents the kinetic energy losses.The term g^* is a correction factor to take compressibility into account.The pressure drop for a fixed bed of non-uniform particles can be calculated by using surface-volume-mean-diameter (the diameter of the sphere having the same external surface/volume ratio as the particle) instead of the particle diameter.

At low Reynolds numbers eqn.(2.8) reduces to,

$$\frac{\Delta P}{L} g^* = 150 \frac{(1-\varepsilon)^2}{\varepsilon^3} \frac{\mu_f . u_o}{(\phi d_p)^2} \qquad Re_p < 20 \qquad (2.9)$$

where Reynolds number is defined as,

$$Re_p = \frac{d_p u_o \rho_f}{\mu_f} \qquad (2.10)$$

At higher Reynolds numbers, only kinetic energy losses should be considered, then eqn.(2.8) reduces to:

$$\frac{\Delta P}{L} g^{*} = 1.75 \frac{1-\varepsilon}{\varepsilon^{3}} \frac{\rho_f \cdot u_o^2}{\phi d_p} \qquad Re_p > 1000 \qquad (2.11)$$

II.1.D. Void Fraction

When particles either with regular or irregular shape are arbitrarily put together, there will be empty spaces referred to as voids, left between the particles.The *void fraction* for a pack of solids is defined as the volume of voids to the total volume of voids and particles, and can be written as:

$$\varepsilon = \frac{V_{voids}}{V_{particles} + V_{voids}} \qquad (2.12)$$

Typically, the values of void fraction in static bulk materials vary between 0.26 to 0.48.The value of void fraction is higher if the particles are extremely irregular in shape (sphericity is lower), and the size distribution in a bed of particles is in a narrow range.

II.2. Characteristics of Particles

II.2.A. Particle Size

There are many methods used for defining the size of particles.Some of the more common are:

(i) Sieve Size

The width of the smallest square opening through which particles will pass

(ii)Volume Diameter

The diameter of a sphere having the same volume as the particle

(iii) Surface/Volume Diameter

The diameter of a sphere having the same external surface/volume ratio as the particle.

(iv) Surface Diameter

The diameter of a sphere having the same surface area as the particle.Standard size screen sets are used to determine the *sieve size*.Among the sets of standard size sieves *"Tyler"* is the most commonly used (Appendix A).Screen analysis approximates *volume diameter* for irregular particles.For particles which are highly irregular, it overestimates the volume diameter.For regular, non-spherical particles it underestimates (flakes, disks),or overestimates (rods, slivers) the volume diameter.

II.2.B. Particle Shape

The particles in a bulk solid may be irregular in shape.The characteristic shape of the particles which form a bed has been shown to have an effect on the packing and flow behavior in the bed.A commonly used definition, the sphericity, indicates how much the particle shape deviates from *spherical*.Several general expressions are also associated with the particle shape; such as flaky, nodular, acicular, etc.The sphericity is defined as follows:

$$\phi = \left[\frac{(\text{Area})_{\text{surface,sphere}}}{(\text{Area})_{\text{surface,particle}}} \right]_{\text{volume=c}} \qquad (2.13)$$

For perfectly spherical particles, the sphericity is unity.Sphericity may have values between 0 and 1.

II.2.C. Particle and Bulk Density

The density of particles in the case where there are no voids is defined as the *particle density*.This is equal to the mass of the particle divided by the volume occupied by the particle.

In contrast, the *bulk density* is defined as the total mass of the bed of particles divided by the total volume of the bed. Bulk density is related to the particle density through the void fraction and the fluid density as follows:

$$\rho_b = (\rho_p - \rho_f)(1 - \varepsilon) + \rho_f \qquad (2.14)$$

In cases where the fluid used is air, eqn. (2.14) can be simplified to:

$$\rho_b = \rho_p(1 - \varepsilon) \qquad (2.15)$$

II.2.D. Average Particle Size and Distribution

In applications of fluidization, there exists a high probability that the solids forming the bed are not in the same size.It is usually important to determine the size of a bulk of solids.In a bulk mass of solids consisting of particles with different sizes, the *surface/volume diameter* can be used to calculate the average size of particles.It is determined by the following:

$$d_{sv} = \frac{\sum_{i=1} N_i d_i^3}{\sum_{i=1} N_i d_i^2} = \frac{\sum_{i=1} x_i}{\sum_{i=1} \frac{x_i}{d_i}} \qquad (2.16)$$

where N is the number of particles with the size d_i and x is the weight fraction of the particles in each size range.Sieve aperture size would be used for d in case the particle sizes are experimentally found.

II.2.E. Particle Classification

The behavior encountered with a gas-fluidized systems is controlled by the type of bubbling behavior which occurs dominantly a consequence of the different bubbling behavior.It has often been suggested that some breadth of size distribution is desirable to achieve stable fluidization.Geldart [3] has argued that it is the mean size on a surface to volume basis which is the important factor, and the addition of a comparatively small amount of fines classed as material less than 45 μm in size has a considerable impact on the fluidization characteristics.Geldart suggested earlier that the materials could be categorized primarily based on particle density and size from tests under ambient conditions as in Fig.2.2.The first group of classification is namely the *"Group A"* materials and fall in the size range of 20-100 μm and with densities less than 1.4 g/cm^3.They exhibit a considerable degree of stable bed expansion when the fluidization velocity is first exceeded, and it may be possible to sustain such uniform or *particulate* fluidization until the minimum fluidization velocity is increased by a factor of two to three times.However, with a further increase in gas velocity, a point will be reached when the bed will collapse back to a less expanded state approximating closely the degree of expansion under minimum fluidization conditions.Most of the excess gas will flow through the bed as the bubble phase.The gas velocity at which bubbles first appear is referred to as the minimum bubbling velocity.

Geldart's *"Group B"* materials tend to have a mean size within the range 40-500 μm and a density in the range of 1.4 to 4.0 g/cm^3.These exhibit considerably less stable bed expansion, and free bubbling occurs at or a little above the minimum fluidization velocity.It was also suggested that when the minimum fluidization velocity exceeds the minimum bubbling velocity, those materials belong to Group B rather than Group A.

"Group C" materials are those of smaller mean size which are usually less than 30 μm and/or of lower density so that interparticle forces have an effect greater than that of gravity.Such materials are very difficult to fluidize.For this group of materials, it is very unlikely that the pressure drop across the bed will be balanced by the weight.Instead, part of the weight is supported by gas channelling.Once a channel opens through the bed, it tends to enlarge with a further increase in gas velocity so that the gas is never evenly distributed into the bed.

"Group D" materials are usually of mean diameter greater than 600 μm and/or dense particles.Although a bubbling fluidized bed looks very turbulent and may be described as being turbulently fluidized when operating at higher fluidizing velocities, the gas flow condition within the interstices tends to be laminar, or at the most transitional when "Group D" materials are examined.

II.3. Characteristics of Bubbles in Fluidized Beds

Previous studies on bubbles in fluidized beds revealed a considerable understanding of bubble characteristics in fluidized beds.When investigating bubble behavior, many studies have made analogies to the state of bubbles in real fluids.Since gas fluidized beds are operated under fluid flow rates higher than that would allow the gas to escape through the voids without disturbing the particles, the bed has a fluid-like behavior at such conditions.The excess gas flows in the bed in the form of bubbles and the bubbles dominate the mechanisms of fluidization.In investigating the bubble behavior, the *single bubble* approach has been used extensively to understand the shape, size and the rising velocities of bubbles.

II.3.A. Bubble Size

Bubbles forming above the distributor grow in the bed due to a decrease in the static head.They may also grow by coalescence by overtaking the bubble rising close to them.After reaching the largest stable size, bubbles start splitting. Coalescence is

assumed to cause the average bubble size to come into an equilibrium close to the maximum stable size, which is known to be a function of particle characteristics.

There are several models available to predict the bubble size in fluidized beds.A few to mention are by Mori and Wen [4], Rowe [5], Darton et al. [6] and Werther [7].The model by Mori and Wen is used throughout this study.It is explained in more detail in the Section III.1.A.

II.3.B. Bubble Shape

The bubble shapes in fluidized beds are somewhat different than those in real fluids.In real fluids, the bubbles are highly distorted when they are relatively large.But in fluidized beds, the bubbles are spherical on the front surface during their entire period of rise with an indentation in the lower part.A typical bubble is shown in Fig.2.4 with the related nomenclature.The *wake angle* is defined as the angle from the nose to the rim of the bubble and is used to describe the bubble shape.The *wake* portion is the lower portion of the bubble, which would complete the bubble to a perfect sphere.

Grace [8] showed that the wake angle is a function of the bubble Reynolds number.

II.3.C. Bubble Wake Fraction

Bubble wake fraction is defined as the ratio of the bubble wake volume to the total volume of the wake and the bubble cavity.The bubble becomes spherical as the wake fraction approaches zero.Kozanoglu [9] predicts the percent wake fraction by use of the following correlation:

$$f_w = (0.78 + 0.0076 d_p) + \left(\frac{389.9}{d_p^{1.103}}\right) d_b \qquad (2.17)$$

the particle diameter in μm and the bubble diameter has units of mm.

II.3.D. Bubble Flow Rate

Visible bubble flow rate is defined as the flow rate at a certain elevation in the attributed just to the bubbles.The visible flow rate is:

$$Q_b = (u - u_{mf})A_b \qquad (2.18)$$

The two-phase theory of fluidization states that the excess gas of that required for minimum fluidization is carried only by bubbles.

The motion of bubbles can be examined in the following categories as they move upwards.Visible bubble flow associated with the rise of bubbles, flow through the bubbles relative to them, interstitial flow relative to particles in the emulsion phase, flux of interstitial voids moving with the particles.The first two contitutes the *bubble phase flow*, where the last two constitutes to as *flow through the dense phase*.

In practice, eqn. (2.18) tends to overpredict the visible bubble flow.The reason for the deviation is attributed to the interstitial flow and the thru-flow in the bubbles.As expressed in detail in Section III.1.B, an analysis of the results yielded in a correction for equation (2.18) to fit the results. The corrected visible bubble flow is in the form:

$$Q_b = \gamma(u - u_{mf})A_b \qquad (2.19)$$

where the values of gamma can be determined experimentally.

II.3.E. Bubble Velocity

Equations derived for the rise of a single bubble in real liquids were used for fluidized beds in many previous studies.Such equations were also used to derive equations for the single rise of single bubbles in the fluidized beds.The following is derived from real fluids.

$$u_b = 0.71\sqrt{gd_{eq}} \qquad Re_b > 100 \tag{2.20}$$

If the relative velocity between the bubble and emulsion phase are unaffected by the interaction between the surrounding bubbles, the average velocity of bubbles can be written as follows:

$$u_{b,ave} = (u_o - u_{mf}) + u_b \tag{2.21}$$

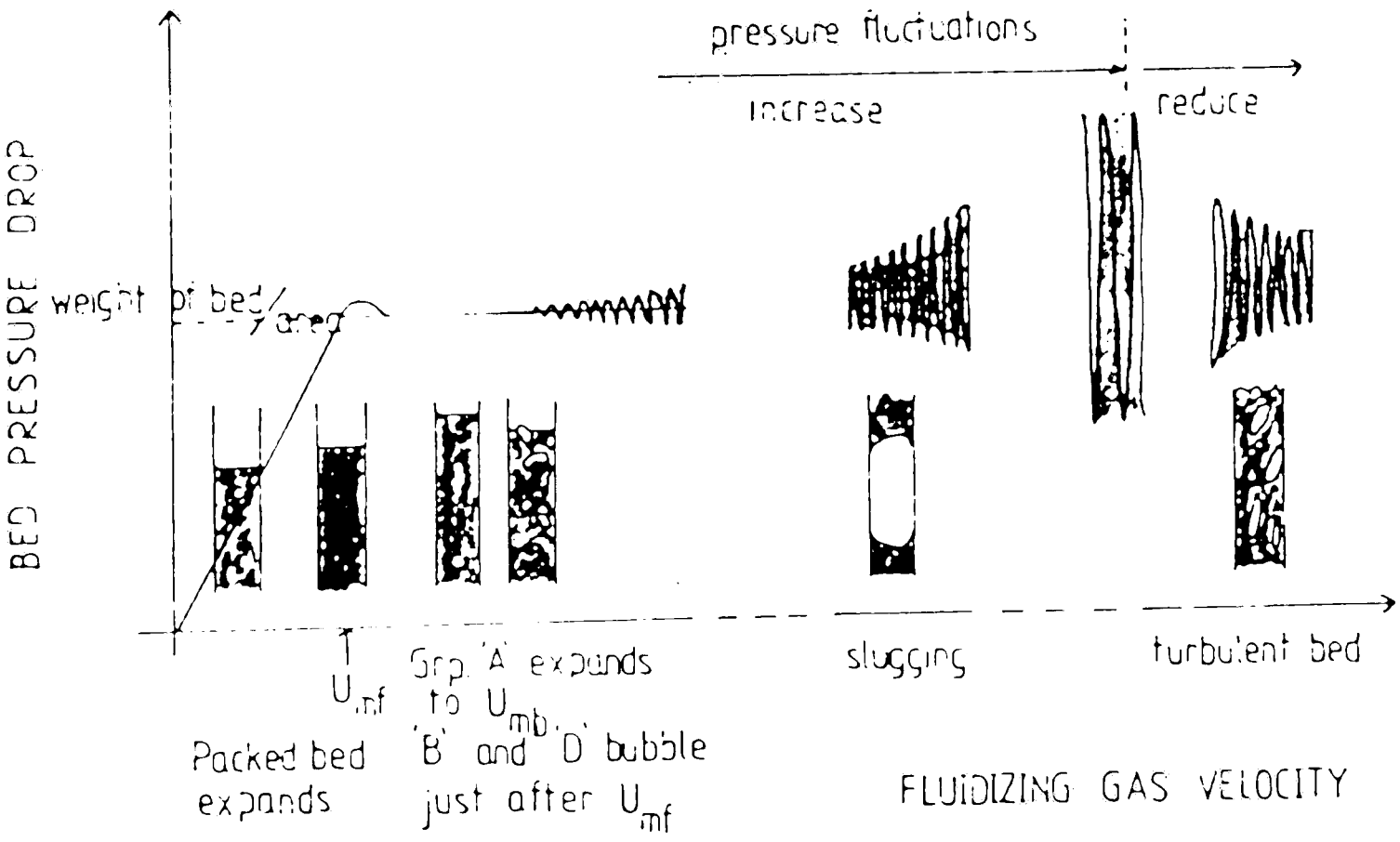

Fig.2.1 Variation in bed pressure drop with superficial gas velocity [3].

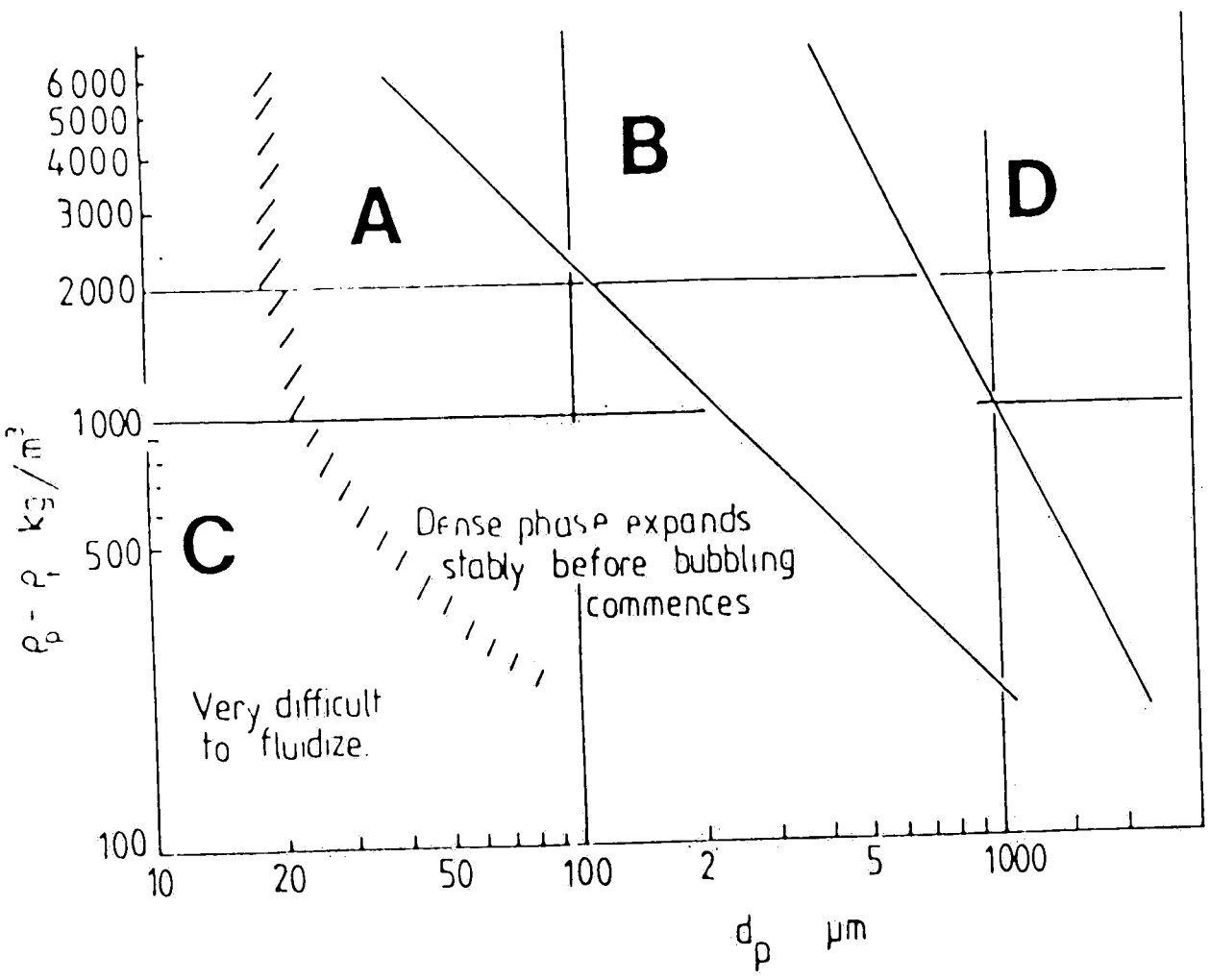

Fig.2.2 Powder classification diagram [3].

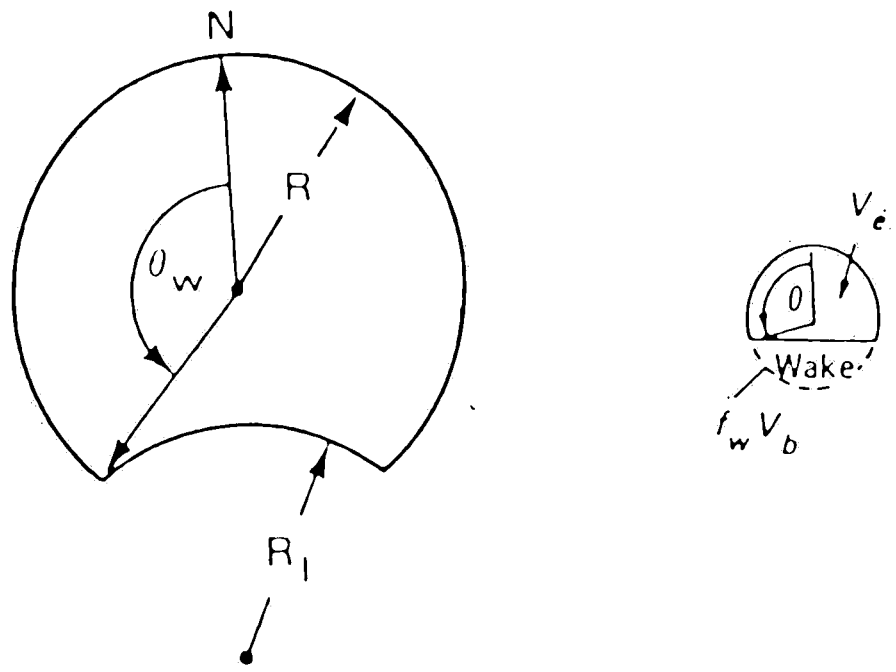

Fig.2.3 Shape of a bubble in a bed of particles when rising

III. MIXING AND SEGREGATION MECHANISMS

In a fluidized bed, both segregation and mixing rate processes occur simultaneously (Fig. 3.1).The bubbles which are formed at the very bottom of the bed will grow, and rise to the top.The bed material is thought of as consisting of two phases; they are the wake phase and the emulsion phase.Solids are picked up at the bottom and lifted up toward the surface in the wake of the bubbles.At the top, the wake contents are deposited in the emulsion phase. Then particles carried up by the bubbles fall through the bubble-free regions. The circulating motion of particles is referred to as *circulation* (Fig.3.2).While bubbles are carrying the solid particles in their wakes, some of the particles are shed en route.This motion of particles between the wake and emulsion phases is referred to as *wake exchange* (Fig. 3.3).Essentially, the mixing in a segregating bed is due to each bubble gathering some jetsam in its wake and lifting and shedding a part of it en route [10].While bubbles rise in the bed, the denser and larger particles tend to fall faster due to a disturbance of the region behind the bubble wake. This motion is referred to as *segregation*.Nienow et al [10] mentioned the existence of other secondary effects such as overlayering.Considering the mechanisms of mixing and segregation, several mathematical models have been established to predict the distribution of different particle components in a fluidized bed.Circulation and wake exchange occur whether or not there are physical differences between the particles which form the bed.Segregation, on the other hand, occurs only when there are physical differences in the particles such as density and size.

III.1. Circulation

Based on the emulsion phase a circulation rate can be defined by balancing the upward and downward motion of solids.That is,

$$\omega (1 - \delta) = u_b f_w \delta \tag{3.1}$$

$$\omega = \frac{u_b f_w \delta}{1 - \delta} \tag{3.2}$$

The volumetric fraction of bubbles and wakes in the bed is ,

$$\delta = \frac{\delta_b}{1 - f_w} - \frac{u_o - u_{mf}}{u_b (1 - f_w)} \tag{3.3}$$

where, f_w is the wake fraction.The bubble rising velocity is given by Nicklin [11] as:

$$u_b = u_o - u_{mf} + 0.711\sqrt{g d_b} \tag{3.4}$$

The minimum fluidization velocity of a mixture of particles is as follows:

$$u_m = u_{fl}\left[\frac{u_j}{u_{fl}}\right]^{x_j^2} \tag{3.5}$$

III.1.A. Bubble Growth Models to Determine Bubble Size

Throughout this study, the bubble growth model by Mori and Wen [4] is used.One of the reasons for using it is that it is the only growth model which takes the bed diameter into account. It is also derived from more data than the other models.The initial bubble diameter just above the porous distributor is given by .

$$d_{b,o} = 0.00376(u_o - u_{mf})^2 \tag{3.6}$$

Maximum attainable bubble diameter would exist when the bubbles form in a single column in the center and carry all the gas that is above minimum fluidization conditions.It is given by,

$$d_{b,m} = 0.652\left[A(u_o - u_{mf})\right]^{0.4} \tag{3.7}$$

And the equivalent bubble diameter has practical use in different fluidization conditions.It is given as follows:

$$d_{b,eq} = d_{b,m} + \left(d_{b,o} - d_{b,m}\right)\exp\left(-\frac{0.3h}{D_{bed}}\right) \tag{3.8}$$

III.1.B. Visible Bubble Flow

Previous studies have shown that visible bubble flow is not accurately predicted by the two-phase flow theory [12].The deviation has been attributed to a possible increase in the interstitial gas velocity in the dense phase above that required for minimum fluidization or to a through flow inside the bubble.Grace and Clift [12] give a summary of studies.The corrections to the equations above can be made as follows:

The volumetric fraction of bubbles and wakes,

$$\delta = \frac{(u_o - u_{mf})\gamma}{u_b(1 - f_w)} \tag{3.9}$$

Bubble rising velocity,

$$u_b = (u_o - u_{mf})\gamma + 0.711\sqrt{gd_b} \tag{3.10}$$

initial bubble diameter,

$$d_{b,o} = 0.00376\left[(u_o - u_{mf})\gamma\right]^2 \tag{3.11}$$

maximum attainable bubble diameter,

$$d_{b,m} = 0.652\left[A(u_o - u_{mf})\gamma\right]^{0.4} \tag{3.12}$$

the correction factor for visible bubble flow,

$$\gamma = \frac{Q_b}{A_b(u_o - u_{mf})} \tag{3.13}$$

III.2. Wake Exchange

Bubbles when rising to the top carry particles in their wakes.A part of their content is shed en route.The wake is also fed from the emulsion phase, resulting in an exchange mechanism.The wake exchange rate is defined as the rate at which particles exchange between the wake and emulsion phases.The exchange coefficient K_w, is defined as the volumetric particle flux into and out of the wake per unit volume of the wake.Basesme [13] in a recent study concludes that the wake exchange coefficient decreases with increasing bubble size and the changes are stronger for particles having relatively lower values of minimum fluidization velocity.

Exchange coefficient is defined as,

$$K_w = \frac{F_p}{V_w} \tag{3.14}$$

where,

$$F_p = \frac{q_s}{1 - \varepsilon_{mf}} \tag{3.15}$$

The material balance on the tracer particles in the wake for a differential element of the bed gives .

$$-\frac{dc_p}{dh} V_w = \frac{K_w}{u_b} V_w c_p \tag{3.16}$$

and when equation (3.16) is integrated,

$$\ln \frac{c_p}{c_{po}} = -K_w \frac{(h - h_o)}{u_b} \tag{3.17}$$

Rowe, Partridge and Henwood [15] observed a stagnant region in the wake of the bubbles in their mixing experiments.Kocatulum's [16] calculations show that the particle velocities become very small near the intersection of the symmetry axis of the bubble and the bubble, solid interface.It is concluded that a relatively small stagnant region exists in the bubble wake around the bubble's symmetry axis.That region is characterized by very low particle velocities where almost no particle exchange occurs.The variation of exchange coefficient is shown against volumetric fraction for different regions in Fig. 3.3.The curve represents particle flux into each control volume by the fraction of the wake bounded by the same control volume.The exchange coefficient varies throughout the wake region.The area under the curve is represented by four regions whose sum is equal to the area under the curve.Each of the four regions is assumed to correspond to a shell which altogether make up the wake. The inner portion is observed to be a stagnant region.The outer shell of the wake exchanges particles with the emulsion phase and the region adjacent to the outer shell exchanges

particles with the outer shell and so the inner shells.Since the innermost region is a stagnant region, no particle exchange occurs between that region and the region next to it.The sum of the ratio of each region to the wake volume is unity.

$$f_{s_1} = f_{s_1} + f_{s_2} + f_{s_3} + f_{s_4} \tag{3.18}$$

III.3. Settlement

Settlement in a fluidized bed occurs only if there are physical differences in the particles which form the bed.The physical differences may be in the size, density and shape.If there are physical differences in the particles, the bed is referred to as heterogeneous, otherwise homogeneous.

In heterogenous beds, particles tend to fall through the voids at the temporarily disturbed region behind the bubbles if they are larger and denser relative to the other particles.Settling and mixing occur simultaneously to produce an equilibrium distribution, which is essentially uniform in a horizontal plane but generally varies with height.Both are the result of bubbling entirely .

III.3.A. Settlement Rate Parameter

The settlement rate parameter k, is defined as the average downward displacement rate of settling particles relative to the rest of the particles in the bed.A negative value of k represents an upward motion.It is calculated from the average segregation distance for a certain bubbling condition according to the following equation:

$$k = \frac{\dfrac{\sum_{i=1}^{n} \Delta x_i N_{ih}}{N_h} - \dfrac{\sum_{i=1}^{n} \Delta x_i N_{it}}{N_t}}{t_f} \qquad (3.19)$$

The first term in the numerator represents the average displacement of the host particles with respect to a fixed reference point in space.The second term represents the average displacement of the tracer particles.The summation term is introduced to account for a weighted average.

III.3.B. Settlement Coefficient

Tanimoto et al. [16] defined the average segregation distance as a dimensional parameter which represents the segregation of jetsam relative to the floatsam by each bubble passage.They propose that the average segregation distance is proportional to the bubble diameter and is given by:

$$Y_j = 0.3\left(\frac{\rho_j}{\rho_f}\right)\left(\frac{d_j}{d_f}\right)^{1/3} . d_b \qquad (3.20)$$

Nienow and Chiba [17] expressed the relationship between the average segregation distance and the settlement rate parameter as follows:

$$k = \frac{3}{2}\frac{Y_j}{d_b} u_b \frac{\delta}{1-\delta} \tag{3.21}$$

The mean jetsam descending velocity can be calculated by knowing the bubble frequency:

$$u_j = Y_j . f_b \tag{3.22}$$

Kozanoglu [9] defines the average segregation distance as a non-dimensional parameter.The relationship between the average segregation distance and the settlement rate parameter k, as given by [9] is the following:

$$k = 0.75 Y_s u_b \frac{\delta}{1-\delta} \tag{3.23}$$

Bubble rising velocity can be calculated by (3.4), the volumetric fraction of bubbles and wakes is given by (3.3) and the wake fraction can be calculated by the following in percent:

$$f_w = (0.78 + 0.076 d_p) + \left(\frac{389.9}{d_p^{1.103}}\right) d_b \tag{3.24}$$

where, mean particle diameter is [μm] and the bubble diameter is [mm].

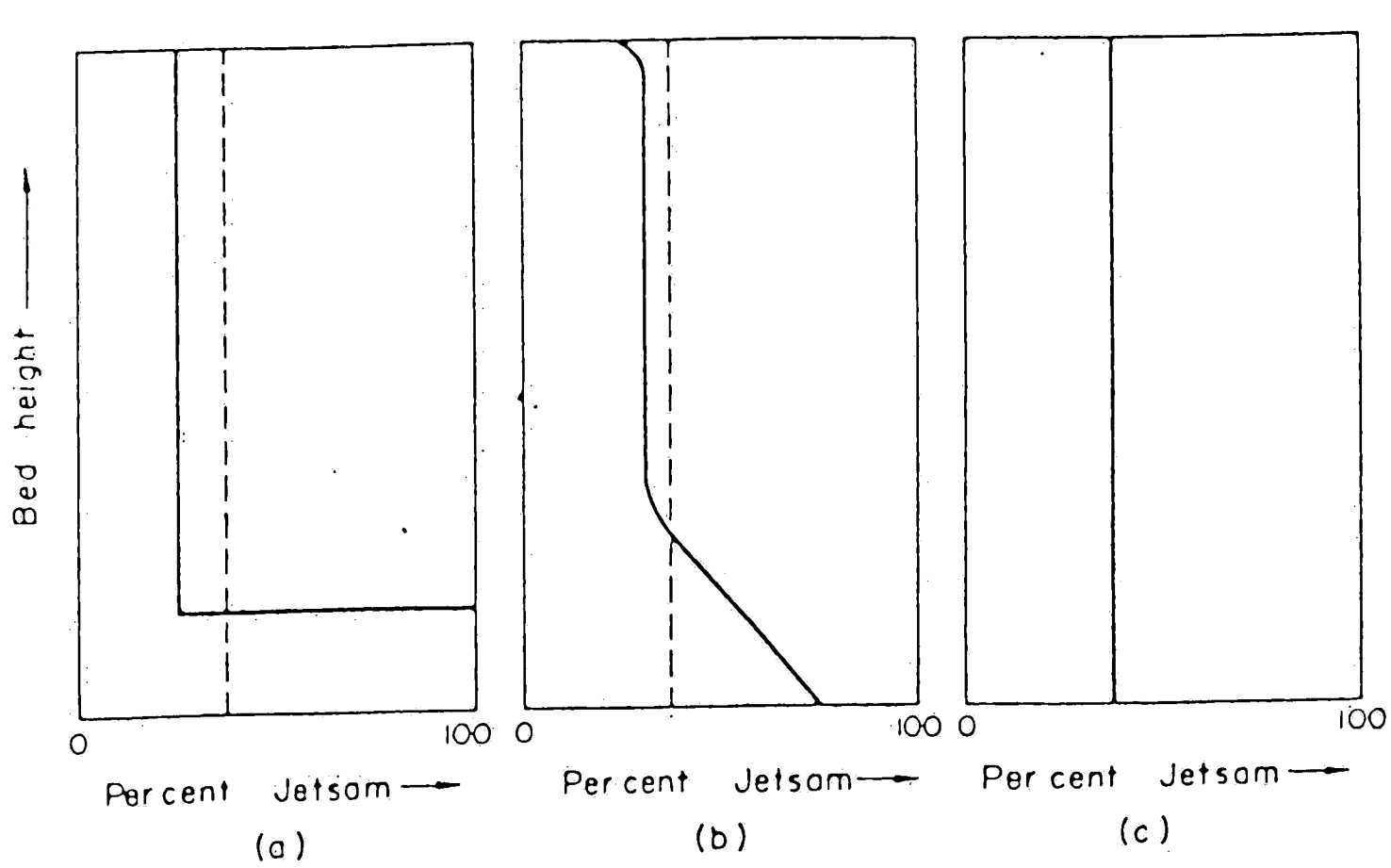

Fig. 3.1 Observed segregation patterns:

(a) strongly segregated

(b) intermediate case

(c) perfect mixing

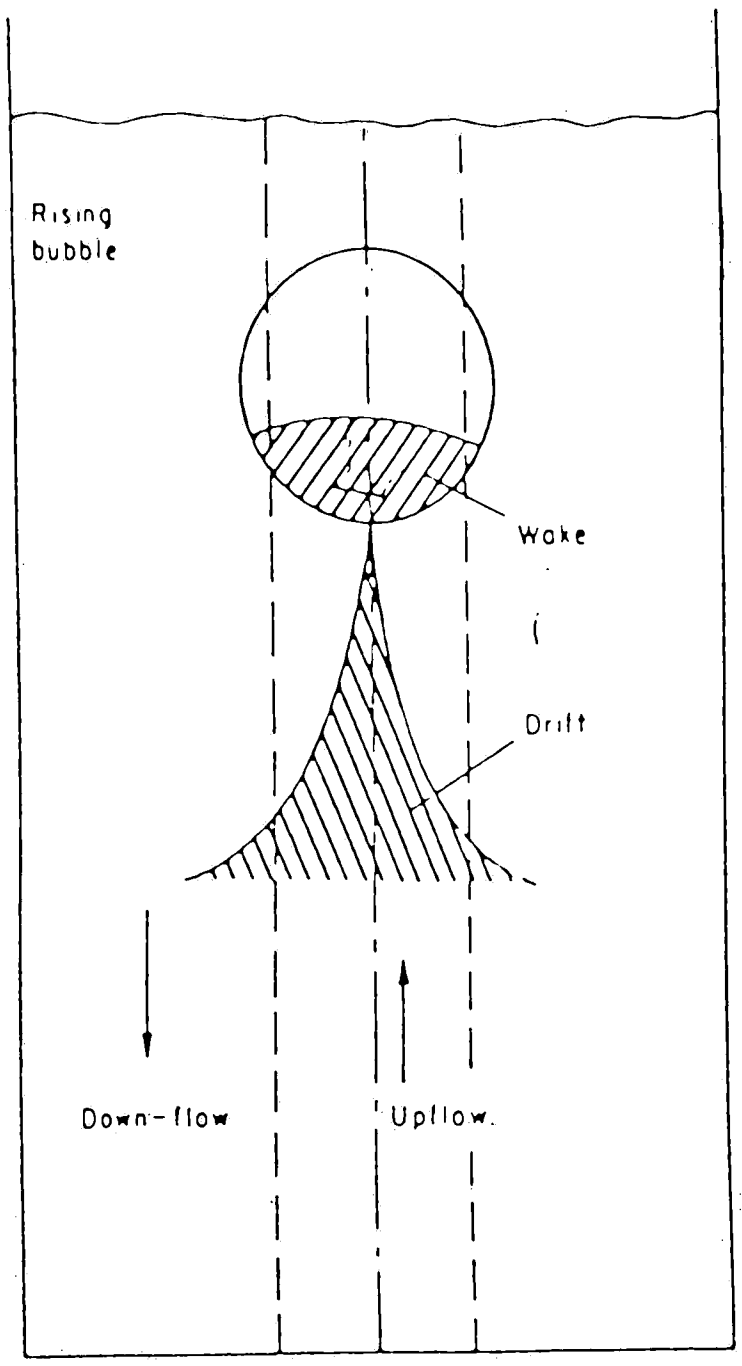

Fig. 3.2 Circulation caused by a bubble

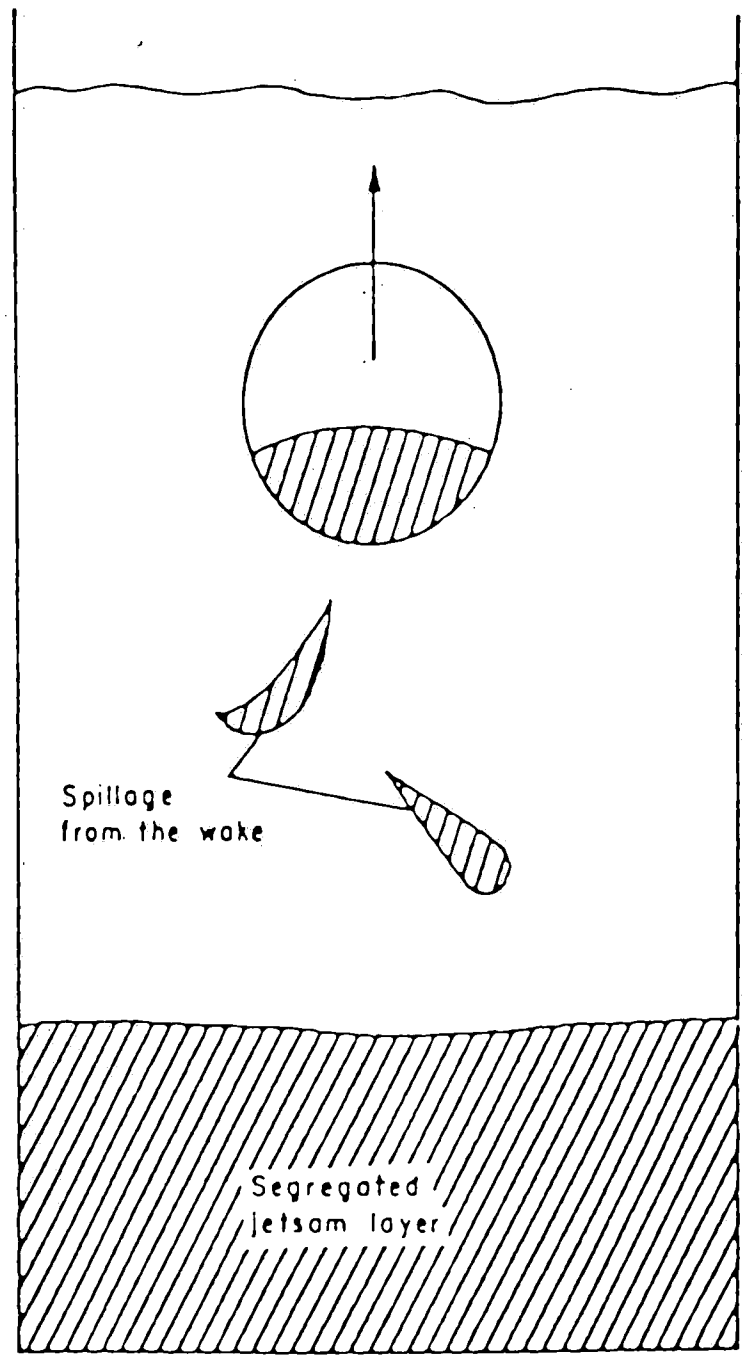

Fig. 3.3 Exchange due to wake shedding

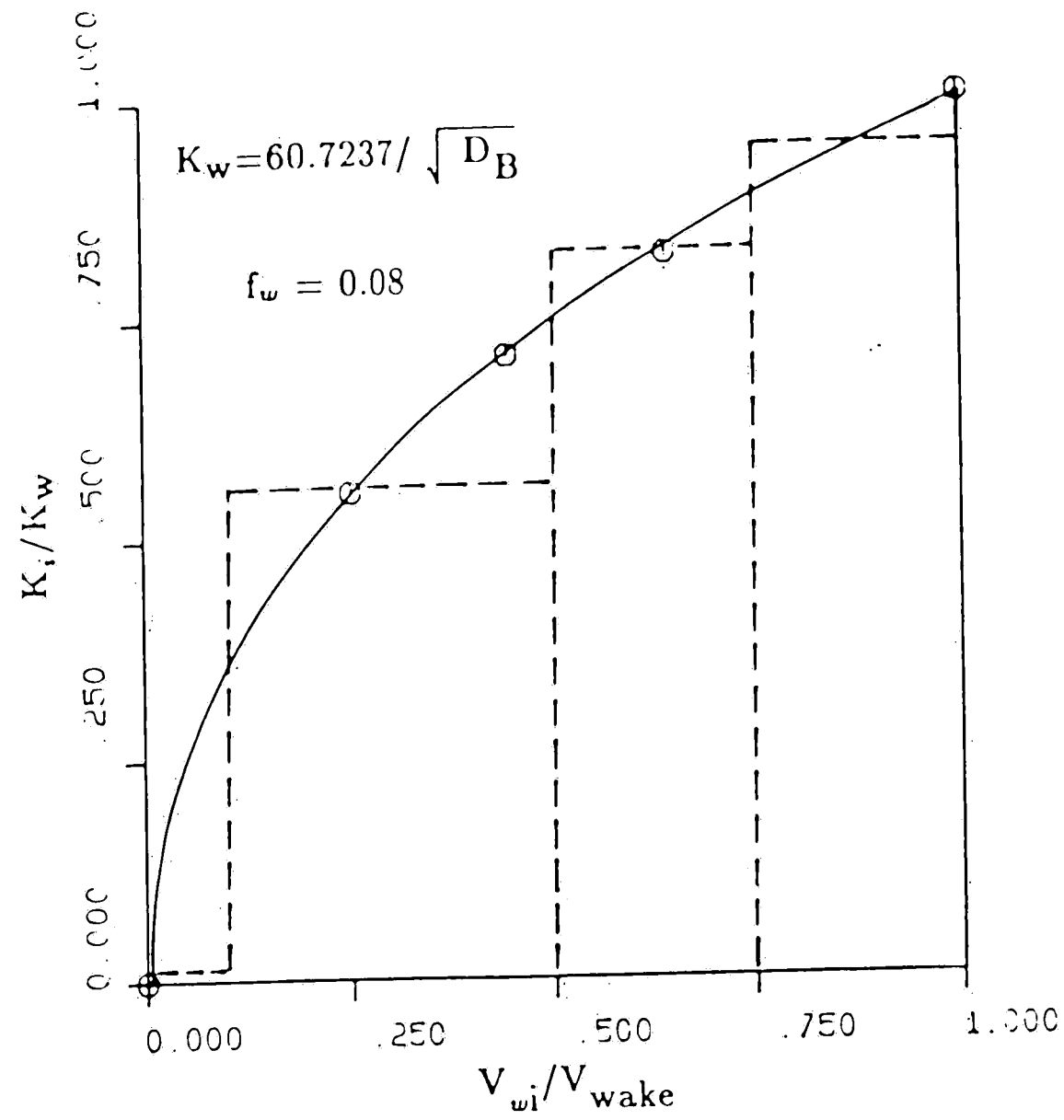

Fig. 3.3 The variation of exchange coefficient [9].

IV. SETTLING RATE EXPERIMENTS

Settling is one of the three mechanisms shown to control the behavior of particles in a fluidized bed.The others are circulation and wake exchange.The mixing in a segregating bed is due to each bubble gathering some jetsam in its wake and lifting and shedding some part of it en route [10].The denser and larger particles tend to fall faster due to a disturbance of the region behind the bubble wake when the bubbles rise in the bed.It is known that circulation and wake exchange occur whether or not physical variations exist in the bed material.Settling (or segregation) can exist only when there are physical differences in the bed material.

IV.1. Theoretical Calculations Related to Settling Experiments

The settlement rate parameter k, is defined as the net downward flux of settling particles relative to the rest of the bed.It is a measure of how particles with different physical properties relocate with respect to each other in a certain differential time. When a particle bed of two types of particles is considered, it is a measure of the rate of displacement of the so-called tracer particles with respect to the host particles. The settling rate parameter k is given by (3.19).An example of how the settling rate parameter can be calculated is shown below provided that the distribution of particles is known.

The settling rate parameter k is related to the settling coefficient factor Y_s by the equation (3.29).The settling coefficient factor is a non-dimensional measure of how particles relocate with respect to each other (whether they settle or they rise) on the average.A negative value of Y_s indicates a rising behavior whereas a positive value indicates a settling behavior.The bubble rising velocity u_b and the volumetric concentrations of bubbles and wakes δ can be calculated by (3.4) and (3.3) respectively.Volume fraction of the wake in the bubble f_w can be calculated by the correlation by (3.24).For the equivalent bubble diameter $d_{b,eq}$, Mori and Wen's model [4] given by equations (3.6) through (3.8) can be used.

When the above parameters are determined, the settling coefficient factor can be calculated.The data from different combinations of particles were used to establish a correlation for the settlement coefficient.Establishment of a correlation in general will help in predicting the behavior of many combinations of materials. Kozanoglu [9] proposes his correlation for combinations of spherical particles. Even though it is believed that his correlation is correct, the applicability is restricted.In this study however, an investigation on highly angular particles is needed since the behavior of coal and magnetite are of major concern.

The settlement coefficient was shown to be a function of the host particle size, tracer particle size, host particle density and tracer particle density by Kozanoglu [9].Even for highly angular particles, one might expect the settlement factor to be a function of the same parameters.

IV. 2. Experimental Set-up

The experiments were performed in a transparent plexiglass cylindrical vessel with 15.24 cm inside diameter.The distributor is a porous glass plate.In order to investigate a possible effect of angularity of the host material on the settling phenomenon, several experiments were made with the magnetite being the host, and glass, plastic and pyrite particles being the tracers.The size range of magnetite was typical of that used in coal cleaning tests.Several sizes of tracers were used throughout the experiments.

The tracers were uniformly located as a thin layer of particles at a distance of about 30.0 cm above the distributor plate in the host material.The total height of the bed was about 43.0 cm through the experiments.

Fluidization of the bed was done at room temperature and at atmospheric pressure.The main air supply is provided by central air compressors.Pressure is regulated by a high flow capacity flow regulator before it enters the rotameters.Air flow through the bed is controlled by various flowmeters with different capacities and several valves, including an on-off solenoid valve, which is controlled by a timer.Humidified air should be supplied to the magnetite in order to minimize eloctrastatic interaction between the particles.This was done before each experiment,

since each experiment typically took only a few seconds.

IV. 3. Experimental Procedure

In order to investigate the behavior of angular particles, settlement experiments with the following hosts and tracers were performed:

Table 4.1 Host and tracer materials used in settling experiments.

Hosts:	Magnetite # -120,+140
	Magnetite #-100,+120
	Magnetite #-70,+80
	Magnetite #-60,+70
Tracers:	Plastic #-60,+70
	Plastic #-50,+60
	Plastic #-40,+50
	Plastic #-25,+40
	Plastic #-20,+25
	Plastic #-16,+20
	Glass #-70,+80
	Glass #-60,+70
	Glass #-40,+45
	Glass #-20,+30
	Pyrite #-100,+120
	Pyrite #-60,+70
	Pyrite #-50,+60
	Pyrite #-20,+25
	Pyrite #-10,+16

The experiments began by loading the bed fully with the host material.The bed material was checked to ensure it was free of impurities and well demagnetized.Tracers were not included in this first step.Then, the superficial gas velocity was chosen to be greater than the minimum fluidization velocity and to provide smooth bubbling characteristics.It was necessary to avoid violent eruptions at the top of the bed.

After selecting an appropriate value for the superficial gas velocity and bubbling the bed for a few minutes, the material in the upper part of the bed (that is above 30.0 cm line) was removed.Then the tracers were placed in the bed at that height as a thin layer of uniformly distributed particles.A great deal of attention was required when placing the tracers evenly, because they were very limited in amount in most cases.Since magnetite is a magnetic material, a certain amount of another non-magnetic material was needed with the same material properties and also with the same size.This was needed to trace the movement of the magnetite.Pyrite was selected as a tracer for the magnetite since it has a specific gravity of about 5, and has almost the same kind of angularity.The pyrite was added on top of the tracer particles.After loading the upper part of the bed with magnetite, the experiments were conducted.Air was supplied to the bed through a rotameter and a solenoid on-off valve for a short time period.The valve opening time was adjusted by a timer.Throughout the experiments, the valve opening time was 2.6 seconds for a single pulse of air and 5.4 seconds for multiple pulses of air.The duration of the air supply contributes to the desired distribution the tracers.The desired distribution should be close to a so-called "*normal distribution*", with the highest tracer concentration around the initial tracer location and decreasing concentration towards the top and bottom of the bed.Accumulation of tracers at the top of the bed should be avoided since a normal probable distribution is expected.However, the net fluidization time was shown to be different than the valve opening time.Fig. 4.1 shows the time lags and the relation between the valve opening and the net fluidization times.

At the time of the experiment, the float level of the flowmeter drops due to back pressure.That must be considered in flow measurements and in the calculation of the net flow velocity.

After completion of the experiment, successive layers of particles were removed by means of a suction nozzle.Magnetic and non-magnetic materials in each layer were separated by the magnetic separator.Particles removed were either counted or weighed.A careful examination of the distribution of tracer particles in some cases may reveal an accumulation of the lightest particles at the very top layers of the bed.Those are generally the plastic particles.In some cases, they might be even glass particles.Results such as these are considered to be unreliable when an accumulation occurs at the free surface.In other words, the distrubution is expected to be close to a *normal distrubution*.In order to avoid accumulation at the top, either the fluidization time or the superficial gas velocity must be reduced or the depth of magnetite on top of the tracers must be increased.

IV.4. Net Fluidization Time

It was previously shown that the valve opening time is not equal to the *net fluidization time*, depending on the time lags of the fluidization.The net fluidization times are usually lower than the valve opening times.The data showed that there were delays between both the opening of the solenoid valve and the appearance of the first bubble at the location of the tracers, and between the closing of the valve and the presence of the last bubble at the tracer location. High speed video recordings were used to determine the fluidization characteristics in the bed.For different valve opening times, superficial gas velocities, and bed heights, the net fluidization must be determined independently.For this purpose, high speed video cameras and oscilloscopes were used.The experimental procedure to determine the net fluidization time was the following:

After the solenoid valve was opened to supply air into the bed, the time of appearance of the first bubbles at a certain bed height was determined by means of high speed video recordings.There is a time lag between the opening of the valve and appearance of first bubbles in the bed.The duration of valve-opening was controlled by a timer.The valve opening time can be measured more accurately by an oscilloscope, since the opening time is a few seconds.After the valve is closed, bubbling can be

observed to continue for a short time.That time lag was also determined by the high speed video recordings.With all the information on the bubbling characteristics in the bed , the net fluidization time can be calculated.Referring to Fig. 4.1, the net fluidization time t_f can be shown by the arithmetic relation below.

$$t_f = t_3 - t_o + t_2 \qquad (4.1)$$

where, t_3: solenoid valve opening time

t_o: time for the first bubble to reach tracer location

t_2: bubbling time after closing of the solenoid valve

IV.5. Results of Settling Rate Experiments

The results of the settling experiments are tabulated in terms of average settlement coefficients in Table 4.2.The results of repeated experiments are given in Table 4.3.Those values of settlement coefficient factor resulted in a correlation as given below.The results showed that settling coefficient Y_s can be expressed as a function of density ratio ρ_r and size ratio d_r, where ρ_r is the ratio $(\rho_l - \rho_h)/\rho_h$ and d_r is the ratio $(d_l - d_h)/d_h$.However, the range of size ratio d_r is expected to be from 0.0 to 0.80 for the conditions of operation and as shown in Fig.4.1, the relation between Y_s and ρ_r is changing proportionately for each size ratio d_r.Then an average value of 0.30 for d_r was used in the correlation (4.2).Results from the settling experiments also showed that the correlation by Kozanoglu [9] for spherical particles cannot be used for angular particles.The predicted correlation for angular particles is the following:

$$Y_S = 0.058 + 0.147\rho_r \qquad (4.2)$$

where, $\rho_r = (\rho_l - \rho_h)/\rho_h$.

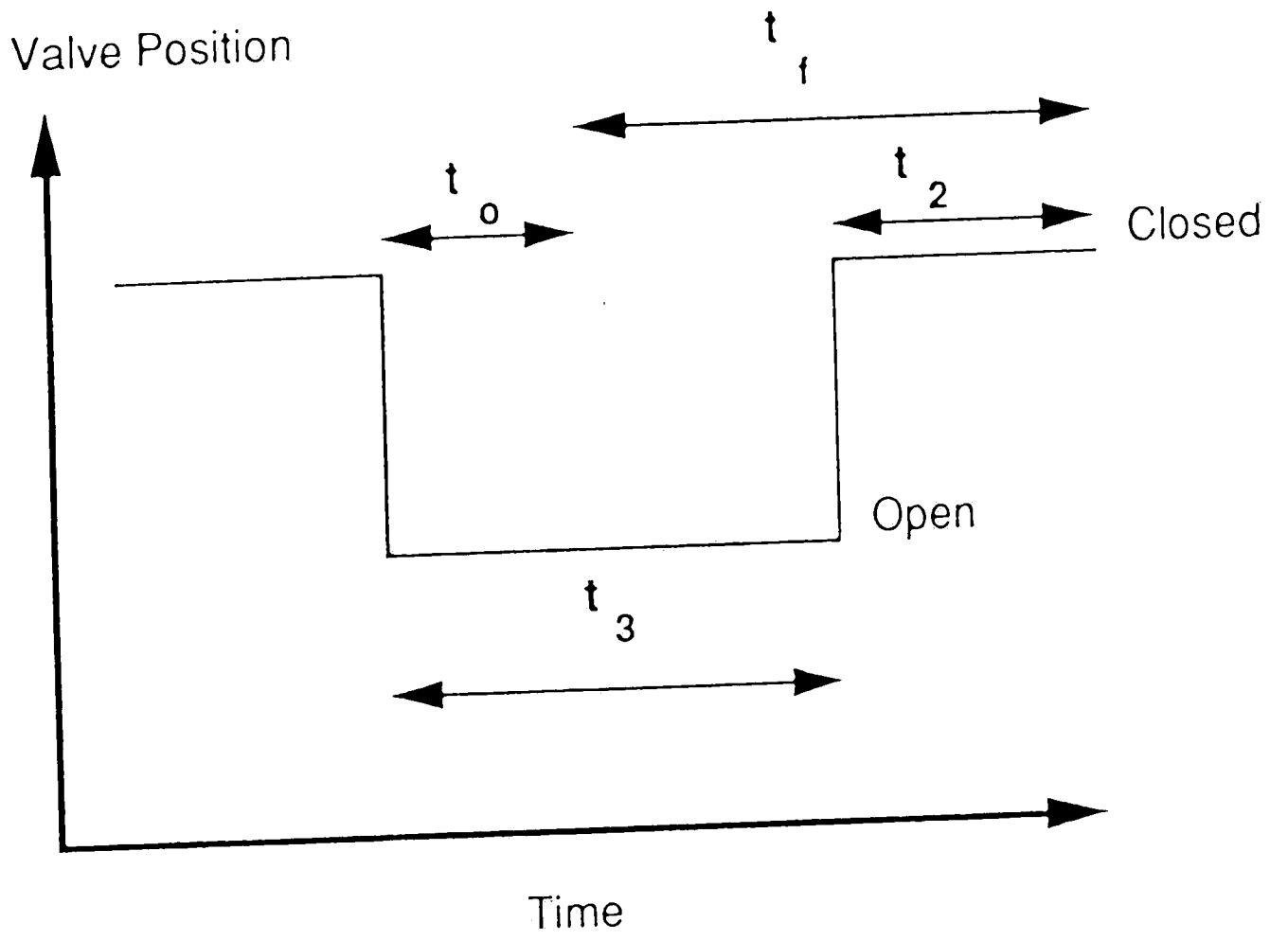

Fig. 4.1 The valve position and the bed response times

Table 4.2 Settling coefficients from experiments; average values.

Exp. #	Host Material			Tracer Particles			$(d_t-d_h)/d_h$	$(\rho_t-\rho_h)/\rho_h$	Y_s
	Type	d_p [μ]	ρ_p $[g/cm]^3$	Type	d_p [μ]	ρ_p $[g/cm]^3$			
1	Plastic	1015	1.05	Plastic	363	1.05	-0.643	0.0	-0.0100
2	"	"	"	"	568	"	-0.041	"	-0.0044
3	"	"	"	"	780	"	-0.232	"	-0.0022
4	"	"	"	"	1015	"	0.0	"	0.0000
5	"	"	"	Glass	725	2.25	-0.286	1.143	0.0530
6	"	"	"	Pyrite	780	5.00	-0.232	3.762	0.1120
7	"	"	"	"	1015	"	0.0	"	0.1190
8	"	"	"	"	1415	"	0.394	"	0.1370
9	"	"	"	Glass. nd.	1015	0.3	0.0	-0.714	-0.0360
10	Magnetite	196	5.00	Plastic	1015	1.05	4.179	-0.790	0.0076

Exp. #	Host Material			Tracer Particles			$(d_t-d_h)/d_h$	$(\rho_t-\rho_h)/\rho_h$	Y_s
	Type	d_p [μ]	ρ_p $[g/cm]^3$	Type	d_p [μ]	ρ_p $[g/cm]^3$			
11-13	"	"	"	"	231	"	0.179	"	-0.0540
14-15	"	"	"	"	273	"	0.393	"	-0.0670
16	"	"	"	Glass	725	2.25	2.699	-0.550	0.0301
17	"	"	"	Pyrite	1415	5.00	6.219	0.0	0.0860
18-20	"	"	"	"	273	"	0.393	"	0.0800
27-29	Magnetite	116	5.00	Plastic	568	1.05	3.913	-0.790	-0.0400
22-24	"	"	"	"	780	"	5.753	"	-0.0240
30	"	"	"	"	1015	"	7.788	"	0.0092
26-29	"	"	"	Glass	231	2.25	1.000	-0.550	0.0100
21,25	"	"	"	"	390	"	2.377	"	0.0180
31	"	"	"	"	725	"	5.277	"	0.0252
32	"	"	"	Pyrite	116	5.00	0.0	0.0	0.0
21-23	"	"	"	"	231	"	1.000	"	0.0500

Exp. #	Host Material			Tracer Particles			$(d_t-d_h)/d_h$	$(\rho_t-\rho_h)/\rho_h$	Y_s
	Type	d_p [μ]	ρ_p $[g/cm]^3$	Type	d_p [μ]	ρ_p $[g/cm]^3$			
27-29	"	"	"	"	780	"	5.753	"	0.0840
33	"	"	"	"	1415	"	11.251	"	0.0952
34-35	"	231	"	"	273	"	0.182	"	-0.0520

Table 4.3 Repeated settlement experiments.

	Y_s, Settling Coefficients			
	Host	**Tracers**		
	Magnetite	Pyrite	Glass	Plastic
	#-120,+140	#-60,+70	#-40,+45	#-20,+25
Particle dia., d_p [μm]	116	231	390	780
Experiment no.				
21		0.054	0.015	
22		0.045		-0.017
23		0.051		-0.029
24				-0.027
25			0.020	
Average		0.050	0.018	-0.024

	Host	**Tracers**		
	Magnetite	Pyrite	Glass	Plastic
	#-120,+140	#-20,+25	#-60,+70	#-25,+40
Particle dia., d_p [μm]	116	780	231	570
Experiment no.				
26			0.013	
27		0.083	0.009	-0.039
28		0.092	0.006	-0.047
29		0.077	0.011	-0.034
Average		0.084	0.010	-0.040

	Y_s, Settling Coefficients			
	Host		**Tracers**	
	Magnetite	Pyrite	Glass	Plastic
	#-70,+80	#-50,+60		
Particle dia., d_p [μm]	196	273		
Experiment no.				
18		0.126		
19		0.041		
20		0.074		
Average		0.080		

	Host		**Tracers**	
	Magnetite	Pyrite	Glass	Plastic
	#-70,+80			#-60,+70
Particle dia., d_p [μm]	196			230
Experiment no.				
11				-0.048
12				-0.071
13				-0.044
Average				-0.054

	Y_s, Settling Coefficients			
	Host			**Tracers**
	Magnetite	Pyrite	Glass	Plastic
	#-70,+80			#-50,+60
Particle dia., d_p [μm]	196			273
Experiment no.				
14				-0.068
15				-0.066
Average				-0.067

	Host		**Tracers**	
	Magnetite	Pyrite	Glass	Plastic
	#-60,+70			#-50,+60
Particle dia., d_p [μm]	230			273
Experiment no.				
34				-0.053
35				-0.050
Average				-0.052

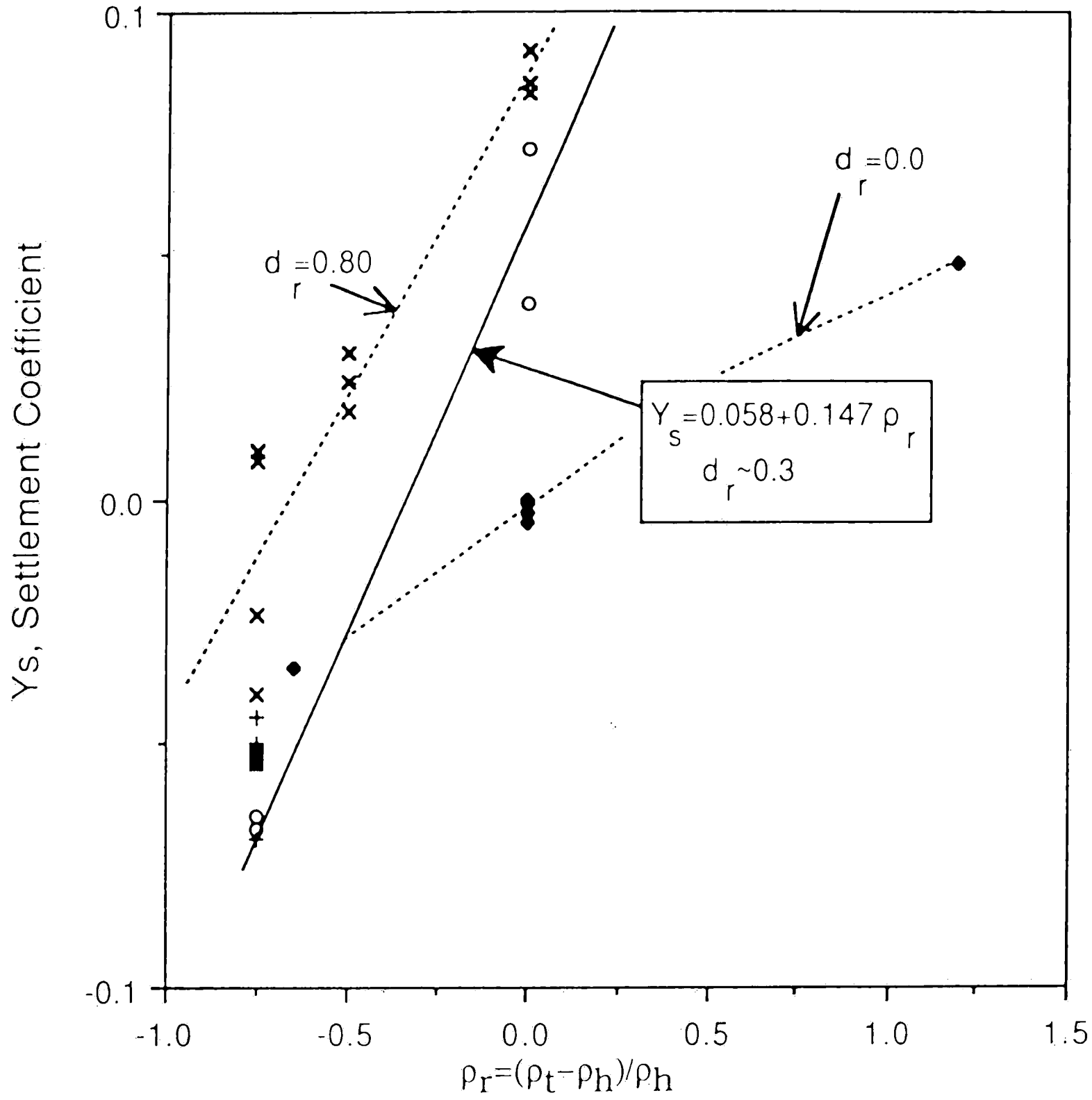

Fig. 4.2 Prediction of a correlation after the settling experiments.

V. PERFORMANCE PARAMETERS

V.I. Coal Cleaning Experiments

Coal cleaning tests were performed with the same batch bed which was mentioned in Section IV.2.The batch bed is cylindrical transparent plexiglass with an inside diameter of 6 inches (15.24 cm).The magnetite is loaded in first in the amount desired.Then the coal is placed on top of the magnetite.The fluidization procedure is the same as the settling experiments described in Section IV.2 except that the duration of fluidization is longer.The superficial gas velocities range from 1.6 to 3.2 times the minimum fluidization velocity of the magnetite.Superficial gas velocity is adjusted and the duration of fluidization is set by a stop-watch. In each experiment 6 layers were collected by the suction nozzle.Then each layer was weighed separately. After noting the total weight of each layer, the coal was separated from magnetite by the magnetic separator.Then the coal from each layer was measured.The magnetite used throughout the experiments was angular magnetite.

V.2. Generalized Distribution Curve

The generalized distribution curve is a plot of the percentage of each specific gravity fraction of the feed that is recovered in the clean coal product as the ordinate, against the median of the specific gravity fraction.A typical distribution curve is shown in Fig.5.1.The specific gravity of separation which is shown by SGS in this study is the value of the specific gravity that corresponds to a weight percent of 50%.The specific gravity of separation indicates the material which is equally divided between the clean and the refuse portions of the coal.

A theoretically perfect separation is obtained if the distribution curve consists of a simple vertical line.In other words, performance is better when the slope of the distribution curve gets steeper.A measure of the sharpness of a distribution curve is the error area.The error area approaches zero as the actual distribution curve approaches

the theoretical.Another measure of performance is obtained by calculating the probable error.That is equal to one half the difference between specific gravity values at 25 percent and 75 percent distribution to clean coal. and is shown by E_p. The generalized performance parameter is shown by GE_p and is found by dividing the probable error E_p by the specific gravity of separation SGS.

V.3.Calculation of Performance Parameters from Experiments

V.3.A. Calculation of Sulfur and Ash Removal, Energy Recovery

Calculation of sulfur and ash removals together with energy recovery reveals the cleaning performance.The experimental results of sulfur and ash percentage and heating values for individual layers are needed with the coal content in each layer.The sample calculation is given below to illustrate the interpretation of the experimental results.

Sample Calculation:

		A	B	C	D
	Layer	**Coal [g]**	**Weight % Sulfur Content of Coal**	**Weight % Ash Content of Coal**	**Heating Value [Btu/lb]**
Top	1	38.94	2.02	18.05	12563
	2	53.84	2.78	28.94	10752
	3	74.37	3.20	31.06	10290
	4	54.78	3.25	33.61	9788
	5	24.89	6.75	49.87	6621
Bottom	6	2.71	16.15	69.87	3149

In order to find the total sulfur and ash in each layer, the coal and sulfur and coal and ash are multiplied (A*B and A*C).The heating value must be multiplied by the coal content in each layer to find the heating value in each layer (A*D).The results are given as follows:

Layer	Sulfur [g]	Ash [g]	Heating Value [Btu]
1	0.79	7.03	1078
2	1.50	15.58	1275
3	2.38	23.10	1686
4	1.78	18.41	1181
5	1.68	12.41	363
6	0.44	1.89	19
Total	8.57	78.42	5602

Then the amounts of sulfur and ash removal are calculated as follows:

$(\text{Sulfur removal, \%})_{\text{i'th layer}}$= (Total sulfur in bed-Total of sulfur from 1 to i'th layer)/Total sulfur in bed

$(\text{Ash removal, \%})_{\text{i'th layer}}$= (Total ash in bed -Total of ash from 1 to i'th layer)/Total ash in bed

$(\text{Energy Recovery, \%})_{\text{i'th layer}}$= (Total of Energy from 1 to i'th layer)/Total Energy in bed

An example for the 2nd layer:

Sulfur removal=[8.57-(0.79+1.50)]/8.57=73.3 %

Ash removal=[78.42-(7.03+15.58)]/78.42=71.2 %

Energy recovery=(1078+1275)/5602=42.0 %

Then the results for the other layers are obtained to be as follows:

Layer	Sulfur Rem.,%	Ash Rem.,%	Energy Recovery,%
1	90.8	91.0	19.2
2	73.3	71.2	42.0
3	45.5	41.7	72.1
4	24.7	18.2	93.2
5	5.1	2.4	99.7
6	0.0	0.0	100.0

V.3.B. Calculation of Generalized Performance Parameter (GE_p)

The distribution of eight components of coal in each layer are obtained by the washability analysis and tabulated along with the coal mass in each layer.The following example is for coal #-30,+50 Rushton.

Coal Component	Weight % in Layers					
specific grav.	1	2	3	4	5	
<1.3	55	40	22	10	5	
1.3-1.4	25	25	16	9	4	
1.4-1.6	11	12.7	10	7	3.5	
1.6-1.8	5	8	9	7	4	
1.8-2.0	2	4.6	8	8	5	
2.0-2.45	1.6	5	13	17	14	
2.45-2.9	1.0	4.6	18	34	40	
2.9>	0	0.7	3	9	24	
Total mass [g]	472	365	531	350	298	(total=2016 g)

Assuming layers 1 to 3 are *products* and 4 to 5 are *refuse*, the percentage of products and refuse coal in the total coal are calculated for each coal component as follows:

Coal component Specific gravity	Product	Refuse
<1.3	(472*0.55+365*0.4 +531*0.22)/2016=0.26	(350*0.1+298*0.05)/2016 =0.025
1.3-1.4	(472*0.25+365*0.25 +531*0.16)/2016=0.146	(350*0.09+298*0.04)/2016 =0.022
1.4-1.6	(472*0.11+365*0.127 +531*0.10)/2016=0.075	(350*0.07+298*0.035)/2016 =0.0174
1.6-1.8	(472*0.05+365*0.08 +531*0.09)/2016=0.05	(350*0.07+298*0.04)/2016 =0.018
1.8-2.0	(472*0.02+365*0.046 +531*0.08)/2016=0.034	(350*0.08+298*0.05)/2016 =0.021
2.0-2.45	(472*0.016+365*0.05 +531*0.13)/2016=0.047	(350*0.17+298*0.14)/2016 =0.05
2.45-2.9	(472*0.01+365*0.046 +531*0.18)/2016=0.059	(350*0.34+298*0.40)/2016 =0.118
>2.9	(472*0.0+365*0.007 +531*0.03)/2016=0.0094	(350*0.09+298*0.24)/2016 =0.051

The *feed* percent of coal is the sum of the *product* and the *refuse* parts for each component, and is given by the following table,

Coal Component specific grav.	Product	Refuse	Feed	Product/Feed
<1.3	0.26	0.025	0.295	0.912
1.3-1.4	0.146	0.022	0.168	0.869
1.4-1.6	0.02	0.0174	0.0924	0.812
1.6-1.8	0.05	0.018	0.068	0.735
1.8-2.0	0.034	0.021	0.055	0.618
2.0-2.45	0.047	0.05	0.097	0.484
2.45-2.9	0.059	0.118	0.177	0.333
2.9>	0.0094	0.051	0.0604	0.1556

Therefore, the specific gravity of separation, SGS=2.1 (evaluated at 50% product/feed).

The probable error E_p=(3.0-1.8)/2=0.60,

and the generalized performance parameter,

GE_p=(3.0-1.8)/2*2.1=0.286

(Specific gravity at 25% product/f eed =1.8, and specific gravity at 75% product/feed=3.0)

V.4. Computer Programs

Two computer programs were written for manipulating the experimental and theoretical results from the extensively used computer code.Both programs are in Fortran and run on the CDC Cyber 850 mainframe computer.

The first program was used to calculate sulfur and ash removals, and energy recoveries by using the data from the analysis of the experiments and is given in Appendix C.1.The data of local coal mass (in grams), weight percentages of sulfur and ash, and heating values in (Btu/lb) of each layer are taken from the results of coal

analysis of experiments.They must be entered into the program.The output of the program is written in an output file called "EXOUT1".The output list includes local coal mass in grams, local sulfur and ash percentages, sulfur and ash removals, and energy recoveries for the indicated layers.The technique used for calculating sulfur and ash removals and energy recoveries is given in Section V.3.A.

The second program is used to manipulate the theoretical results from the computer runs and is given in Appendix C.2.It is used to calculate sulfur and ash removals, and energy recoveries from the volumetric concentrations of coal components in the emulsion phase.For this purpose, the output file from the main batch program must be edited in order to be read.Inputs needed for the program include specific gravity of each coal component together with sulfur, ash and energy content of each coal component as given by the washability tests for that specific coal.Typical washability test results are shown in Appendix D for #-50,+80 Rushton coal.The data are read from a read file called "WRK8" and written in a file called "cout".The technique of calculation of sulfur and ash removals, and energy recoveries from the coal concentrations in the emulsion phase is the same as used in the main batch program and explained by [18].

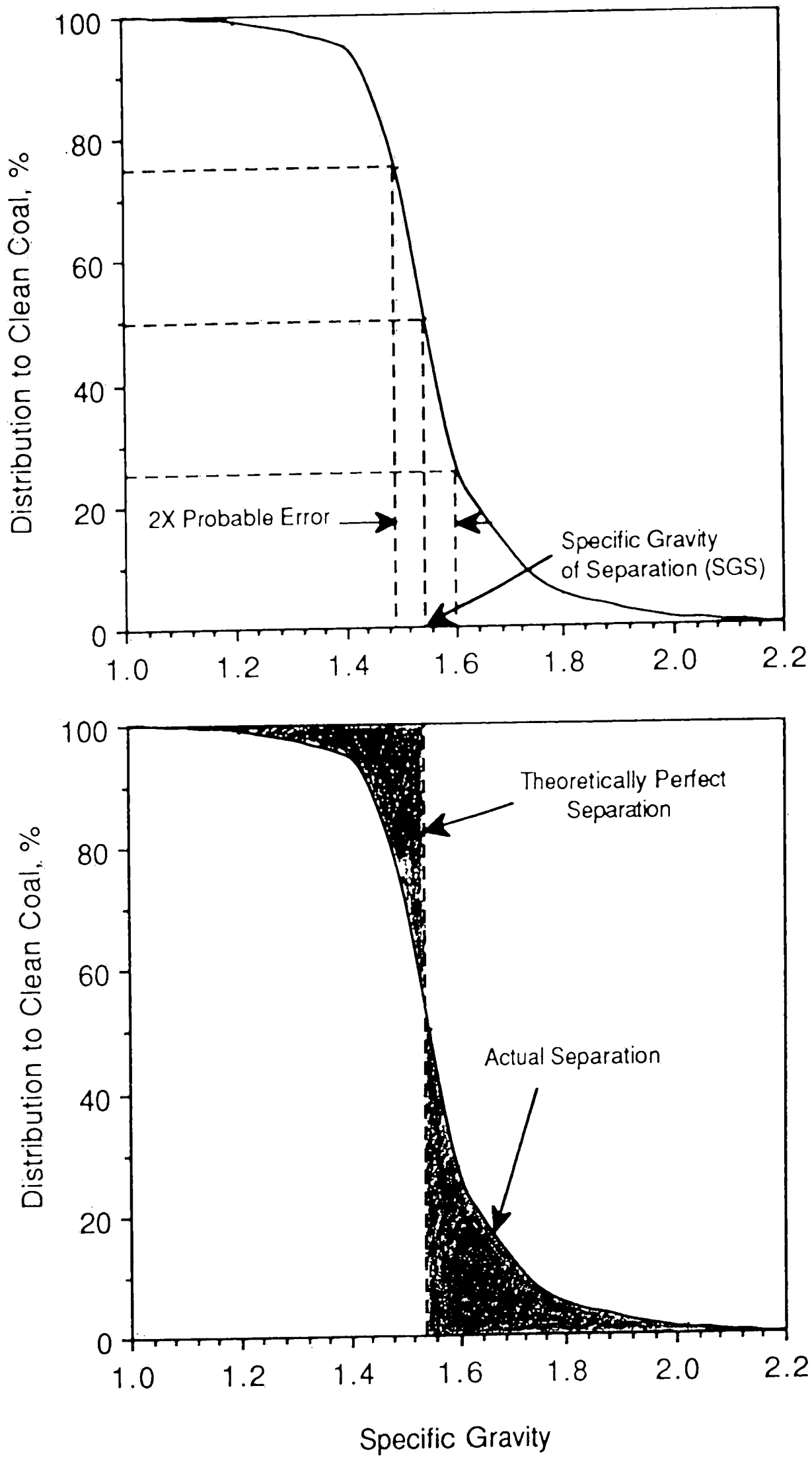

Fig. 5.1 Generalized distribution curve; the probable error and error area approach

VI. RESULTS AND DISCUSSION

The results presented in this section are both experimental and theoretical.The experimental results are with #-50,+80 Rushton coal and #-100.+120 angular magnetite only.Theoretical results are presented for #-50,+80 Rushton coal and #-100.+120 angular magnetite; and #-140,+325 Rushton coal and #-140,-200 and #-200,+325 angular magnetite.The magnetite type which the theoretical results are based on is angular magnetite only.

The experiments with #-50,+80 Rushton coal and #-100.+120 angular magnetite for various operating conditions are listed in Table 6.1.The variations in the bed depths, concentrations of coal which is indicated by the parameter "*mm*", the ratio of the superficial gas velocity to the minimum fluidization velocity and the fluidization periods are given.The parameter "*mm*" indicates the number of layers occupied by magnetite at the bottom part of the bed out of 15 total layers.If the whole bed is considered to be divided into 15 layers, *mm=1* indicates the bottom of the bed .The bed depths of operation changed from 3.0 to 12.0 cm; the mass of coal to mass of magnetite ratio changed from 0.10 to 5.7 (corresponding to mm=12 and mm=1); the ratio of superficial gas velocity to minimum fluidization velocity changed from 1.6 to 3.2; and the duration of fluidization changed from 30 to 600 seconds.

The performance for the experiments with Rushton coal #-50,+80 and magnetite #-100,+120 is presented by Tables 6.2 through 6.4.Sulfur and ash removals at 85% energy recovery are listed for each gas velocity ratio of u_o/u_{mfm}.The experimental conditions varies in coal to magnetite weight percent in the range between 0.7 and 5.7. The bed depths and processing times are 3.0 cm and 30 seconds respectively.

The performance of a coal cleaning process can be measured by various parameters for different operational conditions.Those are sulfur removal, ash removal, energy recovery, generalized performance parameter, probable error, and specific gravity of separation (generalized distribution curve).A higher sulfur and ash removal for a certain value of energy recovery indicates better performance.The fixed

point of reference for energy recovery throughout this study is 85%.The same is true for ash removal.As mentioned earlier in this study, a steeper generalized distribution curve indicates better cleaning performance.In another sense, lower values of generalized performance parameter and probable error reflect better performance.A lower specific gravity of separation is also indicative of a better cleaning.

The theoretical results are from the computer code written by Kozanoglu [18] which was then modified to handle nine components and a certain number of equations which poses restriction on the refinement of thickness of layers.The eight of the nine components are the coal components which have different physical properties such as particle densities, sulfur and ash contents, and heating values.The computer code uses a standard differential solver subroutine to solve a set of fifth order differential equations.The computer code by [18] consists of three subroutines which are referred to as the *Initial*, *Derivative*, and *Write* subroutines.A batch program is used to call the code, for running it in the batch mode.The code computes coal, sulfur and ash profiles together with sulfur and ash removals, energy recoveries, and distribution to clean coal for each specific gravity of coal component.

Fig. 6.1 through Fig.6.6 show the results from the computer runs and experiments no. 2-8-91-16 and no. 3-27-91-17 for mm=6 (mass of coal/ mass of magnetite=0.7), superficial gas velocity/minimum fluidization velocity=2.5, bed depth of 3.0 cm and 30 seconds of processing time for Rushton coal #-50,+80 and magnetite #-100,+120.These results are of typical of those obtained in this study.Fig.6.1 shows the local coal concentration profile.The local coal concentration is the ratio of the mass of coal to the total mass in each layer.Fig. 6.2 and Fig. 6.3 show the local sulfur and ash concentrations.The local concentrations are plotted against non-dimensionalized level of each layer "z/L", where $z/L=0$ indicates the top and $z/L=1$ indicates the bottom of the bed. They are calculated as the mass percent in coal for each layer.Sulfur removal and ash removal curves are plotted against energy recovery in Fig. 6.4 and Fig. 6.5.Generalized performance curve is given by Fig.6.6.The performance of the process is relatively high as observed by the sharp slope.The specific gravity of separation is

approximately 1.95.The generalized performance parameter was calculated to be 0.13.

(i) The effect of bed depth

The bed depth appeared to be the most important parameter in the coal cleaning process.In this study, the bed depth ranged from 3.0 to 12.0 cm, and the performance consistently improved as the bed depth became shallower.The theoretical results also indicate a dramatic improvement of performance with lower bed depth.This effect can be seen in Fig. 6.7. The effect of bed depth can be seen for a wide range of superficial gas velocities in Fig. 6.8 through Fig. 6.11.It can be observed that the performance is steady and processing time is short to reach a satisfactory state of performance for the bed depth of 3.0 cm (Fig. 6.8).Experimental and theoretical comparison of results given by Table 6.5 shows poorer performance for higher bed depths. Theoretical results under the best estimated superficial velocities is given by Table 6.6 through Table 6.8.Comparison of the data also confirms that operating the bed can be satisfyingly efficient alone with a low bed depth in a certain range of operating velocities.

(ii) The effect of coal concentration (mass of coal/mass of magnetite)

The ratio of mass of coal to mass of magnetite also came out to be a very important factor in the process of segregation of coal.The higher mass of coal to mass of magnetite ratio (from 0.7 to 5.7) results in significant improvement in coal cleaning performance in deeper beds.This effect can be seen in Fig.6.12 through Fig.6.16.Fig.6.12 through Fig.6.14 shows the generalized performance parameter GE_p as a function of the bed depth for coal to magnetite mass ratios of 0.10 to 0.70 for the processing times of 30, 60 and 120 seconds.The difference in GE_p with respect to processing time seems to stay constant.The effect of coal concentration on sulfur removal and specific gravity of separation was observed to be more significant for deeper beds as seen in Fig.6.15 and Fig. 6.16.The experiments with #-50,+80 coal shows that the effect of concentration vanishes for the shallow beds under a certain range of superficial gas velocities as seen in Fig. 6.19 through Fig. 6.21, since sulfur removals of approximately 70 percent were achieved independent of the coal concentrations.

(iii) The effect of superficial gas velocity

Experiments and theoretical results revealed a significant effect of superficial gas velocity for obtaining improved performance.Throughout this study the operating velocities are expressed in terms of a ratio of superficial gas velocity to the minimum fluidization velocity of the magnetite u_o/u_{mfm}, magnetite as always being the host material.The operating velocities should be slightly higher than the minimum bubbling velocity.The ratio u_o/u_{mfm} for the best performance has been observed to be less than 3.0 and above 1.8 in general throughout this study.Theoretical results show that the best velocity ratio u_o/u_{mfm} is the same about 2.5 for the bed depths of 3.0 and 12.0 cm as seen in Figs. 6.17 and 6.18 respectively.The best operating velocity ranges from the experiments are shown in Fig. 6.19 through Fig.6.21 for coal to magnetite ratio based on mass.It is observed that the best velocity ratio u_o/u_{mfm} is about 2.2 for coal to magnetite mass ratio of 0.7 as seen in Fig.6.19, and coal to magnetite mass ratio of 1.6 also, as seen in Fig.6.20.There appears to be a shift to about 2.0 in the best velocity ratio of u_o/u_{mfm} for coal to magnetite mass ratio of 5.7 as seen in Fig.6.21.

(iv) The effect of processing time

Processing time is considered as the time of fluidization of the bed.The results show that the processing time has a significant effect on the cleaning performance.Theoretical results show that the time needed to reach steady state cleaning performance is longer for the deeper beds.This effect can also be seen in Fig. 6.8 through Fig. 6.11. However, the cleaning efficiencies obtained in processing times as short as 30 seconds can be quite satisfactory for the shallow beds.

(v) Selection of the host material (magnetite)

Throughout this study, highly angular magnetite has been used as the host material.The selection of the host material is considered to be based on the minimum fluidization velocities of the host material and the coal.The minimum fluidization

velocities of those have to be close in order to avoid a packed top or bottom part in the bed in the process of fluidization. However, the results show that the criterion of matching the minimum fluidization velocities of magnetite and coal may not give the best cleaning efficiciency.The host with a slightly higher minimum fluidization velocity was observed to result in an improved performance as seen in Fig.6.22 and in Fig.6.23.

(vi) An analysis of governing mechanisms

The analysis presented in this section provides an insight to which mechanisms may dominate the behavior of the fluidized bed of particles under different operational conditions.Such an analysis of dominating mechanisms from one condition to another could enable us to predict the most favorable operating conditions.

Kozanoglu [9] presents equation (6.1) in which the governing mechanisms of particle behavior are expressed separately.The first term on the right is the settlement term, whereas the second and the third terms are circulation and wake exchange terms respectively.

$$\frac{\partial C_E}{\partial t} = \frac{1}{1-\delta} 0.75 Y_s \frac{\partial\left[u_b \delta C_E (1-C_E)\right]}{\partial z} + \frac{1}{1-\delta} \frac{\partial(\delta f_w u_b C_E)}{\partial z} + \frac{K_1.\delta.f_w f_{s_1}(C_{w_1} - C_E)}{1-\delta} \qquad (6.1)$$

The parameters time t, and vertical distance z, can be non-dimensionalized as follows:

$$\hat{t} = \frac{t.u_b}{d_b} \qquad \hat{z} = \frac{z}{L}$$

Inserting the non-dimensional parameters into equation (6.1),

$$\frac{u_b}{d_b}\frac{\partial C_E}{\partial \hat{t}} = \frac{1}{1-\delta}0.75Y_s\frac{\partial\left[u_b\delta C_E(1-C_E)\right]}{L.\partial\hat{z}} + \frac{1}{1-\delta}\frac{\partial(\delta f_w u_b C_E)}{L.\partial\hat{z}} + \frac{K_1.\delta.f_w f_{s_1}(C_{w_1}-C_E)}{1-\delta} \tag{6.2}$$

where the fraction of the bubbles and wakes in the bed is given by,

$$\delta = \frac{u_o - u_{mf}}{u_b(1-f_w)} \tag{6.3}$$

the settlement term in equation (6.2) is,

$$\frac{d_b}{u_b(1-\delta)}0.75Y_s\frac{\partial\left[u_b\delta C_E(1-C_E)\right]}{L.\partial\hat{z}} \tag{6.4}$$

the circulation term is,

$$\frac{d_b}{u_b(1-\delta)}\frac{\partial(\delta f_w u_b C_E)}{L.\partial\hat{z}} \tag{6.5}$$

the wake exchange term is,

$$\frac{d_b.K_1.\delta.f_w f_{s_1}(C_{w_1}-C_E)}{u_b(1-\delta)} \tag{6.6}$$

Equation (6.2) can be evaluated at the following locations in the bed as follows:

the settlement term,

$$\left[\frac{d_b}{u_b(1-\delta)}0.75Y_s\right]_{L/2}.\frac{1}{L}\frac{1}{(1/2)}\left\{\left[u_b\delta C_E(1-C_E)\right]_{L/2}-\left[u_b\delta C_E(1-C_E)\right]_{Bottom}\right\} \tag{6.7}$$

the circulation term,

$$\left[\frac{d_b}{u_b(1-\delta)}\right]_{L/2}.\frac{1}{L}\frac{1}{(1/2)}\left\{\left[\delta f_w u_b C_E\right]_{L/2}-\left[\delta f_w u_b C_E\right]_{Bottom}\right\} \tag{6.8}$$

the wake exchange term,

$$\left[\frac{d_b.K_1.\delta.f_w f_{s_1}(C_{w_1}-C_E)}{u_b(1-\delta)}\right]_{L/2} \tag{6.9}$$

The following data are taken directly from the computer output for #-50,+80 Rushton coal, and #-100,+120 magnetite for the three characteristic beds with the indicated operating parameters:

(a) Case I

mm=6 (m_{coal}/m_{mag}= 0.70), L=12.0 cm, t=30 s

At the top:

d_b=1.241 cm

f_w=0.145

C_E=0.91223

δ=0.070

u_b=0.2481 m/s

<u>At the bottom:</u>

d_b=0.103 cm

f_w=0.036

C_E=0.01120 (C_E at the bottom can be taken as zero)

δ=0.180

u_b=0.0715 m/s

<u>At L/2:</u>

d_b=0.714 cm, u_b=0.1882 m/s, $K_w=60.7237/(d_b)^{1/2}$ =71.86 1/s

(assume K_1=0.85. K_w referring to Fig. 3.3)

f_w=0.097

fs_1=0.043 cm

δ=0.072

Cw_1=0.408

C_E=0.80716

Y_S=-0.0381

Then substituting the values into equations (6.7), (6.8), (6.9), the terms on the right are calculated to be as follows:

settlement term,

$$\frac{(0.714)*10^{-2}}{0.1882}\,\frac{0.75(-0.0381)}{(1-0.072)}\,\frac{\left[\dfrac{(0.072)(0.1882)(0.8072)(1-0.8072)}{0.12}-0\right]}{1/2}$$

$=-4.11*10^{-5}$

circulation term,

$$\frac{(0.714)*10^{-2}}{0.1882}\frac{1}{(1-0.072)}\frac{\left[\frac{(0.072)(0.1882)(0.097)(0.8072)}{0.12}-0\right]}{1/2}$$

$=7.23*10^{-4}$

wake exchange term,

$$\frac{(0.714)*10^{-2}.(0.85)(71.86)(0.072)(0.097)(0.043)(0.408-0.8072)}{0.1882(1-0.072)}$$

$=-2.99*10^{-4}$

Then,

$=(-4.11*10^{-5})+(7.23*10^{-4})+(-2.99*10^{-4})$

= (Settlement) + (Circulation) + (Exchange)

(b) Case II

mm=6 (m_{coal}/m_{mag}= 0.70), L=3.0 cm, t=30 s

At the top:

d_b=0.353 cm

f_w=0.059

C_E=0.95381

δ=0.118

u_b=0.1323cm/s

At the bottom:

d_b=0.029 cm

f_w=0.024

C_E=0.02800 (C_E at the bottom can be taken as zero)

δ=0.289

u_b=0.0379 cm/s

<u>At L/2:</u>

d_b=0.197 cm, u_b=0.09884 m/s, K_w=60.7237/$(d_b)^{1/2}$ =136.81 1/s

(assume K_1=0.85. K_w referring to Fig. 3.3)

f_w=0.045

fs_1=0.056cm

δ=0.136

Cw_1=0.157

C_E=0.79370

Y_s=-0.0381

settlement term,

$$\frac{(0.197)*10^{-2}}{0.0988}\,\frac{0.75(-0.0381)}{(1-0.136)}\,\frac{\left[\dfrac{(0.136)(0.0988)(0.7937)(1-0.7937)}{0.03}-0\right]}{1/2}$$

$=-9.69*10^{-5}$

circulation term,

$$\frac{(0.197)*10^{-2}}{0.0988}\,\frac{1}{(1-0.136)}\,\frac{\left[\dfrac{(0.136)(0.0988)(0.045)(0.7937)}{0.03}-0\right]}{1/2}$$

$=7.38*10^{-4}$

wake exchange term,

$$\frac{(0.197)*10^{-2}.(0.85)(136.81)(0.136)(0.045)(0.056)(0.157-0.7937)}{0.0988(1-0.136)}$$

$=-4.07*10^{-4}$

Then,

$=(-9.69*10^{-5})+(7.38*10^{-4})+(-4.07*10^{-4})$

= (Settlement) + (Circulation) + (Exchange)

Then from (a) to (b), the variation in the settlement, circulation and exchange terms can be written as follows:

The increase in settlement term,

$=[(-9.69*10^{-5})-(-4.11*10^{-5})]/(-4.11*10^{-5})=$ **136 %**

The increase in circulation term,

$=[(7.38*10^{-4})-(7.23*10^{-4})]/(7.23*10^{-4})=$ **2 %**

The increase in wake exchange term,

$=[(-4.07*10^{-4})-(-2.99*10^{-4})]/(-2.99*10^{-4})=$ **36 %**

By looking at the comparison above, it can be concluded that from (a) to (b), settlement mechanism becomes more dominant when the bed depth is decreased since the incremental factor is higher for settlement than that of circulation and wake exchange.That is expected to result in a strongly segregated bed.

(c) Case III

mm=12 (m_{coal}/m_{mag}=0.10), L=3.0 cm, t=30 s

At the top:

d_b=0.342 cm

f_w=0.059

C_E=0.8178

δ=0.113

u_b=0.1340 m/s

<u>At the bottom:</u>

d_b=0.028 cm

f_w=0.023

C_E=0.001992 (C_E at the bottom can be taken as zero)

δ=0.293

u_b=0.03726 m/s

<u>At L/2:</u>

d_b=0.191 cm, u_b=0.09732 m/s, $K_w=60.7237/(d_b)^{1/2}$ =138.95 1/s

(assume K_1=0.85, K_w referring to Fig. 3.3)

f_w=0.050

fs_1=0.049 cm

δ=0.140

Cw_1=0.0010

C_E=0.04258

Y_S=-0.0381

Then, settlement term,

$$\frac{(0.191)*10^{-2}}{0.0973}\,\frac{0.75(-0.0381)}{(1-0.140)}\,\frac{\left[\dfrac{(0.140)(0.0973)(0.0426)(1-0.0426)}{0.03}-0\right]}{1/2}$$

$=-2.41*10^{-5}$

circulation term;

$$\frac{(0.191)*10^{-2}}{0.0973}\ \frac{1}{(1-0.140)}\ \frac{\left[\dfrac{(0.140)(0.0973)(0.050)(0.0426)}{0.03}\ 0\right]}{1/2}$$

$=4.40*10^{-5}$

wake exchange term,

$$\frac{(0.191)*10^{-2}.(0.85)(138.95)(0.140)(0.050)(0.049)(0.001-0.0426)}{0.0973(1-0.140)}$$

$=-3.93*10^{-5}$

Then,

$=(-2.41*10^{-5}) + (4.40*10^{-5}) + (-3.93*10^{-5})$

= (Settlement) + (Circulation) + (Exchange)

Then from (b) to (c), the variation in the settlement, circulation and exchange terms can be written as follows:

The increase in settlement term,

$=[(-2.41*10^{-5})-(-9.69*10^{-5})]/(-9.69*10^{-5})=$ **-75 %**

The increase in circulation term,

$=[(4.40*10^{-5})-(7.38*10^{-4})]/(7.38*10^{-4})=$ **-94 %**

The increase in wake exchange term,

$=[(-3.93*10^{-5})-(-4.07*10^{-4})]/(-4.07*10^{-4})=$ **-90 %**

From the above results, it can be concluded that from (b) to (c), all of the terms decrease together by almost the same percent, therefore going from one condition to another may not have a significant effect on the performance.

Table 6.1 Experiments with coal: #-50,+80 Rushton, magnetite: #-100,+120.

mass coal / mass magnetite	mm	u_0/u_{mfm}	t [s]	Bed depth [cm]	Experiment no
0.10	12	1.6	60	3	2-5-91-3
0.10	12	2.2	60	7	2-5-91-2
0.10	12	2.5	30	12	2-7-91-4
0.10	12	2.5	600	12	2-8-91-5
0.70	6	1.7	30	3	5-2-91-21
0.70	6	2.0	30	3	4-1-91-18
0.70	6	2.5	30	3	3-27-91-17
0.70	6	2.5	30	3	2-8-91-6
0.70	6	3.2	30	3	4-1-91-19
0.70	6	2.5	30	12	2-11-91-7
1.60	3	1.25	30	3	2-12-91-12
1.60	3	1.25	30	3	3-25-91-13
1.60	3	1.96	30	3	2-11-91-8
1.60	3	1.96	30	3	3-26-91-14
1.60	3	2.35	30	3	4-1-91-20
		(experiment 4-1-91-20 is discarded)			
1.60	3	2.35	30	3	5-6-91-24
1.60	3	2.90	30	3	5-7-91-25

$\frac{\text{mass coal}}{\text{mass magnetite}}$	mm	u_0/u_{mfm}	t [s]	Bed depth [cm]	Experiment no
5.70	1	1.25	30	3	2-12-91-11
5.70	1	1.56	30	3	2-12-91-10
5.70	1	1.56	30	3	3-26-91-15
5.70	1	1.96	30	3	3-26-91-16
5.70	1	1.96	30	3	2-11-91-9
5.70	1	2.35	30	3	5-3-91-22
5.70	1	2.74	30	3	5-3-91-23

Table 6.2 Experimental results with coal: #-50,+80 Rushton, magnetite: #-100,+120, mm=6 (m_{coal}/m_{mag}=0.70), t=30 s, bed depth: 3 cm.

u_o/u_{mfm}	Sulfur Remov. (%) (at 85% Energy Recovery)	Ash Remov. (%)	Exp. no.
1.7	46	43	5-2-91-21
2.0	67	66	4-1-91-18
2.5	70	64	2-8-91-6
2.5	65	64	3-27-91-17
3.2	50	45	4-1-91-19

Table 6.3 Experimental results with coal: #-50,+80 Rushton, magnetite: #-100,+120, mm=3 (m_{coal}/m_{mag}=1.6), t=30 s, bed depth: 3 cm.

u_o/u_{mfm}	Sulfur Remov. (%) (at 85% Energy Recovery)	Ash Remov. (%)	Exp. no.
1.25	45	39	2-12-91-12
1.25	37	31	3-25-91-13
1.96	58	60	2-11-91-8
1.96	65	60	3-26-91-14
2.35	71	70	5-6-91-24
2.90	69	66	5-7-91-25

Table 6.3 Experimental results with coal: #-50,+80 Rushton, magnetite: #-100,+120, mm=1 (m_{coal}/m_{mag}=5.7), t=30 s, bed depth: 3 cm.

u_0/u_{mfm}	Sulfur Remov. (%) (at 85% Energy Recovery)	Ash Remov. (%)	Exp. no.
1.25	33	31	2-12-91-11
1.56	49	46	2-12-91-10
1.56	57	53	3-26-91-15
1.96	65	60	2-11-91-9
1.96	64	60	3-26-91-16
2.35	58	53	5-3-91-22
2.74	68	67	5-3-91-23

Table 6.5 Comparison of experimental and theoretical results;
coal: #-50,+80, magnetite: #-100,+120.

	Experimental results		Theoretical results		Bed depth	Time
Exp. no.	**sulfur removal**	**ash removal**	**sulfur removal**	**ash removal**	**[cm]**	**[s]**
	(at 85% energy recovery)		(at 85% energy recovery)			
mm=12						
2-5-91-3	64	61	68	64	3.0	60
2-5-91-2	57	46	45	43	7.0	60
2-7-91-4	32	26	32	26	12.0	30
2-8-91-5	to be repeated		57	38	12.0	600
mm=6						
5-2-91-21	46	43	34	28	3.0	30
4-1-91-18	67	66	unstable solution		3.0	30
3-27-91-17	65	64	67	63	3.0	30
2-8-91-6	70	64	67	63	3.0	30
4-1-91-19	50	45	unstable solution		3.0	30
2-11-91-7	35	28	42	35	12.0	30

Table 6.6 Theoretical results with the best performed velocities;

coal: #-50,+80, magnetite: #-100,+120,

bed depth: 3.0 cm.

mass coal / mass mag.	Best Performance u_0/u_{mfm}	Time [s]	GE_p	SGS	Sulf. Rem. at 80% ER at t=60 s	d_b [cm]
0.10	2.0	30	0.26	2.53	0.67	0.29
		60	0.24	2.43		
		120	0.23	2.35		
0.28	1.8	30	0.213	2.25	-	0.27
		60	0.185	2.14		
		120	0.185	2.14		
0.70	2.2	30	0.137	1.98	0.71	0.34
		60	0.115	1.87		
		120	0.099	1.87		

Table 6.7 Theoretical results with the best performed velocities;
coal: #-50,+80, magnetite: #-100,+120,
bed depth: 7.0 cm.

mass coal / mass mag.	Best Performance u_0/u_{mfm}	Time [s]	GE_p	SGS	Sulf. Rem. at 80% ER at t=60 s	d_b [cm]
0.10	2.0	30	0.40	2.53	0.44	0.65
		60	0.36	2.43		
		120	0.32	2.35		
0.28	1.8	30	-	-	-	0.58
		60	0.284	2.55		
		120	0.279	2.34		
0.70	2.2	30	0.250	2.78	0.68	0.76
		60	0.220	2.42		
		120	0.190	2.30		

Table 6.8 Theoretical results with the best performed velocities;
coal: #-50,+80, magnetite: #-100,+120,
bed depth: 12.0 cm.

mass coal / mass mag.	Best Performance u_0/u_{mfm}	Time [s]	GE_p	SGS	Sulf. Rem. at 80% ER at t=60 s	d_b [cm]
0.10	2.0	30	0.45	4.41	0.31	1.06
		60	0.42	4.05		
		120	0.38	3.60		
0.28	1.8	30	-	-	-	0.94
		60	-	-		
		120	0.317	2.95		
0.70	2.2	30	0.325	3.37	0.51	1.22
		60	0.276	2.77		
		120	0.245	2.47		

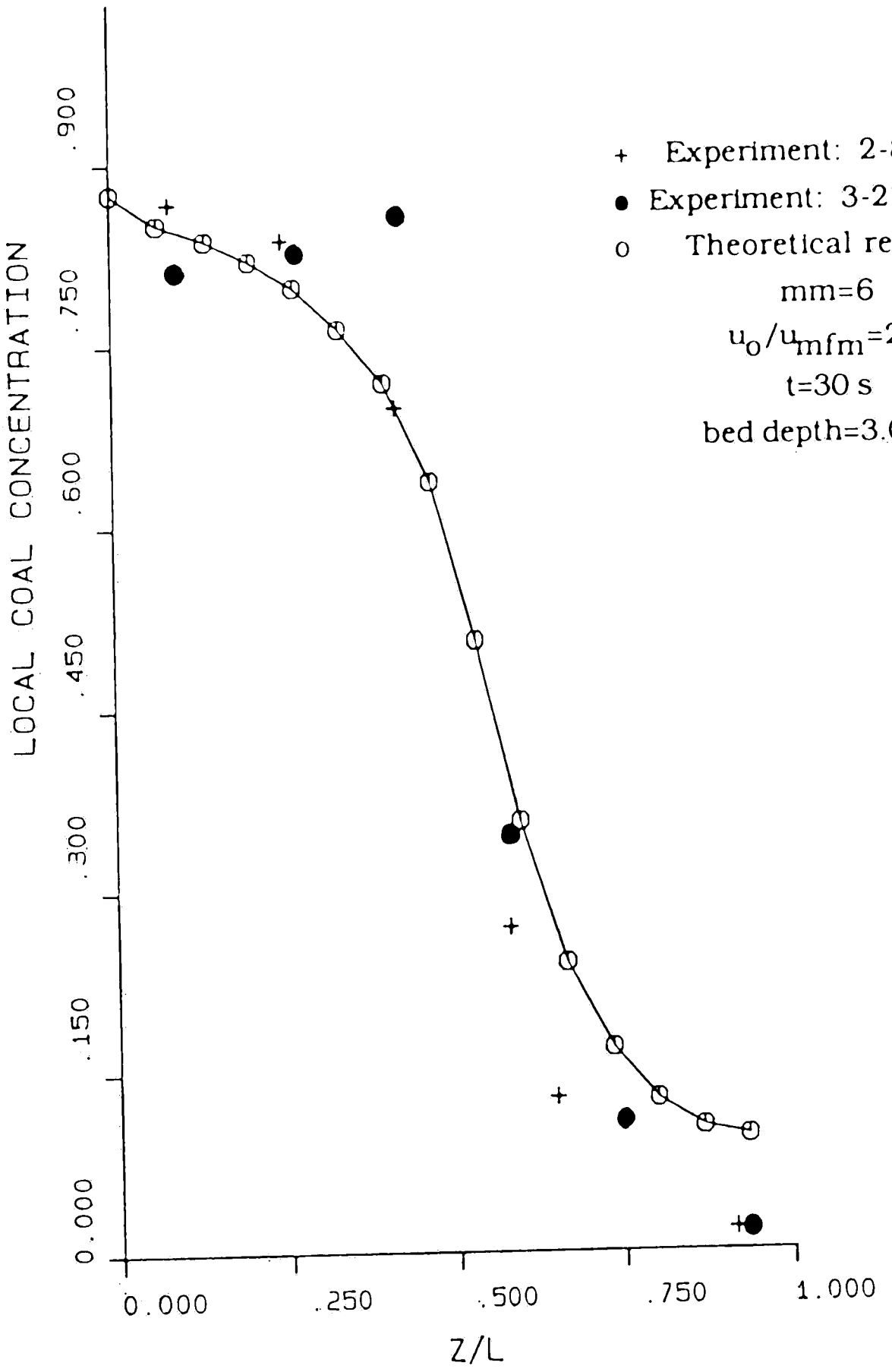

Fig. 6.1 Local coal concentration profile

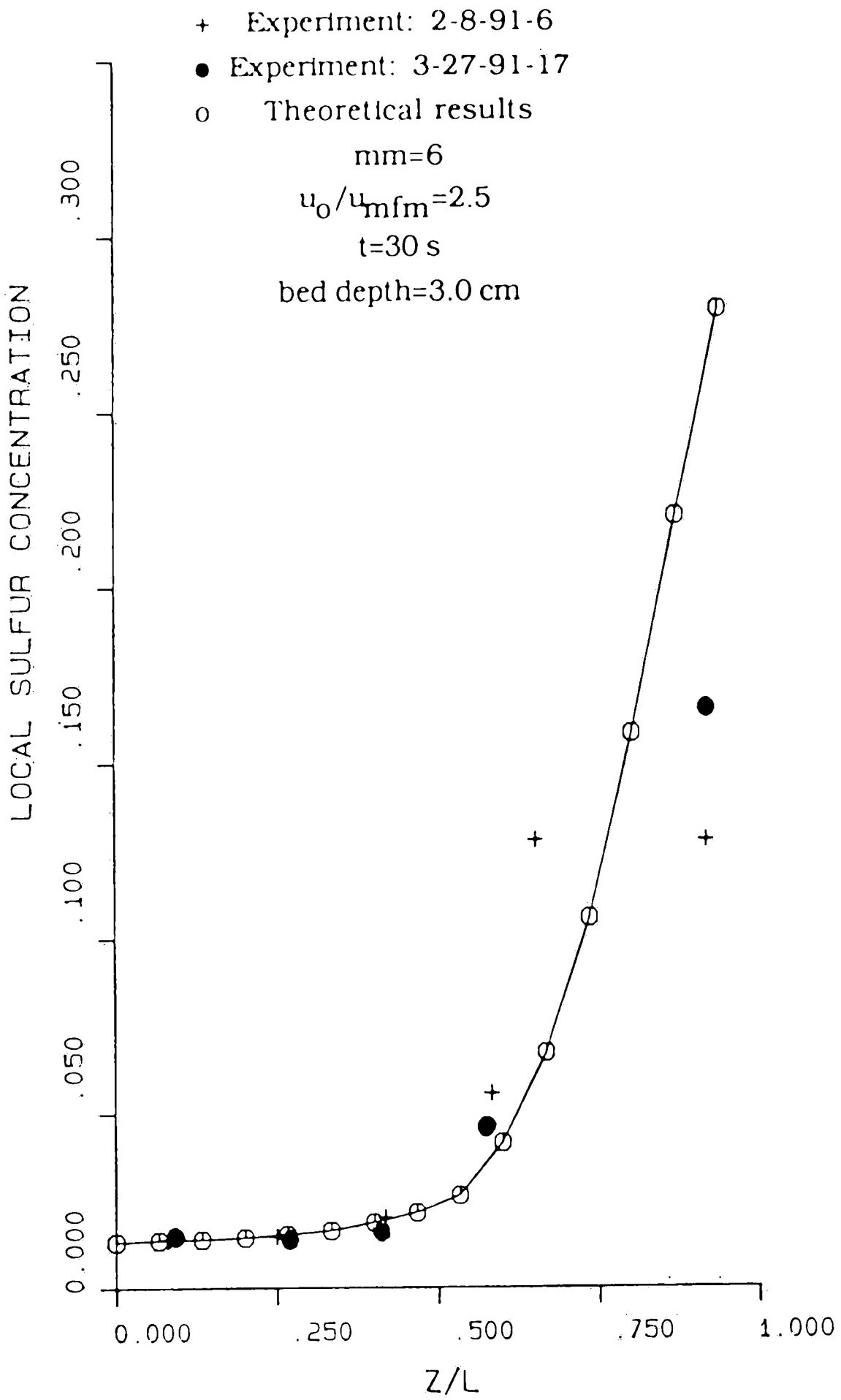

Fig. 6.2 Local sulfur concentration profile

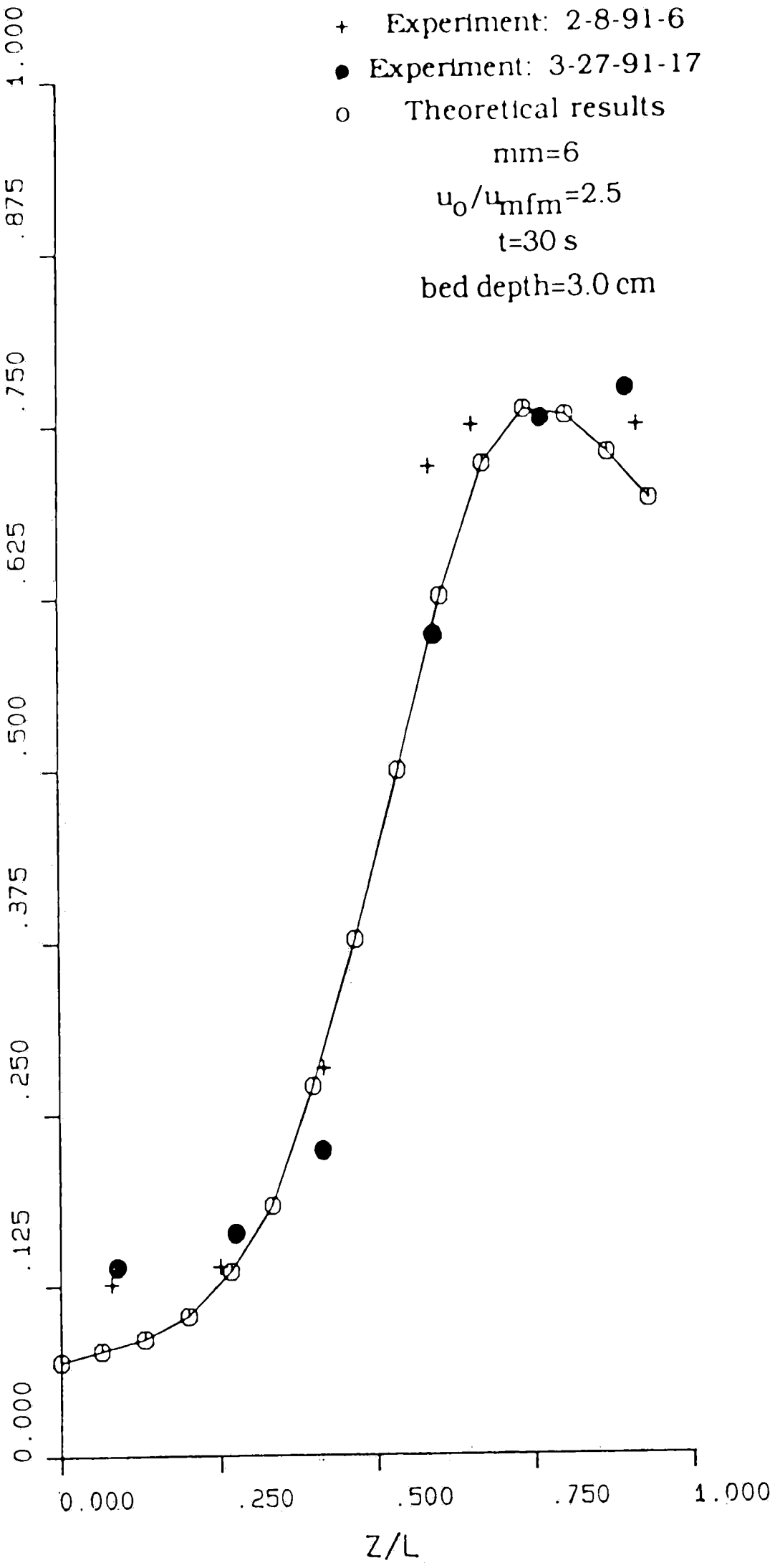

Fig. 6.3 Local ash concentration profile

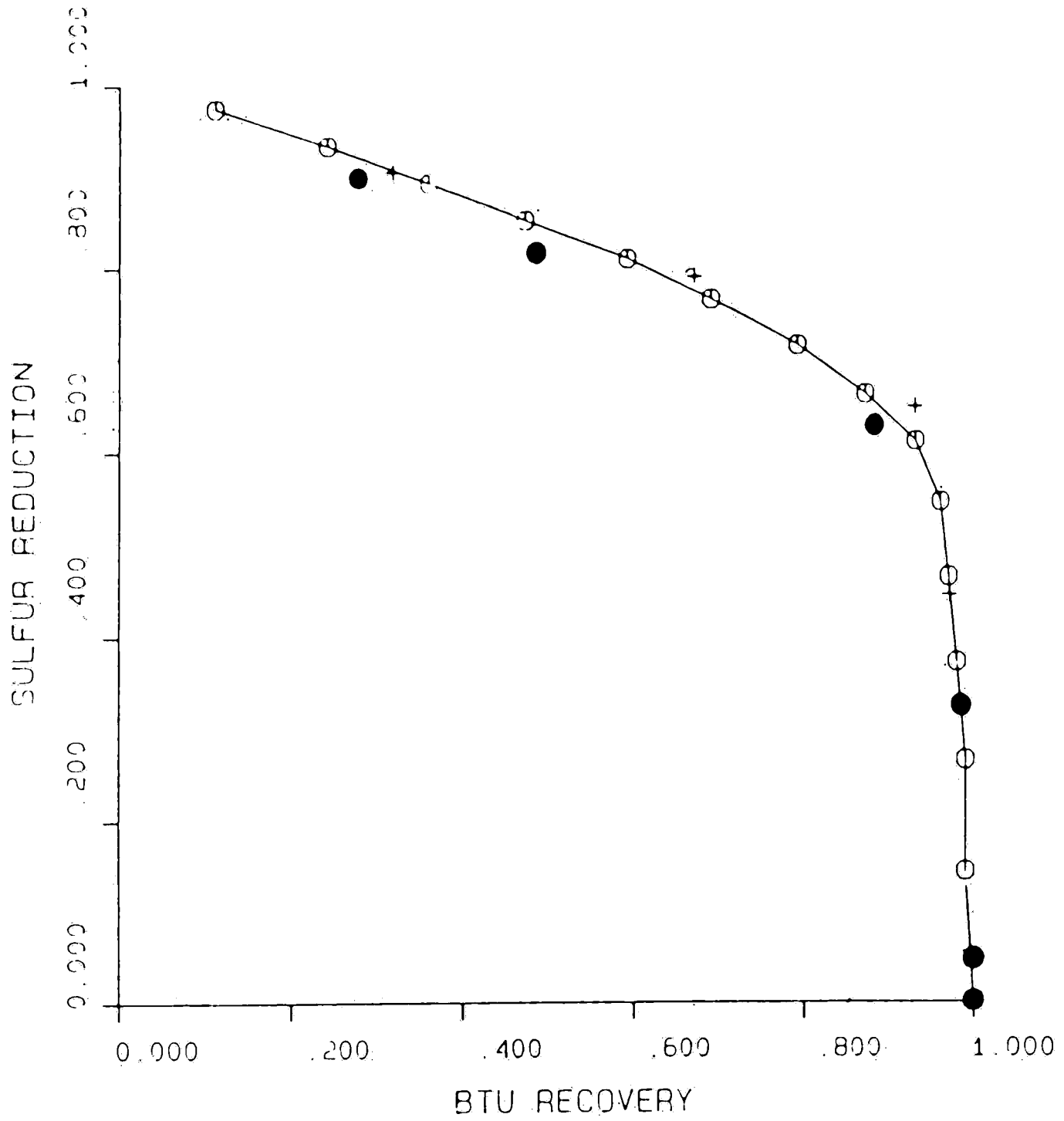

+ Experiment: 2-8-91-6

● Experiment: 3-27-91-17

o Theoretical results

mm=6

u_o/u_{mfm}=2.5

t=30 s

bed depth=3.0 cm

Fig. 6.4 Sulfur removal against energy recovery

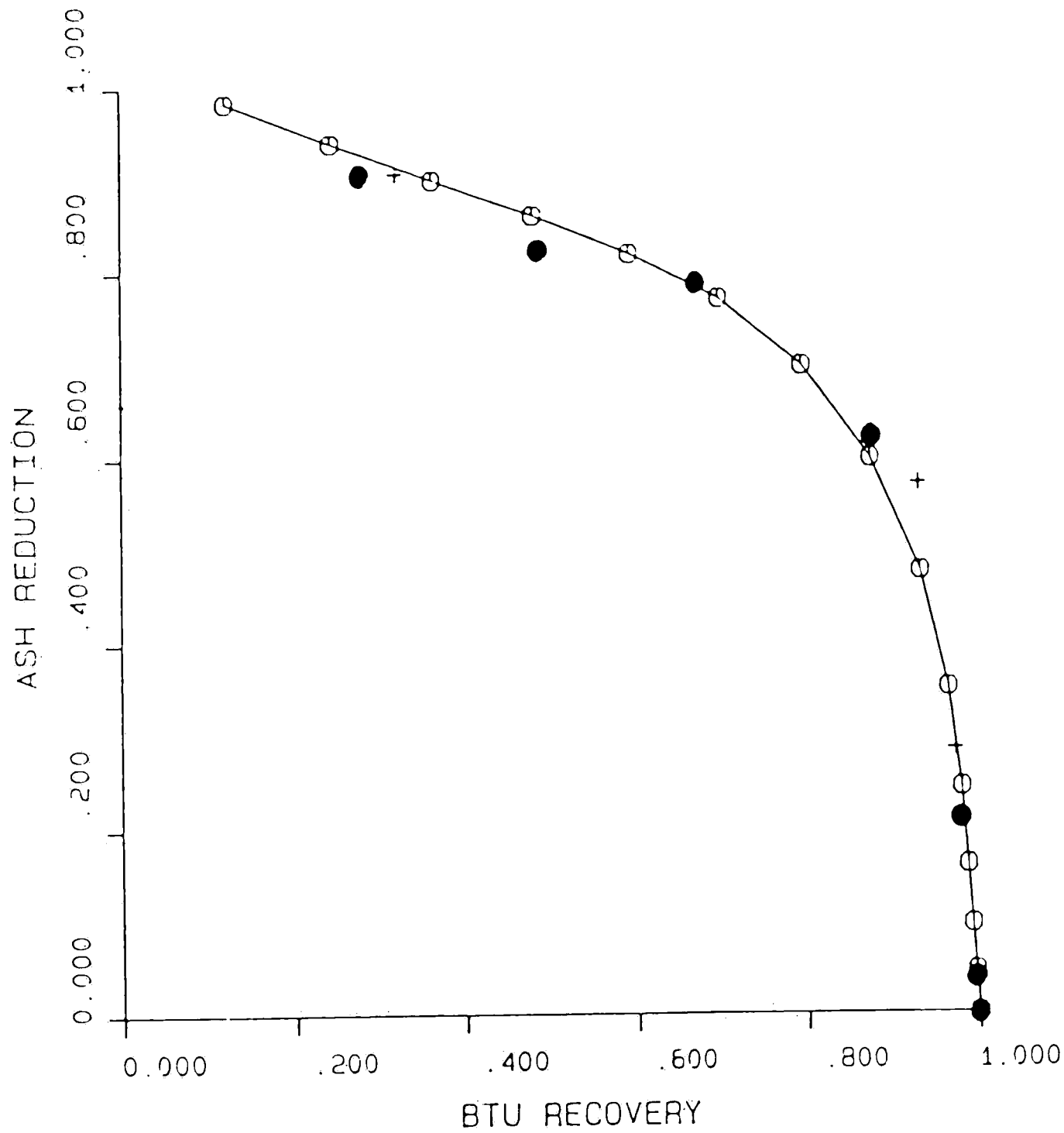

+ Experiment: 2-8-91-6

● Experiment: 3-27-91-17

o Theoretical results

mm=6

u_o/u_{mfm}=2.5

t=30 s

bed depth=3.0 cm

Fig. 6.5 Ash removal against energy recovery

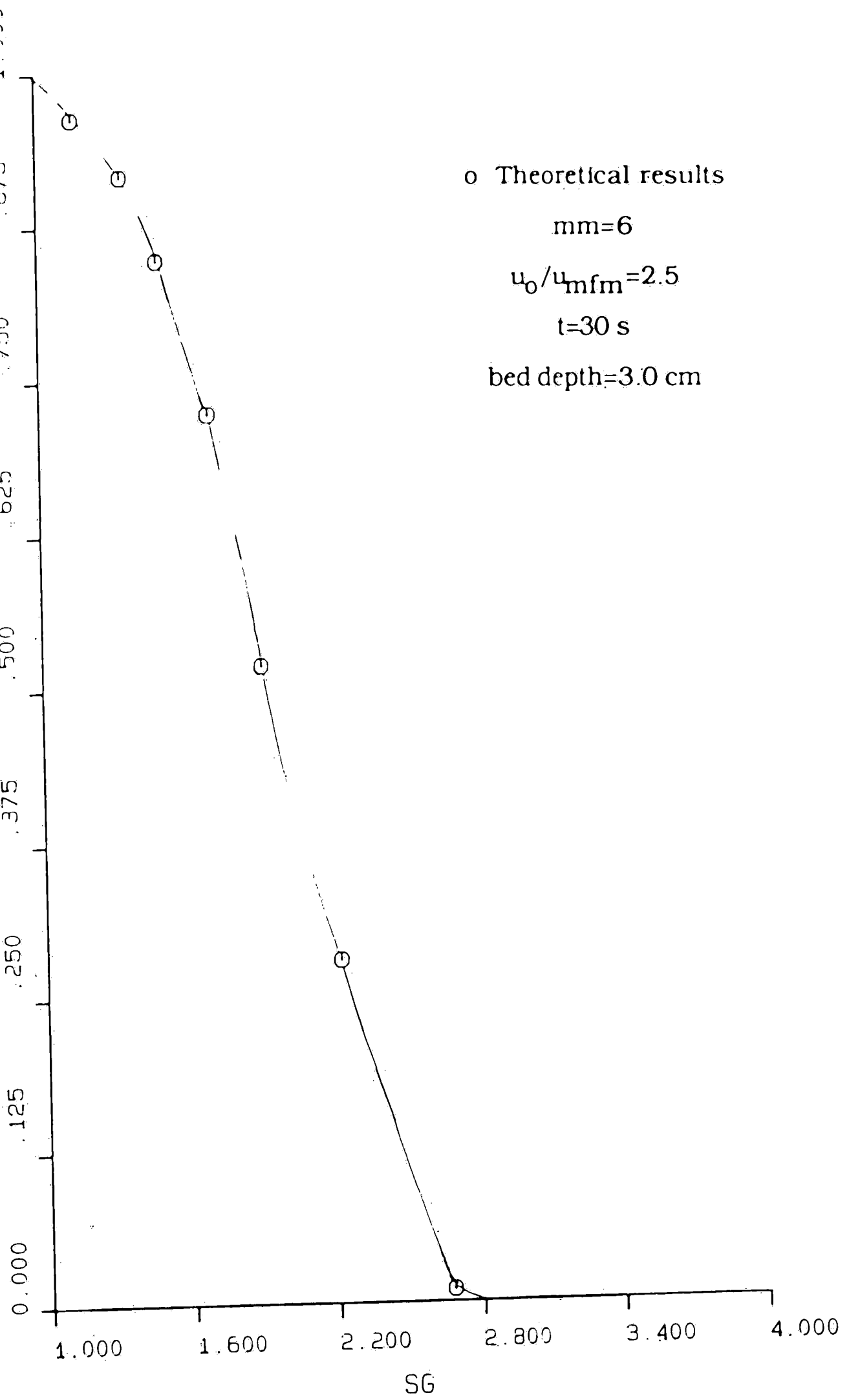

o Theoretical results

mm=6

u_o/u_{mfm}=2.5

t=30 s

bed depth=3.0 cm

Fig. 6.6 Reporting (distribution) to clean coal against specific gravity

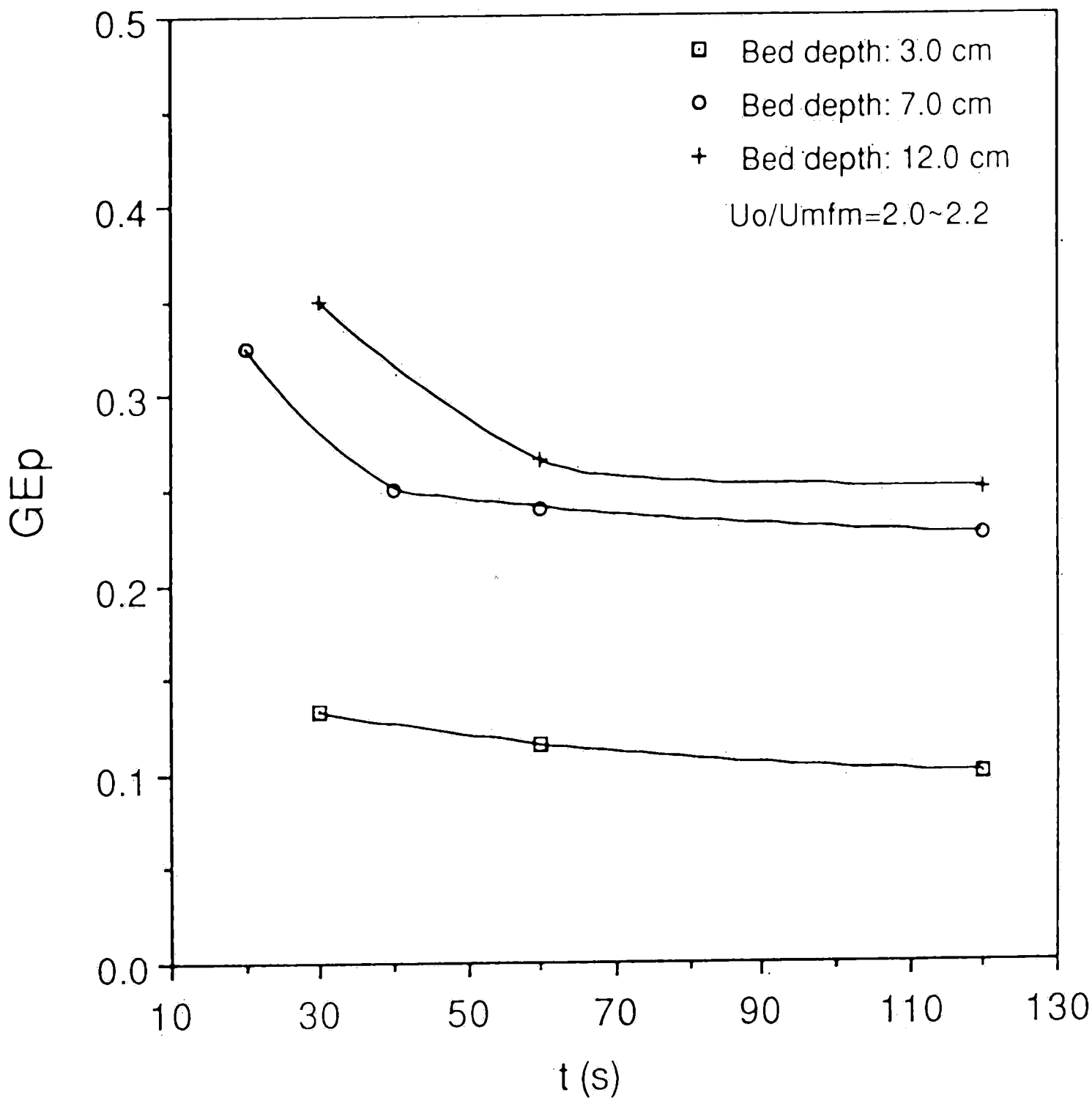

Fig. 6.7 Theoretical results; variation of generalized performance parameter GE_p with time and bed depth, coal: #-50,+80, magnetite: #-100,+120, mm=6 (mass of coal/mass of magnetite=0.7)

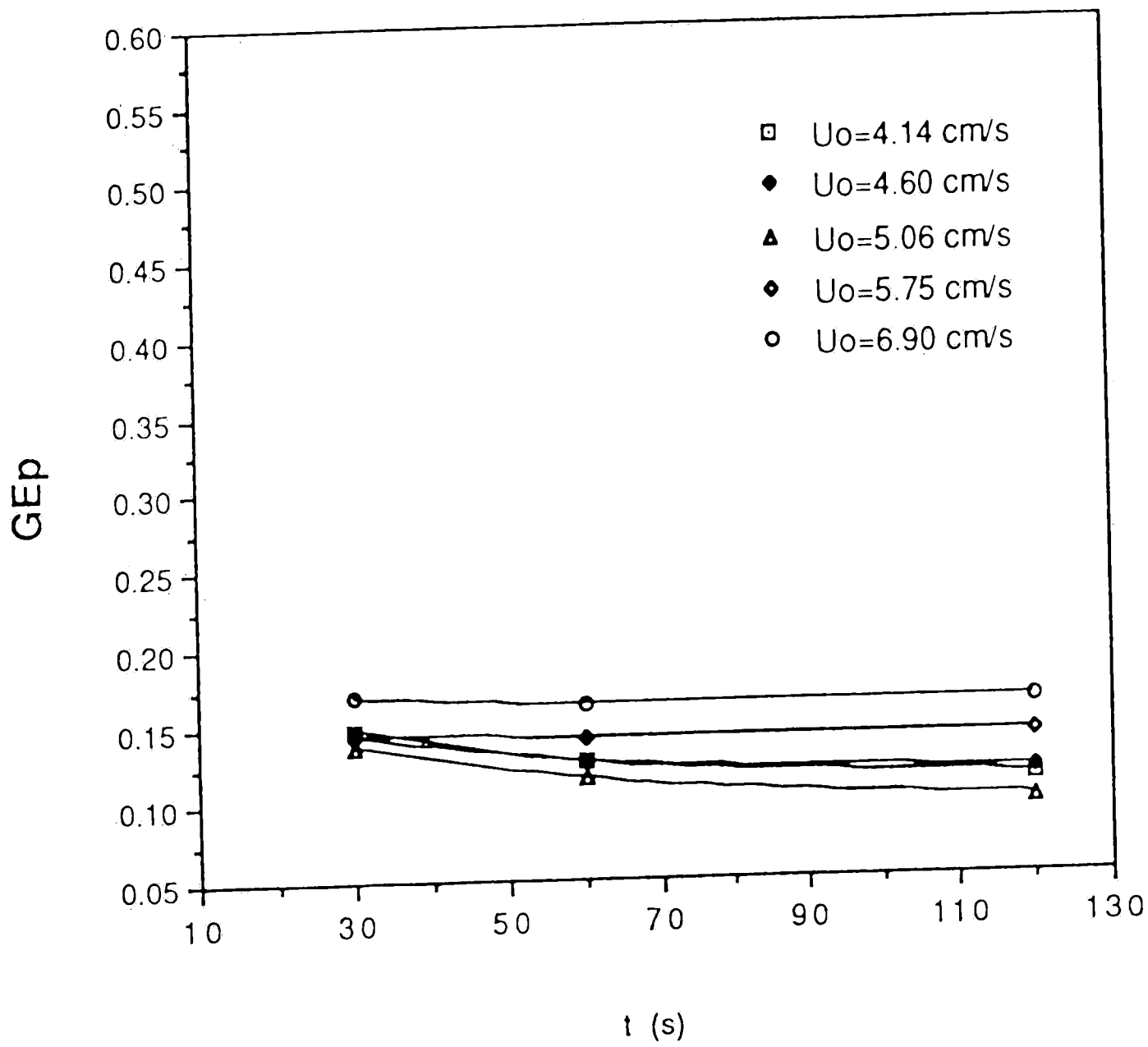

Fig. 6.8 Theoretical results; variation in generalized performance parameter GE_p with time, coal: #-50,+80, magnetite: #-100,+120, mm=6 (mass coal/mass magnetite=0.7), bed depth: 3.0 cm

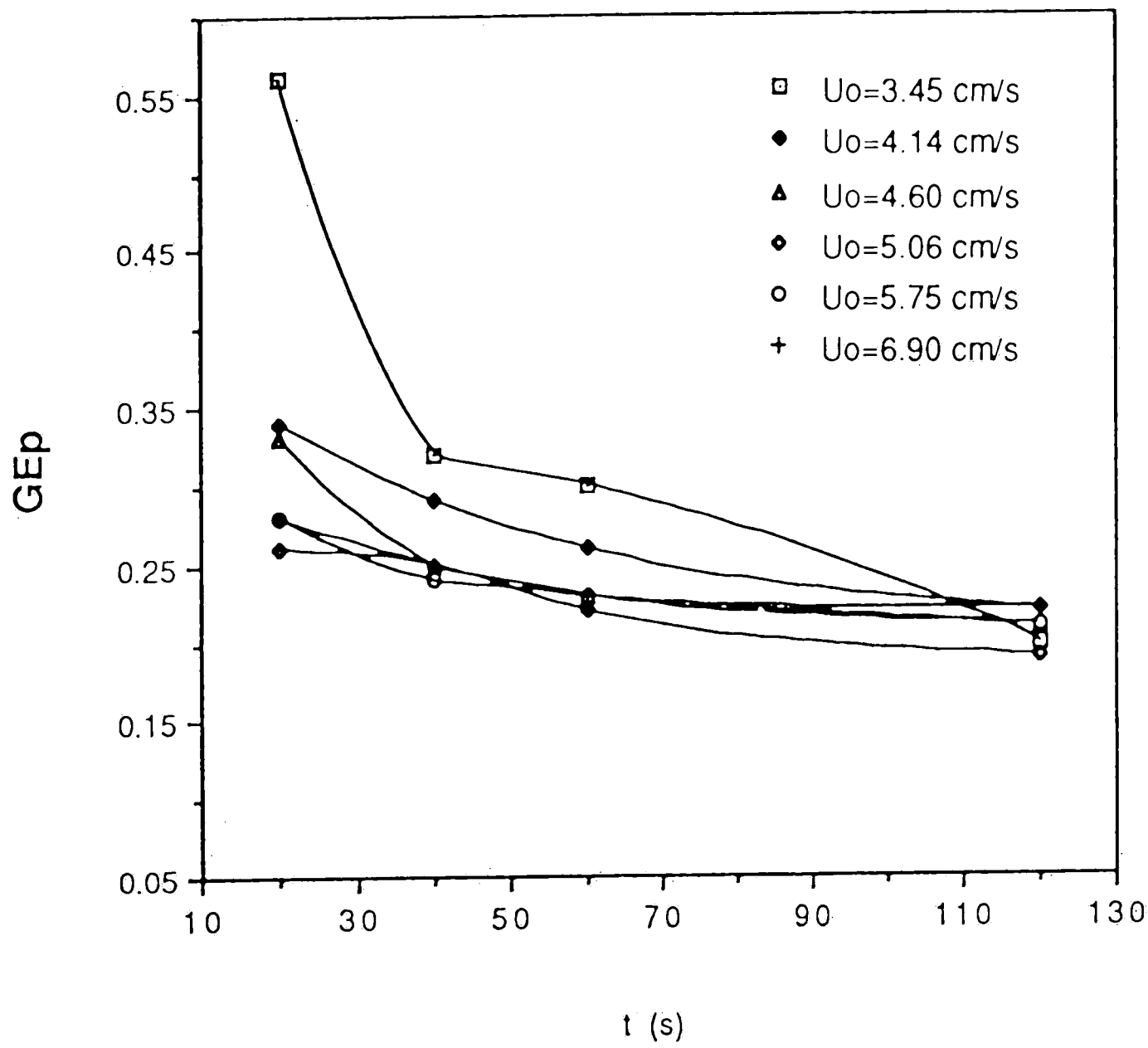

Fig. 6.9 Theoretical results; variation in generalized performance parameter GE_p with time, coal: #-50,+80, magnetite: #-100,+120, mm=6 (mass coal/mass magnetite=0.7), bed depth: 7.0 cm

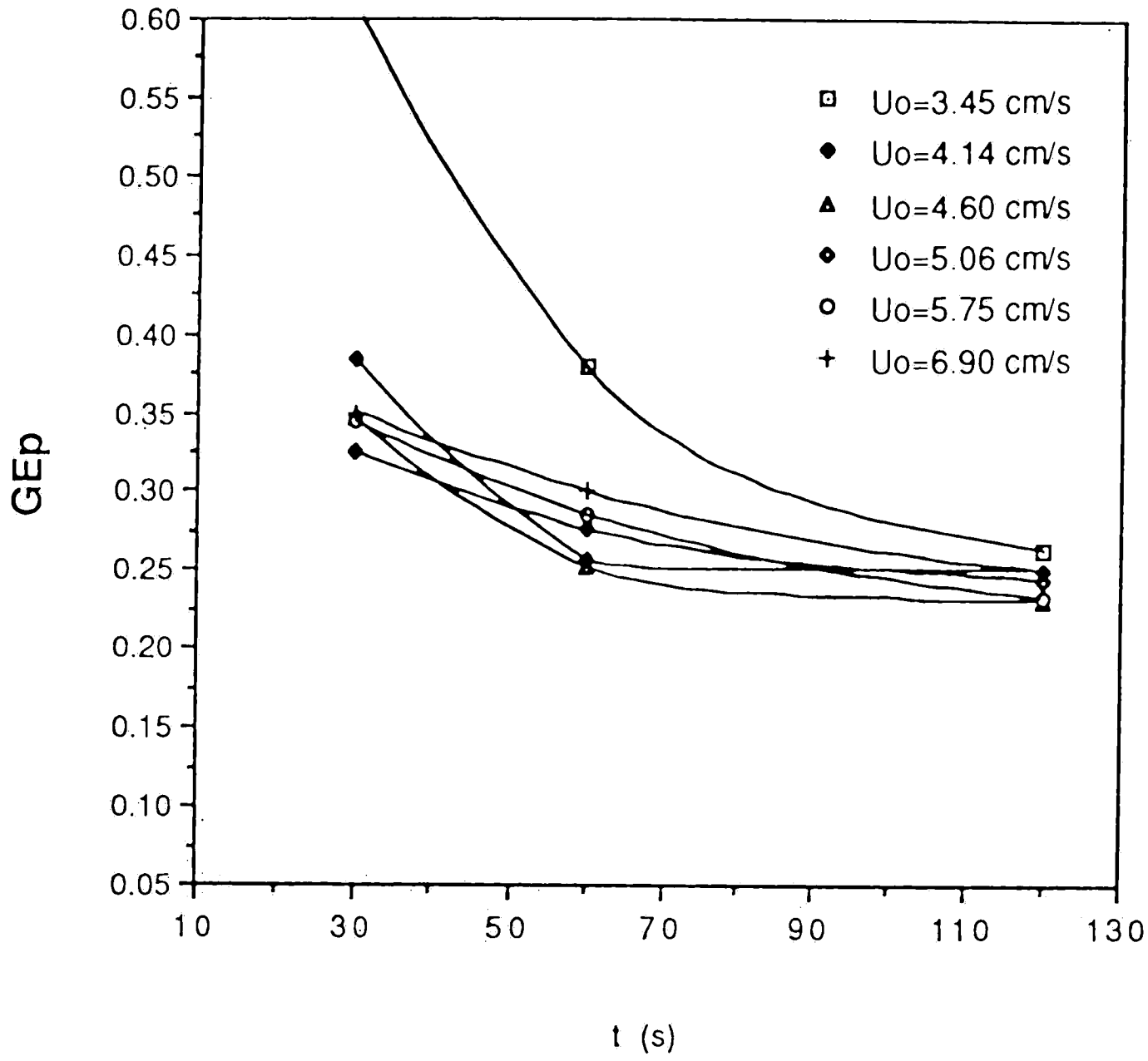

Fig. 6.10 Theoretical results; variation in generalized performance parameter GE_p with time, coal: #-50,+80, magnetite: #-100,+120, mm=6 (mass coal/mass magnetite=0.7), bed depth: 12.0 cm

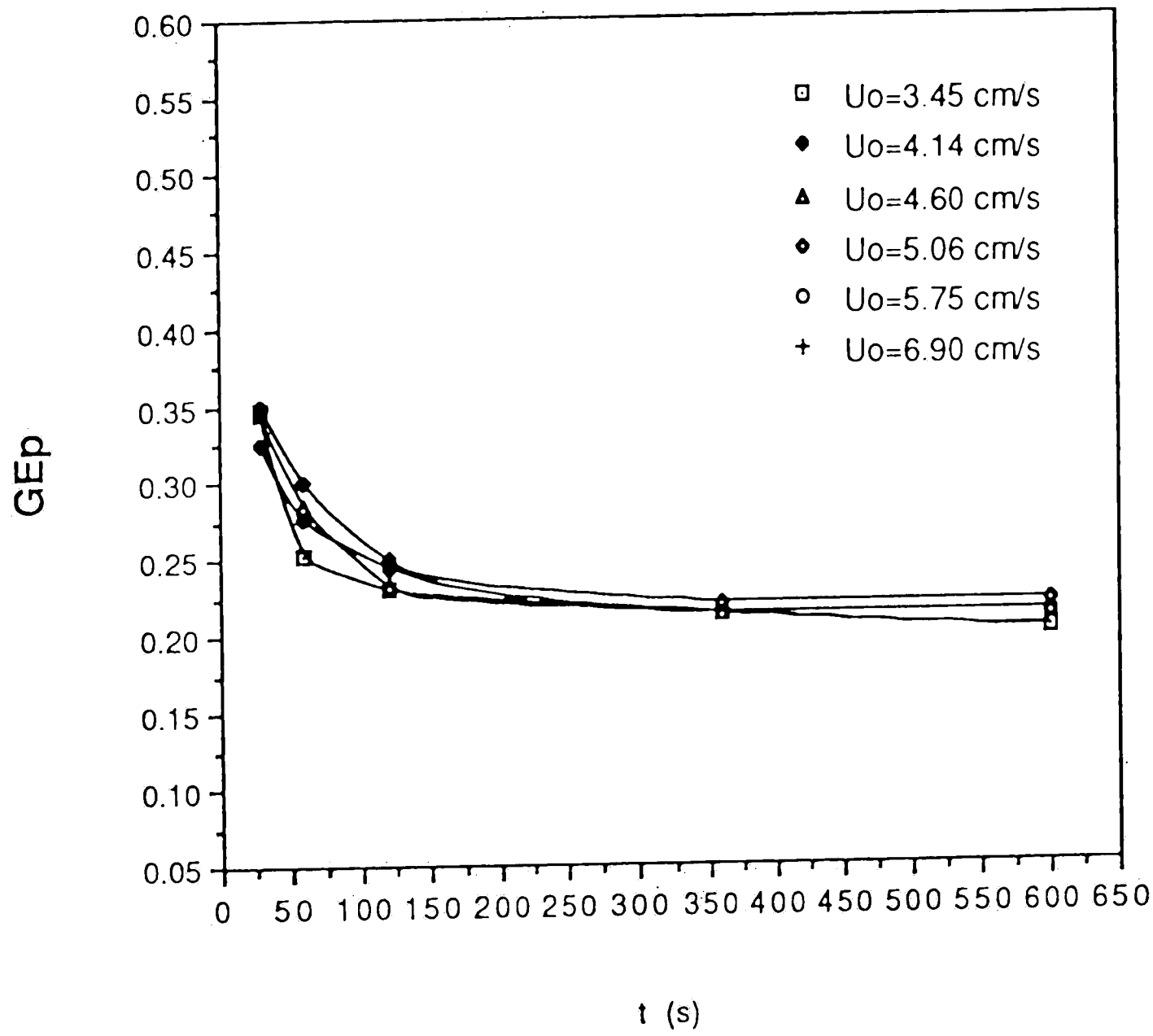

Fig. 6.11 Theoretical results; variation in generalized performance parameter GE_p with time (longer processing), coal: #-50,+80, magnetite: #-100,+120, mm=6 (mass coal/mass magnetite=0.7), bed depth: 12.0 cm

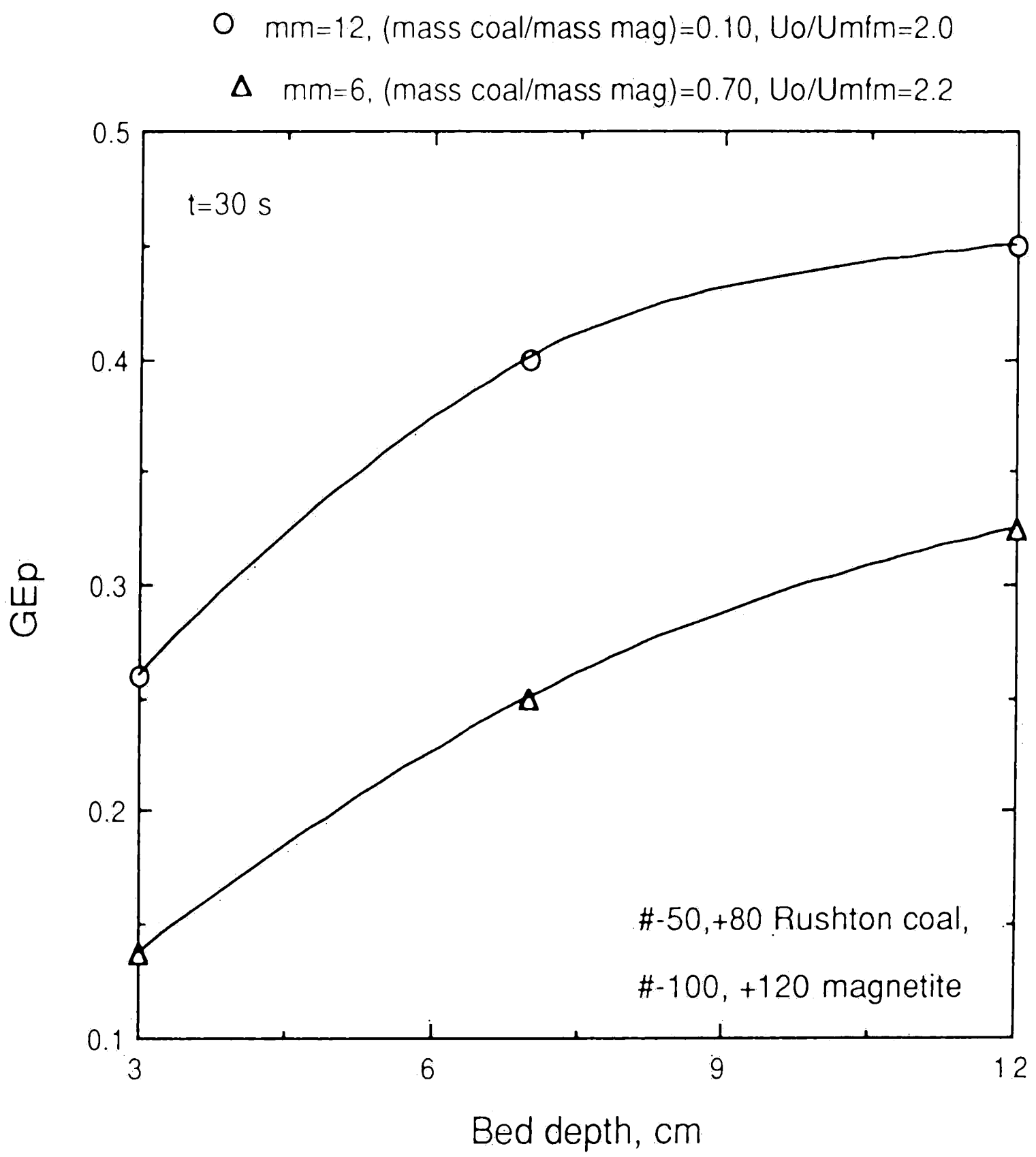

Fig. 6.12 Theoretical results; the effect of bed depth and coal concentration on the generalized performance parameter GE_p, t=30 seconds

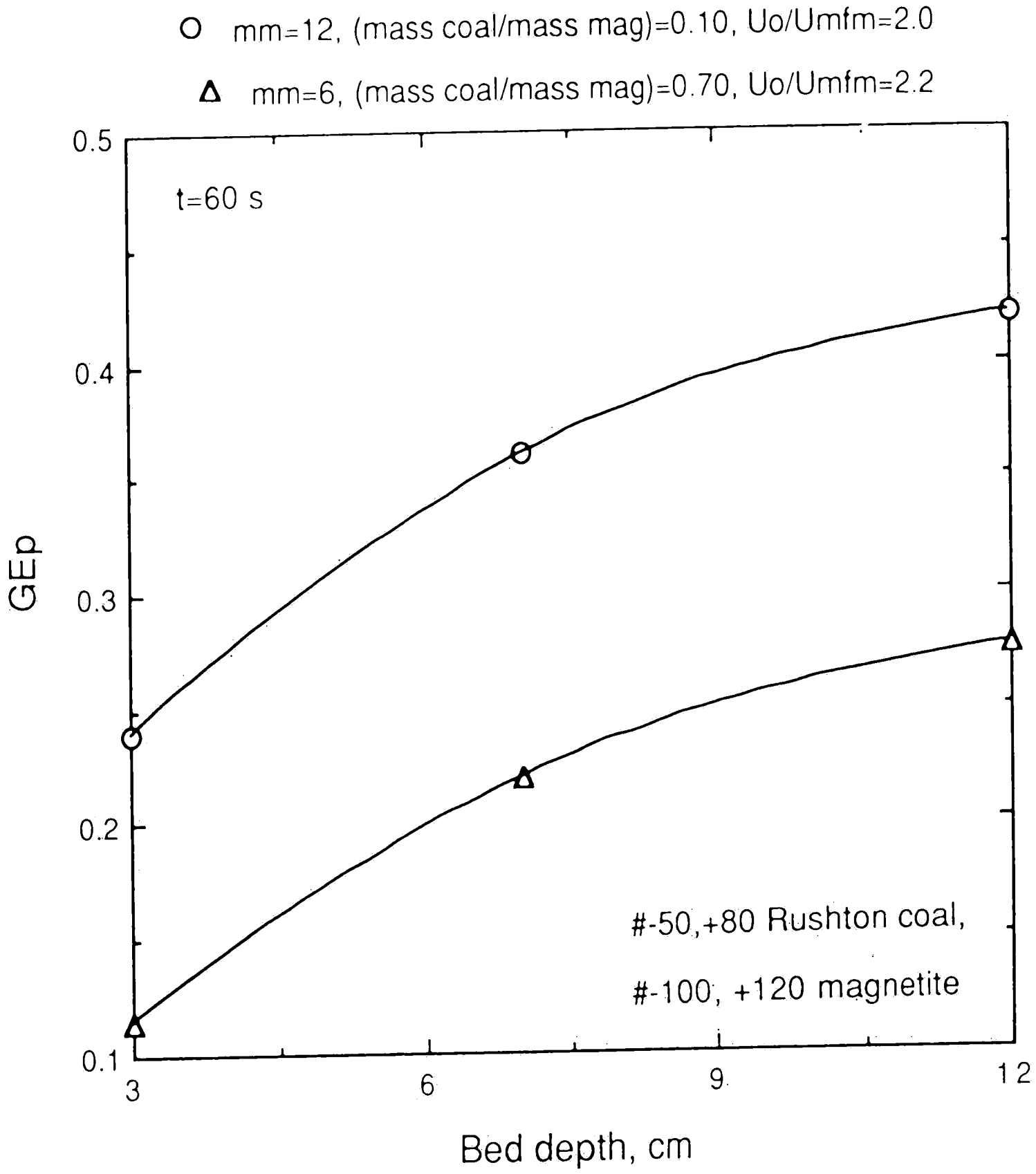

Fig. 6.13 Theoretical results; the effect of bed depth and coal concentration on the generalized performance parameter GE_p, t=60 seconds

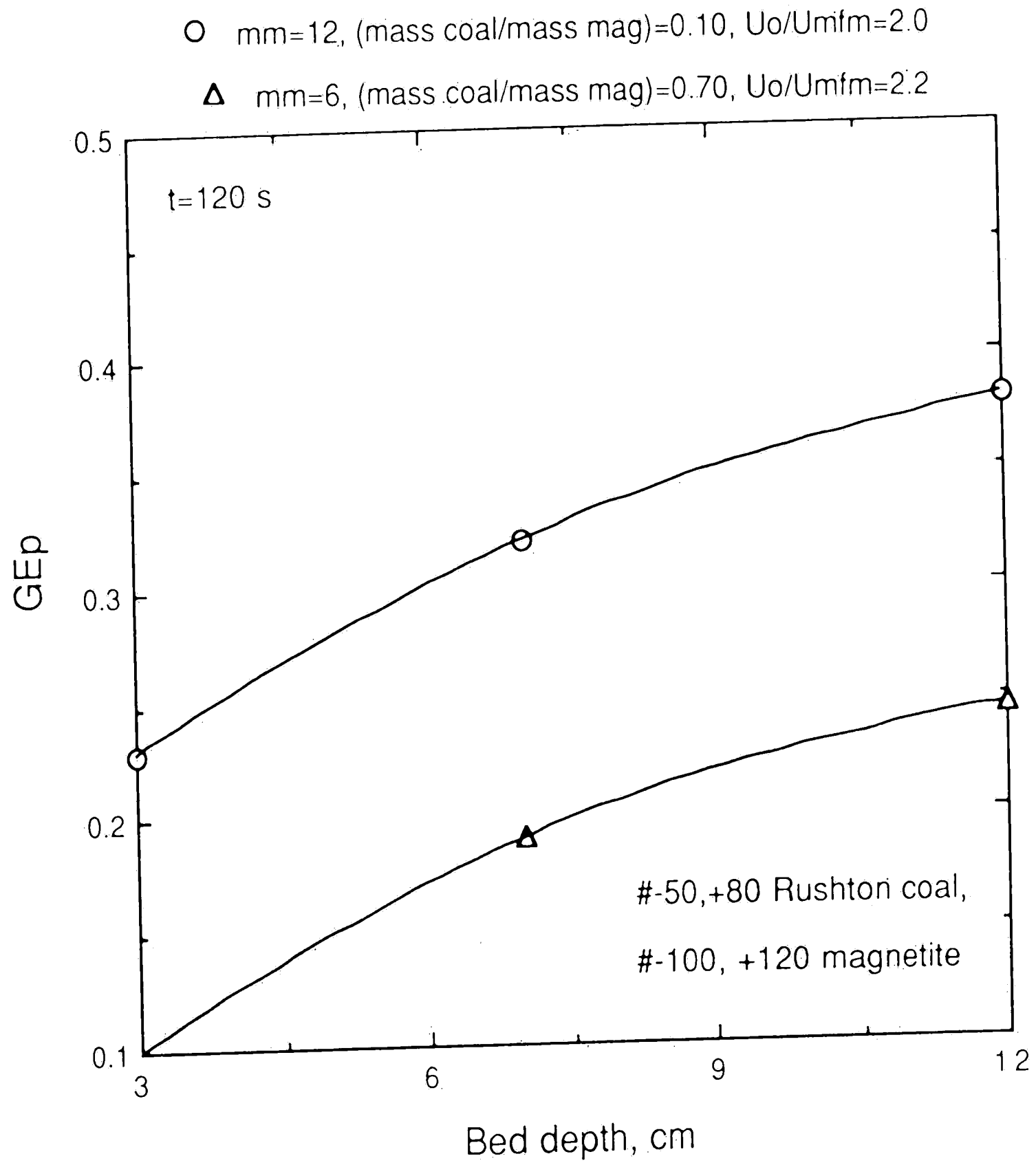

Fig. 6.14 Theoretical results; the effect of bed depth and coal concentration on the generalized performance parameter GE_p, t=120 seconds

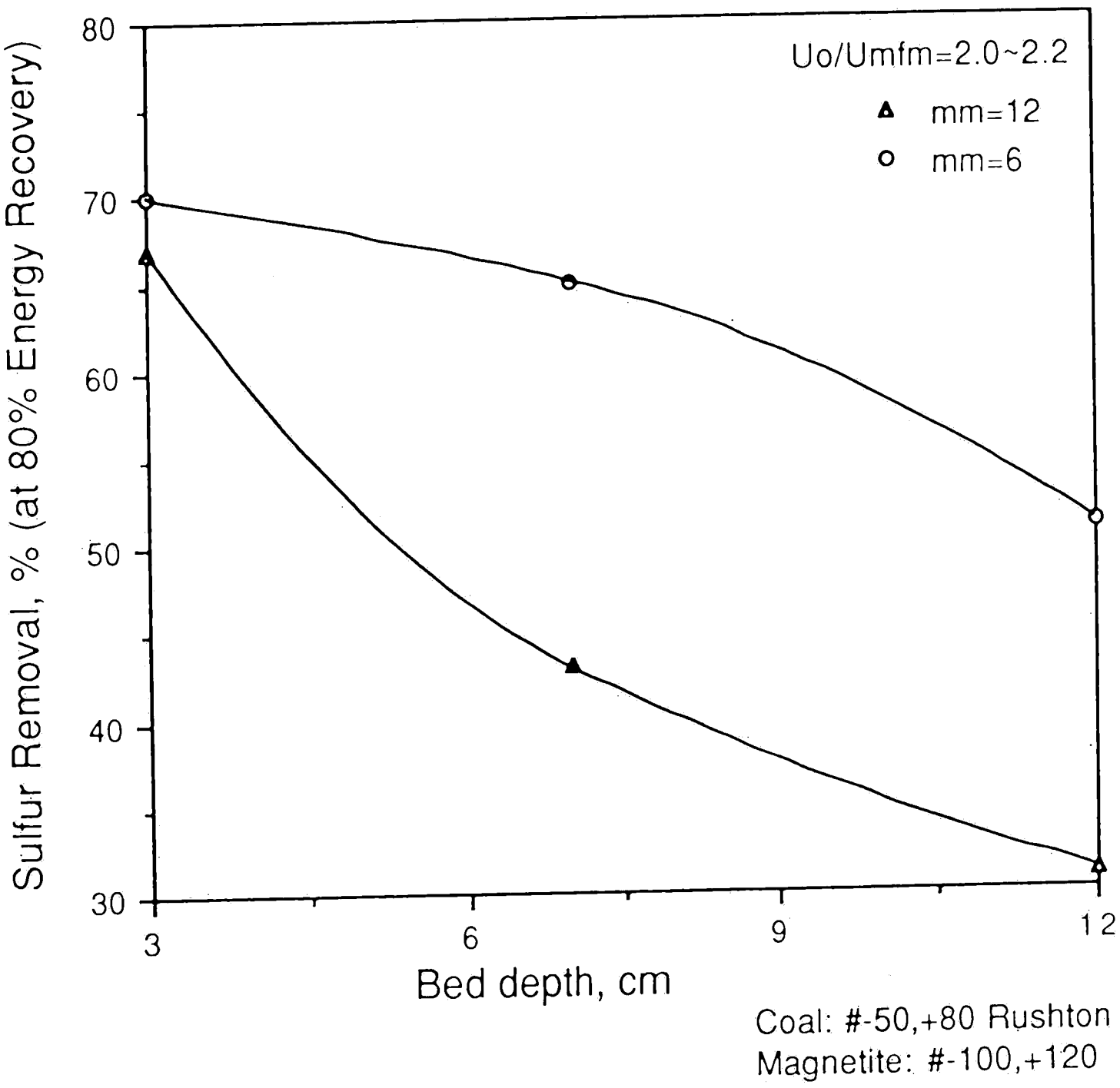

Fig. 6.15 Theoretical results; the effect of bed depth and coal concentration on sulfur removal, t=60 seconds

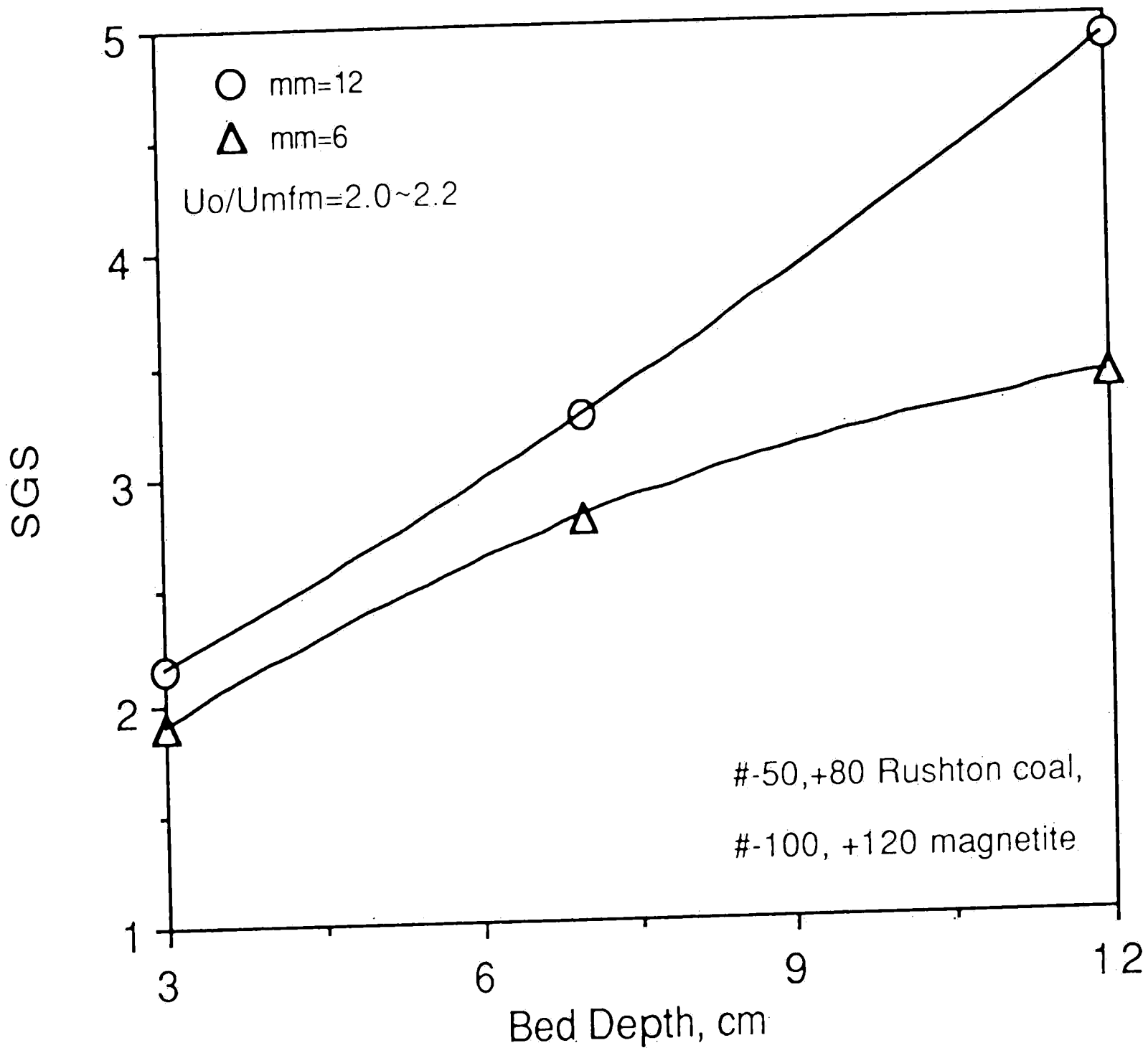

Fig. 6.16 Theoretical results; the effect of bed depth and coal concentration on specific gravity of separation, t=60 seconds

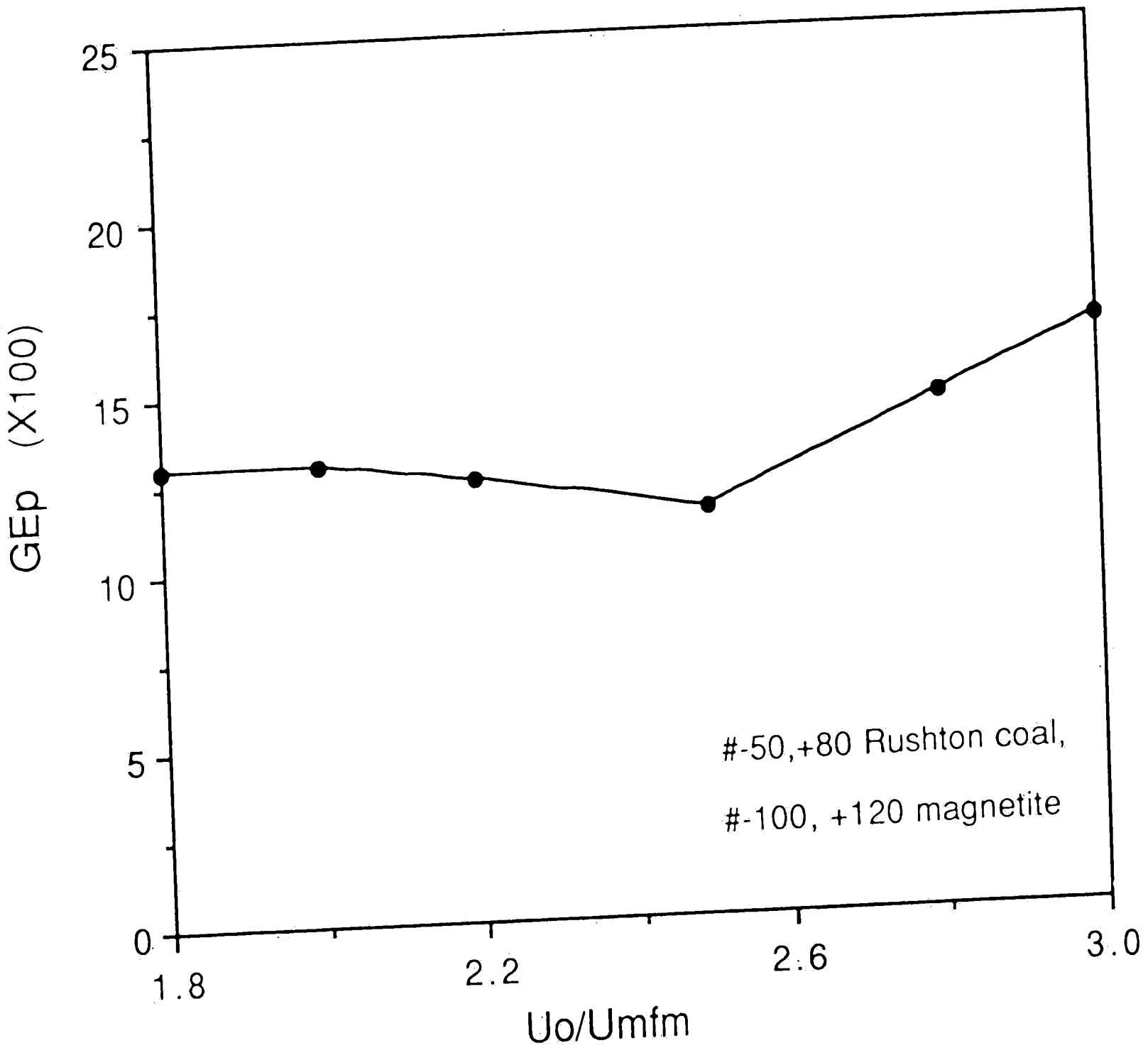

Fig. 6.17 Theoretical results; the effect of superficial gas velocity on generalized performance parameter, mm=6 (mass coal/ mass magnetite =0.70), bed depth: 3.0 cm, t=60 seconds

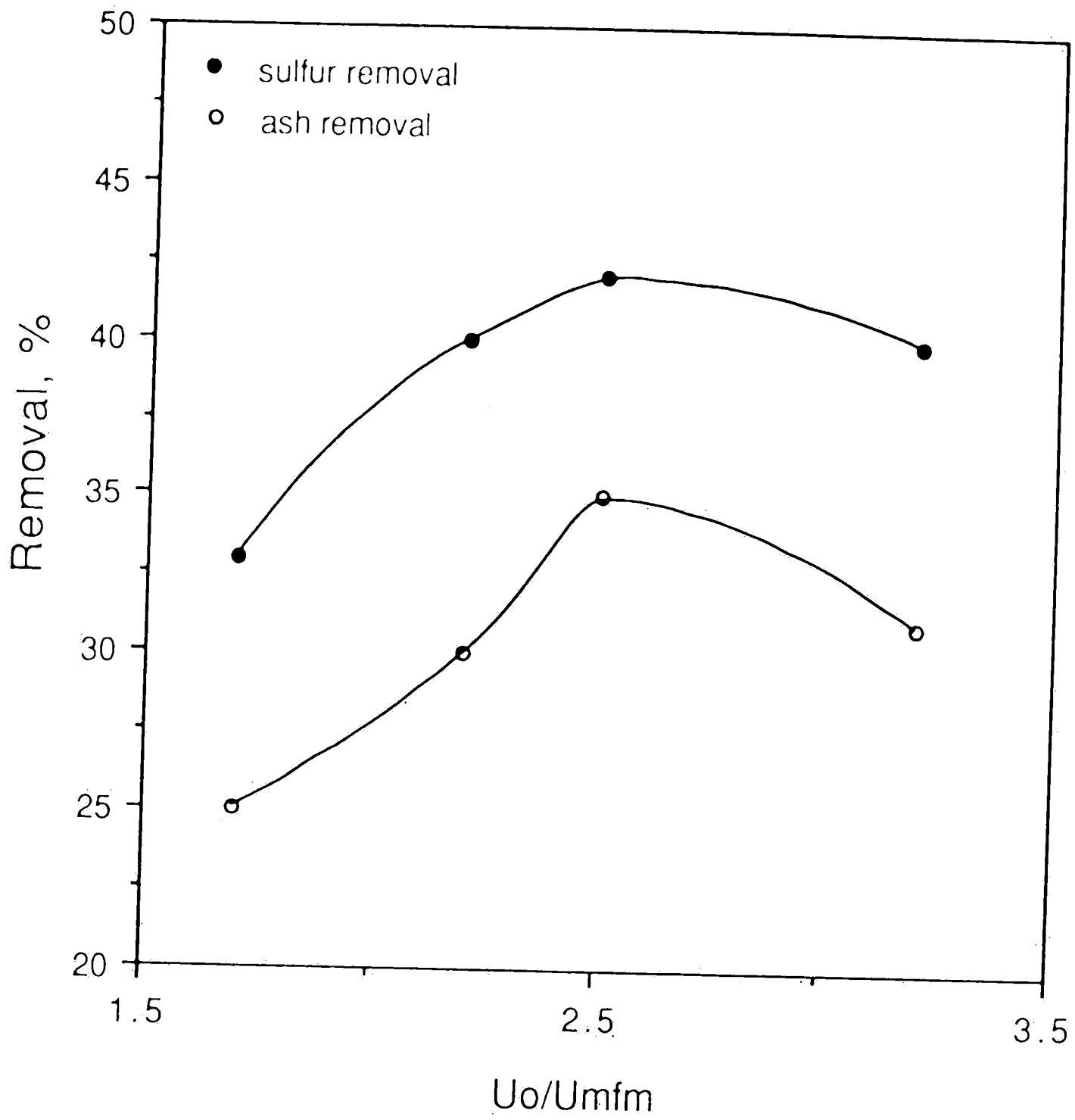

Fig: 6.18 Theoretical results; variation of sulfur removal, and ash removal with superficial gas velocity, coal: #-50,+80, magnetite: #-100,+120, mm=6 (mass of coal/mass of magnetite=0.7), bed depth: 12.0 cm, t=30 seconds.

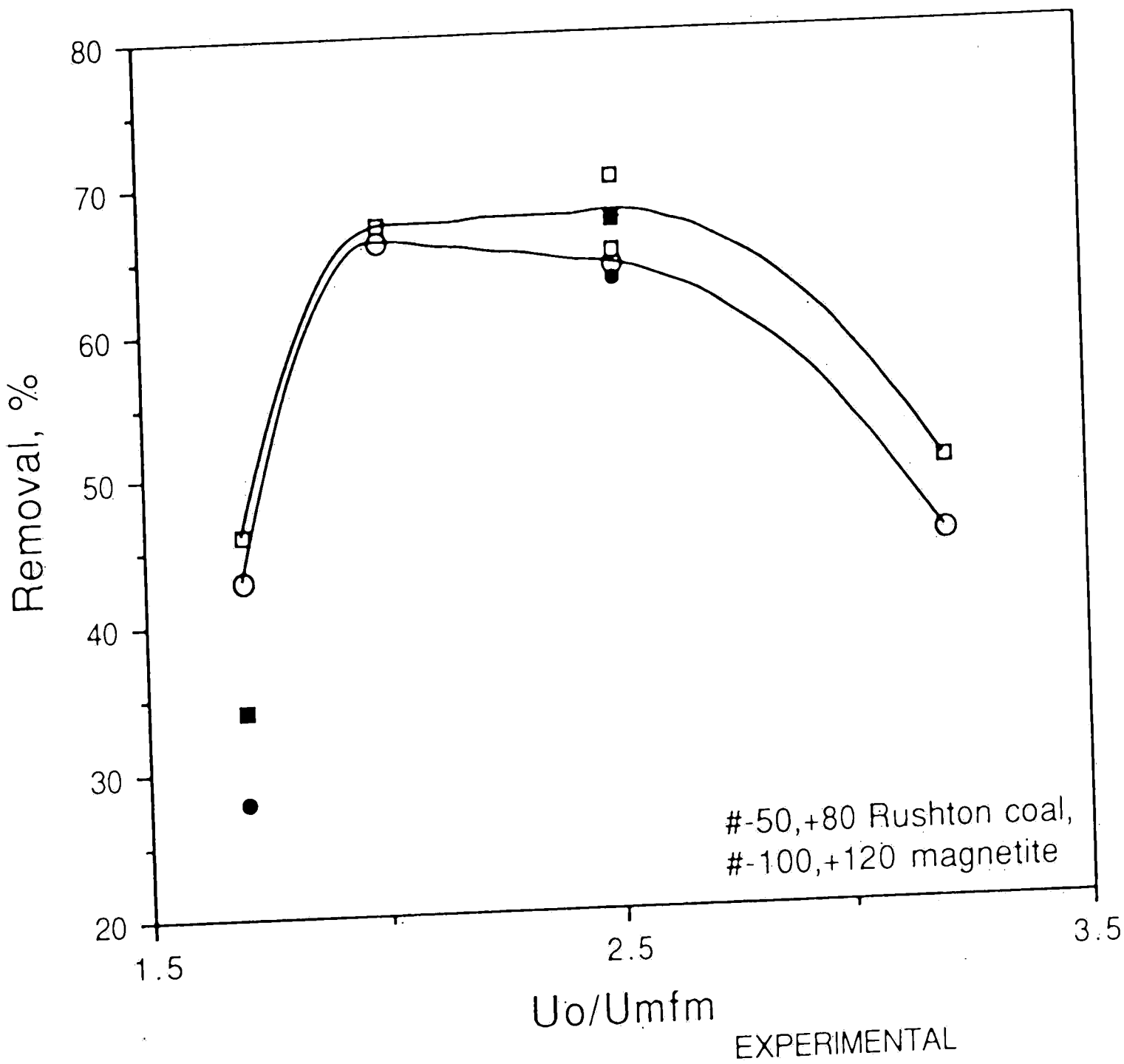

Fig. 6.19 Experimental results; the effect of superficial gas velocity on sulfur and ash removal, mm=6 (mass coal/ mass magnetite =0.70), bed depth: 3.0 cm, t=30 seconds

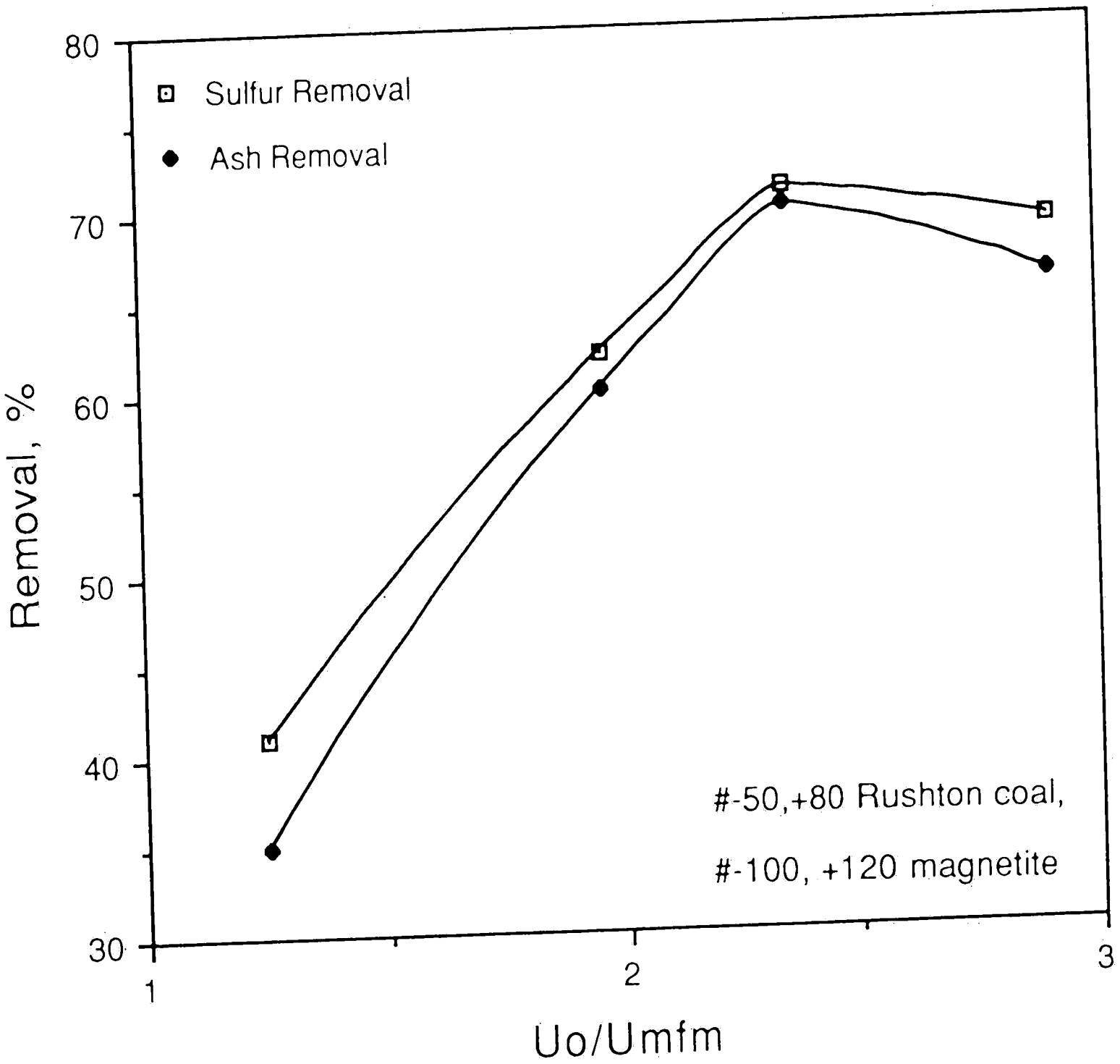

Fig. 6.20 Experimental results; the effect of superficial gas velocity on sulfur and ash removal, mm=3 (mass coal/ mass magnetite =1.6), bed depth: 3.0 cm, t=30 seconds

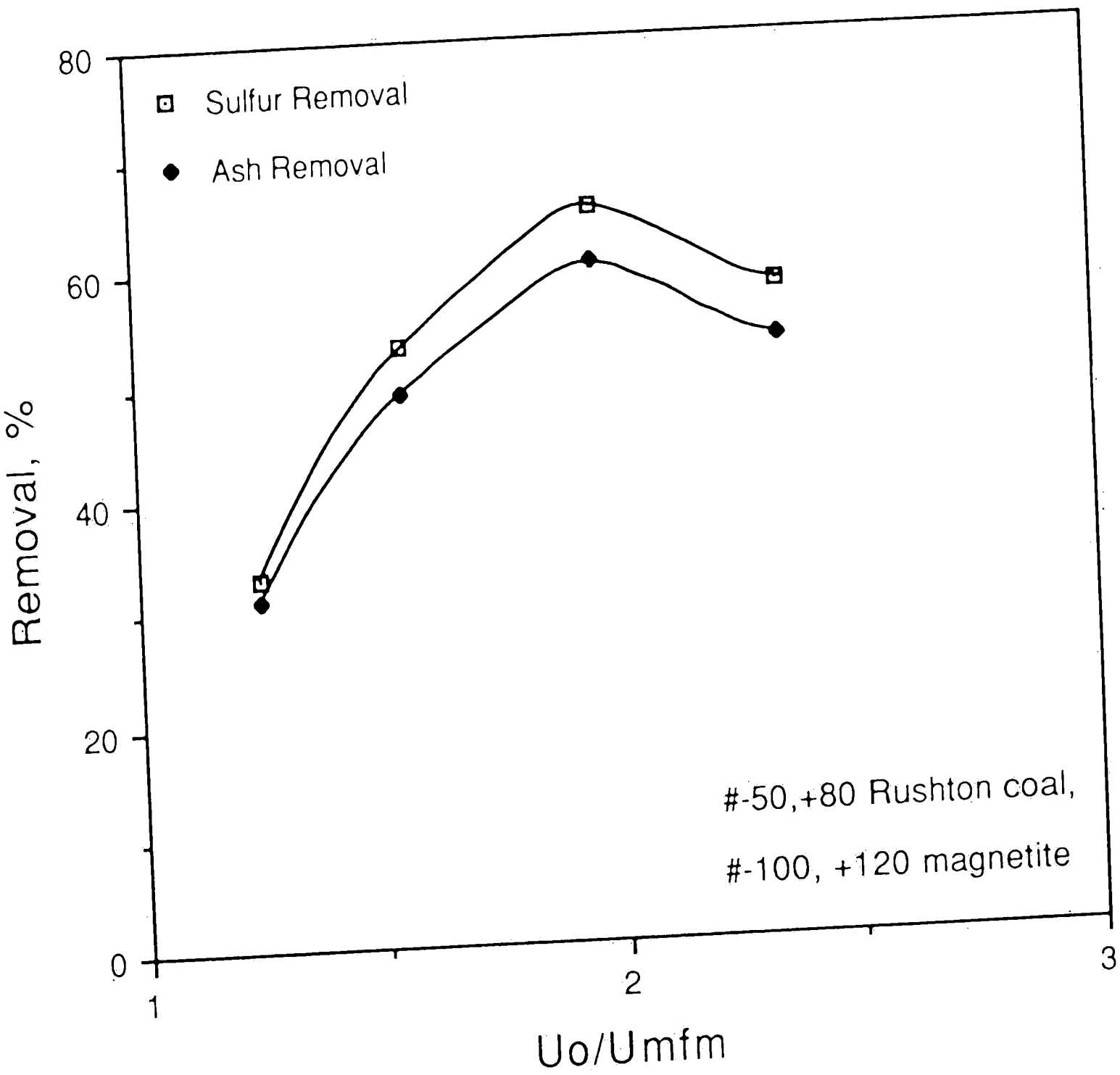

Fig. 6.21 Experimental results; the effect of superficial gas velocity on sulfur and ash removal, mm=1 (mass coal/ mass magnetite =5.7), bed depth: 3.0 cm, t=30 seconds

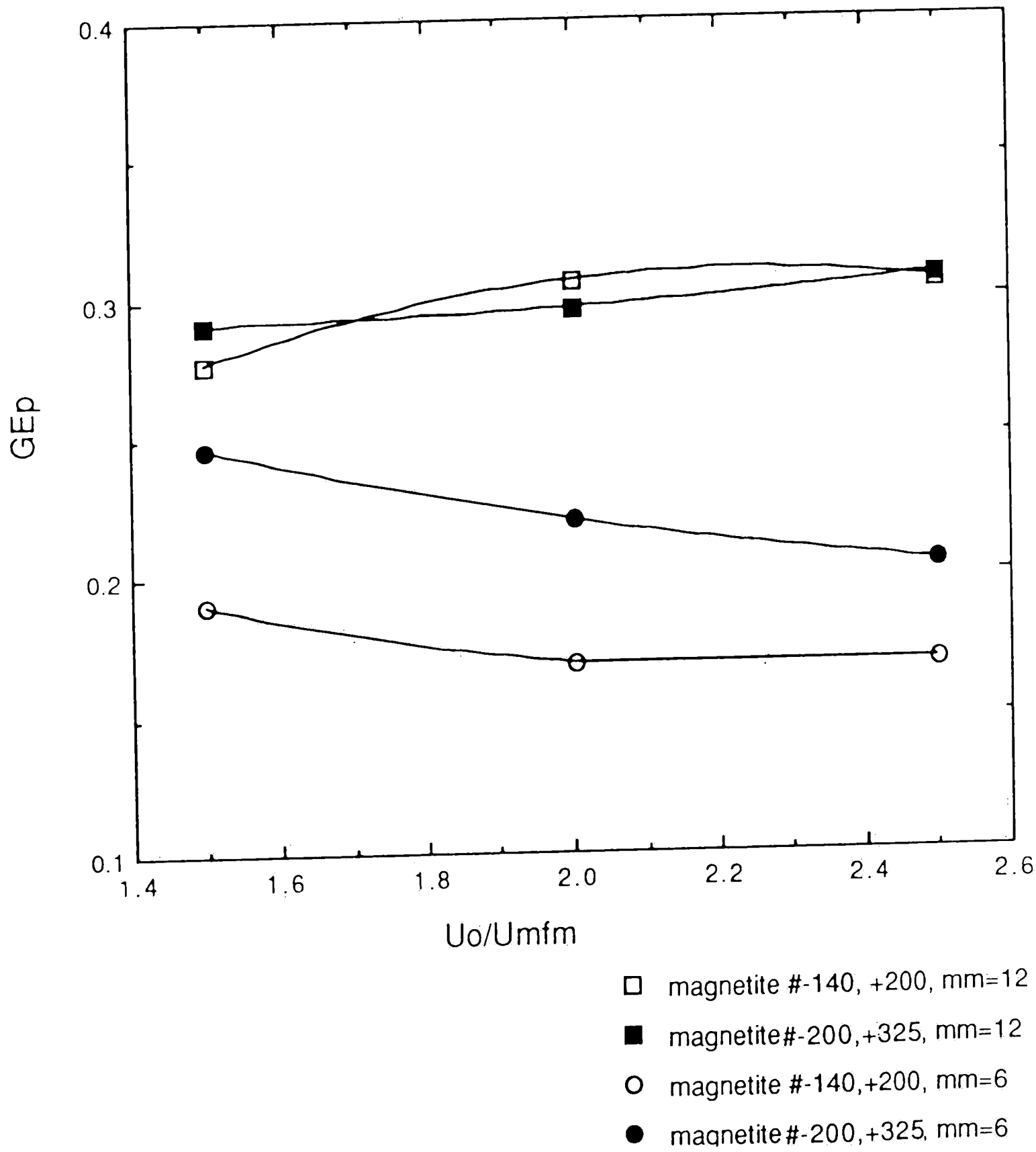

Fig. 6.22 Theoretical results; the effect of magnetite size on performance, coal:#-140,+325 Rushton, bed depth: 3.0 cm, t=30 seconds

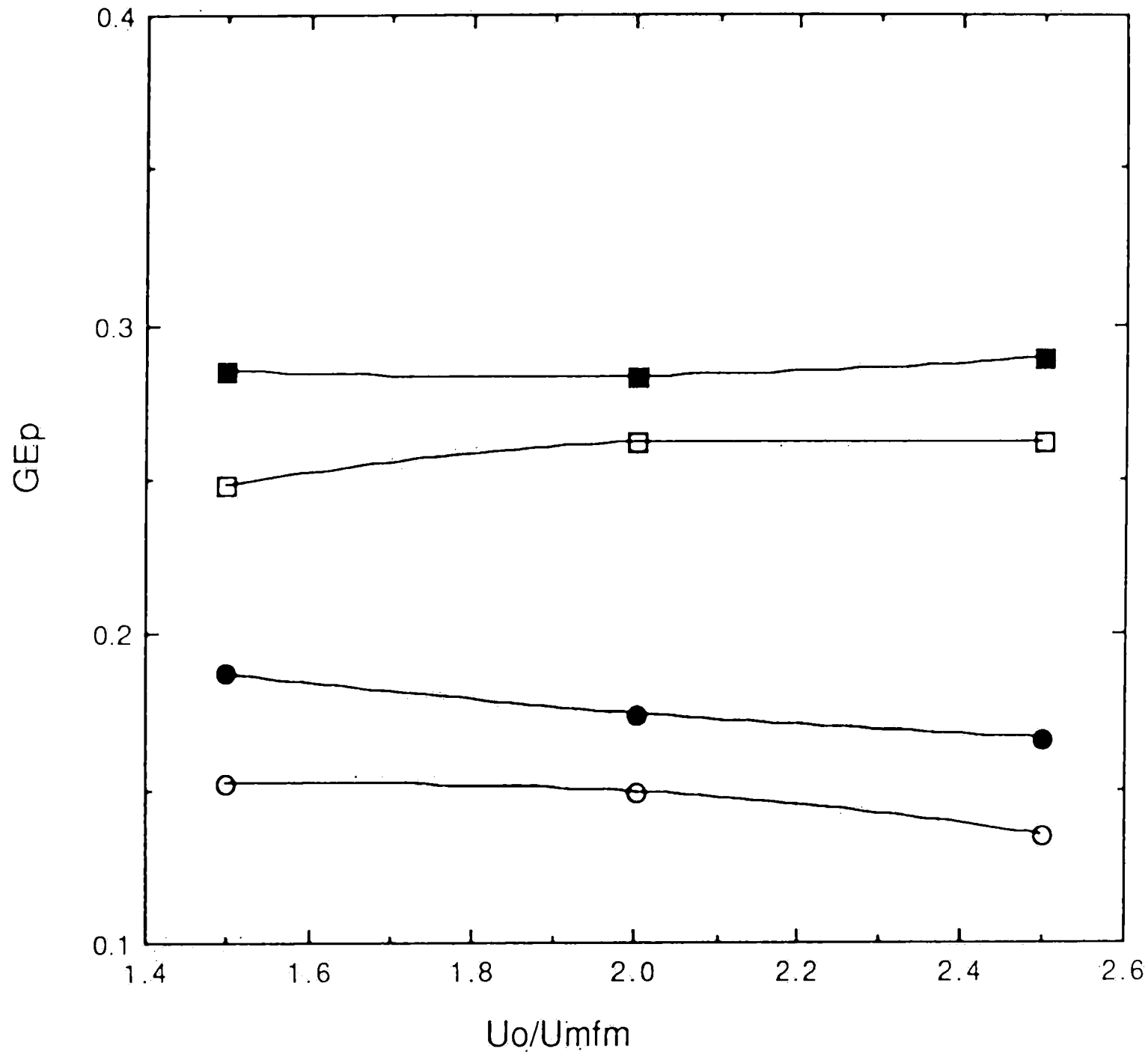

Fig. 6.23 Theoretical results; the effect of magnetite size on performance, coal:#-140,+325 Rushton, bed depth: 3.0 cm, t=60 seconds

VII. SUMMARY AND CONCLUSIONS

Mechanical cleaning of impurities such as pyritic sulfur and ash from coal in a fluidized bed can be performed very efficiently under certain operating conditions.For cleaning of coal from its mineral impurities, a fluidized bed which operates at room temperature was used.Crushed coal was added on top of the angular magnetite particles and fluidized with room temperature air.As a result, the particle mixing and settling processes in the fluidized bed can cause a separation between the clean portion of coal and its higher sulfur and ash containing part.In a non-homogeneous bed of particles with different physical properties such as size, density and shape, solids have a tendency to stratify in the vertical direction as the bubbles move upwards.The cleaner portion of the coal stays at the top of the bed, where the highly liberated impurities move to the bottom. Thus, the pyrite and other mineral contents of the coal at the top is lowered, allowing a recovery of cleaner coal.The type of coal extensively studied was Rushton mesh -50,+80 which has a total dry sulfur concentration of 2.53%, and a dry ash concentration of 26% by weight.The dry heating value is 11226 Btu/lbm and SO_2 concentration is 4.51 lbm/MBtu.Pyritic sulfur concentration constitutes to 69% of total sulfur where the rest is sulfate sulfur and organic sulfur.Results indicated that it is possible to remove the pyritic sulfur completely, and as high as 70% of ash for energy recoveries less than 85%.

Settlement characteristics of angular particles, such as coal and magnetite were determined by the early experiments.The rates of particle settling were expressed as functions of particle density and size and rates of solids mixing as a function of the size of the bubble rising in the bed.Those results are used together with other equations in literature to predict the parameters to establish a correlation.The outcome of these experiments was fed into the theoretical model which was previously developed.The theoretical model is used to predict the particle stratification in a fluidized bed under certain operating conditions.Theoretical model is based on the governing mechanisms in a bubbling fluidized bed and consists of a set of simultaneous differential equations which are solved by a computer code.The computer code was used to investigate the

effect of various operational parameters and bed configurations on the performance of cleaning.

The theoretical model agreed with the results from the coal cleaning experiments that the coal cleaning efficiency is a strong function of operating conditions and bed configuration.For high efficiency cleaning, the shallower beds must be selected.The operating gas velocitites must be carefully selected in a certain range.This velocity range was 2.0 to 2.5 times the minimum fluidization velocity of the host material which was angular magnetite.Even though the magnetite is considered to act as a buffer to enhance segregation, the higher coal to magnetite ratio seemed to help improved cleaning efficiencies in the case of deeper beds.However, higher mass concentrations of coal did not have a significant effect on the cleaning efficiency for the shallow beds.Cleaning performance improves with time, but processing times as short as 30 seconds may result in high performance in the case of shallow beds.The selection of magnetite size for best perfomance is considered to be based on matching the minimum fluidization velocities of the coal and magnetite.The results showed that the magnetite with a minimum fluidization velocity slightly higher than that of the coal should be selected for better performance .

The effect of the magnetite size and sphericity of magnetite may be factors to be investigated in the further studies.Further studies with the lower bed depths may also reveal the trends in the cleaning performance.It is also important to perform experiments with different types of coals and coals which are very fine in size.

VIII. APPENDIX

APPENDIX.A Tyler Standard Screen Apertures

MESH SIZE	APPROXIMATE MICRON SIZE	APPROXIMATE MILLIMETERS	INCHES
4	4760	4.76	0.185
6	3360	3.36	0.131
8	2380	2.38	0.093
12	1680	1.68	0.065
16	1190	1.19	0.046
20	840	0.84	0.0328
30	590	0.59	0.0232
40	420	0.42	0.0164
50	297	0.29	0.0116
60	250	0.25	0.0097
70	210	0.21	0.0082
80	177	0.17	0.0069
100	149	0.14	0.0058
140	105	0.10	0.0041
200	74	0.07	0.0029
230	62	0.06	0.0024
270	53	0.05	0.0021
325	44	0.04	0.0017
400	37	0.03	0.0015
625	20	0.02	0.0008
1250	10	0.01	0.0004
2500	5	0.005	0.0002

APPENDIX B. u_{mf} and u_{mb} of Coal and Magnetite

1. Coal, Rushton

Size	**Mean Particle Dia.** [μm]	u_{mf} [cm/s] (previous)	u_{mf} [cm/s]	u_{mb} [cm/s]
#-30,+50	450	6.6	5.4	7.5
#-50,+80	240	1.8	2.0	3.0
#-80,+140	143	0.5	0.7	1.1
#140,+325	75	0.2	0.4	0.5

2. Magnetite

Size	**Mean Particle Dia.** [μm]	u_{mf} [cm/s] (previous)	u_{mf} [cm/s]	u_{mb} [cm/s]
#-50,+60	274	_	6.6	9.0
#-60,+70	230	_	4.3	5.9
#-70,+80	196	3.8	3.5	4.7
#-80,+100	165	3.5	_	_
#-100,+120	138	2.3	2.3	3.2
#-120,+140	116	1.3	1.5	2.0
#-140,+200	90	1.2	_	_

APPENDIX C Computer Programs

Appendix C.1 Computer Program for Calculating Sulfur and Ash Removals, and Energy Recoveries from Experimental Data

```
      PROGRAM TIME2 (EXOUT1,TAPE2=EXOUT1)
      PARAMETER (n=6)
      DIMENSION coal(n),sulf(n),ash(n),btu(n)
     &,sulr(n),ashr(n),btur(n),zel(n)
      tash=0.0
      tbtu=0.0
      tsul=0.0
      DO 65 i=1,n
C     READ(5,10) coal(i)
C     READ(5,11) sulf(i)
C     READ(5,12) ash(i)
C     READ(5,13) btu(i)
C     READ(5,14) zel(i)
C  10 FORMAT(//,10X,F6.2)
C  11 FORMAT(//,23X,F5.2)
C  12 FORMAT(//,36X,F5.2)
C  13 FORMAT(//,51X,F5.0)
C  10 FORMAT(/,/,11X,F5.2)
C  14 FORMAT(//,F5.3)
C....
      COAL(1)=38.13
      COAL(2)=42.04
      COAL(3)=42.99
      COAL(4)=33.65
      COAL(5)=13.76
      COAL(6)=0.001
C.....
      SULF(1)=1.46
      SULF(2)=1.51
      SULF(3)=1.82
      SULF(4)=5.25
      SULF(5)=10.89
      SULF(6)=0.001
C......
      ASH(1)=12.57
      ASH(2)=13.75
      ASH(3)=21.17
      ASH(4)=63.32
      ASH(5)=74.47
      ASH(6)=1.000
C....
      BTU(1)=13444
      BTU(2)=13260
      BTU(3)=11989
      BTU(4)=4382
      BTU(5)=2151
      BTU(6)=15
C......
      tsul=tsul+sulf(i)*coal(i)
      tash=tash+ash(i)*coal(i)
      tbtu=tbtu+btu(i)*coal(i)
   65 CONTINUE
c....
      rsul=0.0
      rash=0.0
      sbtu=0.0
c....
      DO 70 i=1,n
      rsul=rsul+coal(i)*sulf(i)
      rash=rash+coal(i)*ash(i)
```

```
      sbtu=sbtu+coal(i)*btu(i)
c....
      sulr(i)=(tsul-rsul)/tsul
      ashr(i)=(tash-rash)/tash
      btur(i)=sbtu/tbtu
   70 continue
c....
c....
      zel(1)=0.000
      zel(2)=0.000
      zel(3)=0.000
      zel(4)=0.000
      zel(5)=0.000
      zel(6)=1.000
c....
c....
      WRITE(2,90)
C  90 FORMAT("  Z/L     COAL    SULF     ASH     SULR     ASHR     BTUR",/)
   90 FORMAT("       SULR        ASHR        BTUR",/)
      DO 85 i=1,n
C     WRITE(2,80) ZEL(I),COAL(I),SULF(I),ASH(I),SULR(I),ASHR(I)
C    &,BTUR(I),K
      WRITE(2,75) SULR(I),ASHR(I),BTUR(I)
   75 FORMAT(/,4X,3(F6.3,6X))
C  80 FORMAT(/,2X,7(F6.3,3X))
   85 CONTINUE
      END
```

Appendix C.2 Computer Program for Calculating Sulfur and Ash Removals, and Energy Recoveries Using Volumetric Coal Concentrations in the Emulsion Phase from the Batch Code

```
      PROGRAM TIME2 (WRK8,cout,TAPE5=WRK8,TAPE2=cout)
      PARAMETER (n=15)
      PARAMETER (m=8)
      DIMENSION rot(8),s(15,8),ss(15),su(8),as(8),btu(8)
     &,cave(n,m),top(m),denom(n),sul(n),ash(n),coal(n),sulr(n)
     &,ashr(n),btur(n),sula(n),asha(n)
      DO 65 I=1,n
      READ(5,70) Cave(I,1),cave(i,2),cave(i,3),cave(i,4),cave(i,5)
     &,cave(i,6),cave(i,7),cave(i,8),kk
      do 64 jjj=1,m
      TOP(jjj)=TOP(jjj)+CAVE(I,jjj)
   64 continue
   65 CONTINUE
   70 FORMAT(8(F8.6,1x),1X,I2,/)
c
      rot(1)=1.15
      rot(2)=1.35
      rot(3)=1.50
      rot(4)=1.70
      rot(5)=1.90
      rot(6)=2.225
      rot(7)=2.675
      rot(8)=3.450
c
      roj=5.2
c
      do 19 i=1,n
      over1=1.0
      over2=0.0
      ss(i)=1.0
c
      do 30 jjj=1,m
      over1=over1-cave(i,jjj)
      over2=over2+cave(i,jjj)*rot(jjj)
   30 continue
c
      do 31 jjj=1,m
      s(i,jjj)=(cave(i,jjj)*rot(jjj))/(over1*roj+over2)
      if(s(i,jjj) .lt. 0.0) s(i,jjj)=0.0
      ss(i)=ss(i)-s(i,jjj)
   31 continue
   19 continue
c
      su(1)=1.12
      su(2)=1.48
      su(3)=2.05
      su(4)=2.23
      su(5)=2.31
      su(6)=2.80
      su(7)=3.74
      su(8)=38.28
c
      as(1)=2.64
      as(2)=9.00
      as(3)=21.99
      as(4)=42.86
      as(5)=56.33
      as(6)=72.65
      as(7)=86.35
```

```
      as(8)=62.88
C
C
      btu(1)=34.02
      btu(2)=31.34
      btu(3)=26.19
      btu(4)=18.24
      btu(5)=13.08
      btu(6)=6.83
      btu(7)=1.76
      btu(8)=5.67
C
      btuo=0.0
      asho=0.0
      sulo=0.0
      weight=0.0
      coalo=0.0
      WRITE(2,72)
   72 FORMAT(/," coal     sul     ash   sulr  ashr  btur sula asha i",
     &//,"=============================================================",//)
C
C
C
C
      H=3.00
      dh=H/15
      at=182.41469
      do 507 i=1,n
      do 601 jjj=1,m
      btuo=btuo+at*dh*cave(i,jjj)*rot(jjj)*btu(jjj)
      coalo=coalo+at*dh*cave(i,jjj)*rot(jjj)
      sulo=sulo+at*dh*cave(i,jjj)*rot(jjj)*su(jjj)
      asho=asho+at*dh*cave(i,jjj)*rot(jjj)*as(jjj)
      weight=weight+at*dh*cave(i,jjj)*rot(jjj)
  601 continue
  507 continue
C
C
C
      do 500 i=1,n
      denom(i)=0.0
      sul(i)=0.0
      ash(i)=0.0
C
      do 602 jjj=1,m
      denom(i)=denom(i)+s(i,jjj)
  602 continue
C
      if(denom(i) .lt. 0.0000001) go to 505
C
      do 603 jjj=1,m
      sul(i)=sul(i)+su(jjj)*s(i,jjj)
      ash(i)=ash(i)+as(jjj)*s(i,jjj)
  603 continue
C
      sul(i)=sul(i)/(denom(i)*100)
      ash(i)=ash(i)/(denom(i)*100)
      coal(i)=denom(i)
      go to 500
  505 sul(i)=0.0
```

```
      ash(i)=0.0
      coal(i)=0.0
  500 continue
C
C
C
      srec=0.0
      arec=0.0
      wrec=0.0
      brec=0.0
C
C
C
      do 508 i=1,n
      l=n+1-i
      do 604 jjj=1,m
      srec=srec+at*dh*cave(l,jjj)*rot(jjj)*su(jjj)
      arec=arec+at*dh*cave(l,jjj)*rot(jjj)*as(jjj)
      wrec=wrec+at*dh*cave(l,jjj)*rot(jjj)
      brec=brec+at*dh*cave(l,jjj)*rot(jjj)*btu(jjj)
  604 continue
      sulr(i)=((sulo/weight)-(srec/weight))/(sulo/weight)
      ashr(i)=((asho/weight)-(arec/weight))/(asho/weight)
      btur(i)=brec/btuo
      sula(i)=srec/sulo
      asha(i)=arec/asho
  508 continue
C
C
C
      do 509 i=1,n
      write(2,501) coal(i),sul(i),ash(i),sulr(i),ashr(i),btur(i),
     &sula(i),asha(i),i
  501 FORMAT(/,8(F6.4,2X),1X,I2)
  509 continue
      END
```

APPENDIX D. Washability Analysis for Rushton #-50,+80 Coal

Homer City, PA 15748
412-479-9011

Penelec / GPU

Certificate of Analysis

Pennsylvania Electric Company
Homer City Laboratory

Description:
LEHIGH FLUIDIZED BED
SEGREGATOR RUN #89100901
RUSHTON RAW COAL - B

Lab No.: 891000130
From: EPRI-CQDC
Sampled: / /
Gross Wt.: 0.5062 Kg

FLOAT/SINK OF PLUS BY 0.000 mm FRACTION REPRESENTING 100.00 % OF THE TOTAL SAMPLE

GRAVITY SINK	GRAVITY FLOAT	DIRECT WT %	DIRECT ASH	DIRECT SULFUR	DIRECT BTU/LB	DIRECT SO2/MBTU	CUMULATIVE FLOAT WT %	CUMULATIVE FLOAT ASH	CUMULATIVE FLOAT SULFUR	CUMULATIVE FLOAT BTU/LB	CUMULATIVE FLOAT SO2/MBTU
	1.300	31.07	2.64	1.12	15430	1.45	31.07	2.64	1.12	15430	1.45
1.300	1.400	21.63	9.00	1.48	14216	2.08	52.70	5.25	1.27	14932	1.70
1.400	1.600	11.05	21.99	2.05	11879	3.46	63.76	8.15	1.40	14402	1.95
1.600	1.800	6.16	42.86	2.23	8273	5.39	69.92	11.21	1.48	13862	2.13
1.800	2.000	4.13	56.33	2.31	5932	7.80	74.05	13.73	1.52	13420	2.27
2.000	2.450	8.62	72.65	2.80	3099	18.09	82.67	19.87	1.66	12343	2.68
2.450	2.900	12.46	86.35	3.74	797	93.79	95.13	28.58	1.93	10831	3.56
2.900		4.87	62.88	38.28	2571	297.67	100.00	30.25	3.70	10429	7.10

IX. REFERENCES

[1] Wen, C. Y., Yu, Y. H., *AIChE J.*, Vol. 12 (1966), pp. 610.

[2] Clift, R., in "Fluid Bed Technology" Ed. Geldart, D., New York: John Wiley & Sons (1985)

[3] Botterill, J. S. M.,"Fluidised Bed Behaviour" Ed. Howard, J. R., London: Applied Science Publishers (1983) pp. 1-36

[4] Mori, S., Wen, C. Y., "Estimation of Bubble Diameter In Gaseous Fluidized Beds" *AIChE J.*, Vol. 21 No. 1 (1975), pp. 109-115.

[5] Rowe, P. N., *Chem. Eng. Sci.*, Vol. 31 (1976), pp. 285-288.

[6] Darton, R. C., LaNauze R. D., Davidson, J. F., Harrison, D., "Bubble Growth Due To Coalescence In Fluidized Beds" *Trans. Inst. Chem. Eng.*, Vol. 55 (1977), pp. 274-280.

[7] Werther, J., in "Fluidization" Eds. Davidson, J. F., Keairns, D. L., London: Cambridge Univ. Press, (1978).

[8] Grace, J. R., *Can. J. Chem. Eng.*, Vol 48 (1970), pp. 30-33.

[9] Kozanoglu B., "Transient Mixing of Solids In A Bubbling Fluidized Bed" , Ph.D. Dissertation, Lehigh Univ., Bethlehem PA, U.S.A., (1990).

[10] Nienow, A. W., Naimer, N. S., Chiba, T., "Parameter Estimation for a Solids Mixing/Segregation Model for Gas-Fluidized Beds" *Chem. Eng. Sci.*, Vol. 37 (1982) pp. 1047-1057.

[11] Nicklin, D. J., "Two-Phase Bubble Flow", *Chem. Eng. Sci.*, Vol. 17 (1962) pp. 693.

[12] Grace, J. R. and Clift, R., "On the Two-Phase Theory of Fluidization", *Chem. Eng. Sci.*, Vol. 29 (1974), pp. 324-327.

[13] Basesme E. A., "Solid Exchange Between the Bubble Wake and the Emulsion Phase in a Two-Dimensional Gas-Fluidized Bed", M.S. Thesis, Lehigh Univ., Bethlehem PA, U.S.A., (1990).

[14] Rowe, P. N., Partridge, B. A., Cheney, A. G., Henwood G. A. and Lyall E., "The Mechanisms of Solids Mixing in Fluidized Beds", *Trans. Inst. Chem. Engrs.*, Vol. 43 (1965) , T271.

[15] Kocatulum, B., "A Numerical Study of the Fluid Mechanics Within a Bubbling Fluidized Bed", M.S. Thesis, Lehigh Univ., Bethlehem PA, U.S.A. , (1989).

[16] Tanimoto, H., Chiba S., Chiba. T., Kobayashi H., *J. Chem. Eng. Japan*, Vol. 14 (1981), pp. 273.

[17] Nienow, A. W., Chiba T., Chapter 10 in *Fluidization*, Eds. Davidson, J. F., Clift, R., Harrison, D., London and New York: Academic Press, (1985).

[18] Kozanoglu B., "User's Guide to Computer Simulation of Segregation" , Unpublished Document, Energy Research Center, Lehigh Univ., Bethlehem PA, U.S.A., (1990)

VITA

The author was born in Ankara, Turkey to Sevim and Orhan Ulge on March 8, 1963.He attended Ankara Ataturk Anadolu High School.He received his Bachelor of Science and Master of Science degrees both in Mechanical Engineering from Middle East Technical University.He worked as a R&D design engineer for Aselsan Military Electronics in Ankara, Turkey for two years until he came to Lehigh.He enrolled in the graduate program at Lehigh University in August 1989.With a research assistantship support from the Energy Research Center, he attended the graduate program, obtaining a Master of Science degree in Mechanical Engineering in August, 1991.